Lars-Erik Rännar

On Optimization of Injection Molding Cooling

Thesis for the degree doktor ingeniør

Trondheim, April 2008

Norwegian University of Science and Technology
Faculty of Engineering Science and Technology
Department of Engineering Design and Materials

NTNU

NTNU
Norwegian University of Science and Technology

Thesis for the degree doktor ingeniør

Faculty of Engineering Science and Technology
Department of Engineering Design and Materials

ISBN 978-82-471-8270-3 (printed version)
ISBN 978-82-471-8284-0 (electronic version)
ISSN 1503-8181

Doctoral theses at NTNU, 2008:113

Printed by NTNU-trykk

"It was the best of times,
it was the worst of times, …
it was the season of Light,
it was the season of Darkness…"

Charles Dickens, 1859,
A Tale of Two Cities

Abstract

This thesis is devoted to analysis and optimization of the injection molding process with a focus on the mold. In the analysis, both process parameters and the design of the mold are taken in consideration. A procedure has been developed, i.e. a method and a program code, which enables optimization of different quantities, not only restricted to injection molding simulation, by altering different variables. There are many ways to interpret the word "optimization". In this work, "optimization" means the use of mathematical algorithms in order to maximize or minimize any given quantity. This code, called VerOpt, is written in Matlab. It is versatile since it has the functionality of choosing different optimization routines, and it can make use of parallelization over TCP/IP and different external solvers. The software and different applications are further described in Paper A.

There is a pocketful of softwares on the commercial market today, which enables the analysis of the injection molding process. One example is the software Moldex3D by Coretech System. By using simulation in the product development process, much can be gained since the software allows one to make most of the tedious and cost-consuming trial-and-errors in the virtual world, instead of on the shop floor. In Paper B, Moldex3D is used in order to compare the efficiency, in terms of the dimensional accuracy, between two different cooling channel layouts. One conventional layout uses straight holes and a baffle, and another layout makes use of conformal cooling channels manufactured by Free-Form Fabrication (FFF). In Paper C, a comparative study is presented where numerical results are compared with corresponding experimental results using these two types of cooling channel design. For the FFF layout, the Electron Beam Melting (EBM) method was used to manufacture the core insert to the mold. In Paper D, the surface heat distribution of conventional and FFF inserts was investigated, and the influence of the coolant temperature on the surface of the insert was studied.

FFF, or Rapid Prototyping (RP), has been commercially available since the late eighties, but the method is not that well known within the injection molding industry. The first available material was plastics. Today, FFF has evolved and fully dense forms in different metal alloys can be manufactured which are suitable for mold inserts. Studies have shown that by using FFF mold inserts in injection molding, both that the part quality can be increased and that the costs for manufacturing the insert can be decreased. The effects of different process parameters on the warpage of a plastic part are however rather complicated and the introduction of new types of inserts manufactured by FFF makes these effects even harder to predict. In Paper E, Design of Experiments (DOE) is used in order to investigate the influence of different process parameter on the critical dimensional accuracy of a test part. The same part was used for two different studies: one using conventional cooling and the other one using an FFF layout.

In Paper F, four process parameters were chosen after considering the results obtained from the DOE in Paper E, as variables in an optimization study where the warpage of the test part was minimized using the VerOpt code. In order to measure the efficiency of the FFF mold insert, the optimization was performed on the conventional layout as well.

In conclusion, this work has demonstrated the feasibility of including a versatile optimization environment to a commercial injection molding software, and it has also pointed out some important differences in the influence of different process parameters on the warpage of a plastic part when conventional and FFF cooling channel layouts are used.

Acknowledgement

This work has been carried out at the Department of Engineering Design and Materials in the Faculty of Engineering Science, and Technology, at the Norwegian University of Science and Technology (NTNU) and at the Department of Engineering, Physics, and Mathematics at Mid Sweden University in Östersund. The financial support for this work was provided by the European Union Structural Funds and Mid Sweden University.

This thesis would not have been possible without the help of many people and in particular, I would like to thank Professor Claes-Göran Gustafson for taking me on as a PhD student and making it possible for me to be a member of the research group at NTNU. His cheerful spirits have helped me a lot during the sometimes gloomy periods throughout this work. Thank you for everything.

I wish to express my gratitude to my local supervisor Mats Tinnsten who initiated this work and who, once upon a time offered me a position as an instructor at Mid Sweden University.

Without the possibility to make experiments, this thesis would not have been completed, and therefore I would like to thank the Essge-Plast company and especially Mikael Waldehorn both for his invaluable “shop-floor” experience and for his practical and financial help when I performed the experiments.

One of the main advantages with being a PhD student at another university is that you get the possibility to widen your circle of contacts. I would like to thank my fellow colleagues Rudolf Krondorfer and Bent Laursen at NTNU. Both of you made my stays in Trondheim a lot easier. By mixing three different nationalities together, a group spirit was formed in the department which I have not found in any of the groups I have worked in previously.

A special thanks to the present and former colleagues at the Department of Engineering, Physics, and Mathematics in Östersund. All of you have in one way or another contributed to this work, but I would especially like to thank Joakim Holmberg, for being my inseparable office colleague, co-author, and friend for more than 10 years.

Björn Israelsson has been an invaluable support for me in the discussion of injection molding in periods when I did not have the possibility to be at NTNU. He has also served as a great friend, both when we were traveling around Europe together learning about injection molding simulation and when we were spending time together with our families at home.

A never-ending topic in the conversation with my colleague Jon Johansson at Mid Sweden University is the process of how to get a PhD and how to lead your life while trying to reach that goal. Thank you for all of the memorable moments and discussions I have experienced with you.

And finally, the endless gratitude I feel towards my beloved Kristina, and my children Ellen, Emil, and Thea can not be put into words. Without your support and encouragement, I would not have appreciated the work with this thesis as much as I have.

Lars-Erik Rännar Östersund, April 2008

List of publications

This thesis comprises an introductory summary and the following appended papers:

Paper A
J Holmberg and L-E Rännar
"Versatile Optimization", Nordic Matlab Conference, Oslo, Norway, 2001, pp.207-212.

Paper B
L-E Rännar
"Efficient Cooling of FFF Injection Molding Tools with Conformal Cooling Channels, -An Introductory Analysis", 1:st International Conference on Advanced Research in Virtual and Rapid Prototyping, Leiria, Portugal, 2003, pp.433-437.

Paper C
L-E Rännar, A Glad, C-G Gustafson
"Efficient Cooling With Tool Inserts Manufactured by Electron Beam Melting", Rapid Prototyping Journal, 13(3), (2007), 128-135.

Paper D
L-E Rännar, C-G Gustafson
"Improvement in Surface Heat Distribution of Injection Molding Tooling Using Conformal Cooling Channels", submitted to the Journal of Materials Processing Technology.

Paper E
L-E Rännar, C-G Gustafson
"An Investigation of Optimal Process Settings in Injection Molding Using Inserts Manufactured by Rapid Tooling", submitted to the Journal of Manufacturing Science and Engineering.

Paper F
L-E Rännar, C-G Gustafson
"Effective Injection Molding With Rapid Tooling and Optimization", submitted to the International Journal of Advanced Manufacturing Technology.

Contents

1 Introduction

The know-how of the design engineer is an important part in the product design process, but this experience alone is not enough to be competitive on the market today. One important issue affecting product competitiveness is when, that is in which phase in the design process, major decisions are taken, see Figure 1. Decisions taken early in the process have a major impact in terms of the cost of the finished product, whereas decisions taken later in the manufacturing phase only can influence about 25% of the final cost of the product. A second major impact on competitiveness is product quality. An old approach to define and achieve quality is to measure and inspect the products coming out at the end of the production line. Today, the concept of quality is wider and management strategies like Total Quality Management (TQM) are widely used, and here one of the keywords is customer satisfaction. Different tools to improve quality, like Design of Experiments (DOE) and Robust design, are parts of this management system. In addition to customer satisfaction, the design of a product must be carried out in such a way that the product can be made without defects but at a competitive cost. The third contribution to competitiveness is product cycle time. Here, the cycle time refers to the time for development required to bring a new product to the market. Computer-Aided Engineering (CAE) and rapid prototyping methods have contributed to reduced cycle times in organizations striving for an effective product design process. To summarize, the product design process should be conducted so as to develop cost-competitive products of high quality in the shortest time possible. [1]

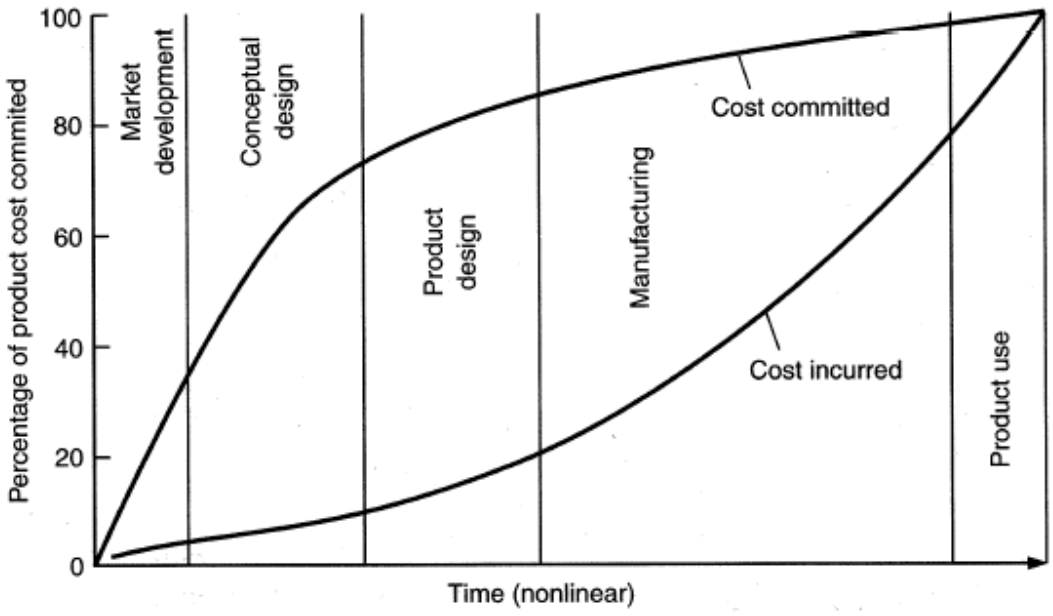

Figure 1. Product costs during the design phase (with a nonlinear timescale). [1]

The use of plastics has been increasing dramatically in the last century, especially since the commercialization of nylon in 1939 by the company Du Pont de Nemours & Coin and, today the total production volume of plastics exceeds that of metals [2]. The most important method of forming complex plastic parts is injection molding. Features like minimal finishing of the molded part, good reproducibility, a fully automated process, and the wide range of weights of parts it is possible to manufacture with injection molding make this method well suited for mass production of complicated parts [3]. See Figure 2 for an example of an injection-molded part.

Figure 2. Housing for a clearing saw, manufactured by injection molding using the material polyamide (PA). Courtesy of Essge-Plast AB.

Asia, and especially China, have for long being a major producer of injection-molded parts, but in the last years, they have also taken over a great share of the market within tool making. The low cost associated with making a mold in China compared to the cost of a mold manufactured in the Western world is the main reason for this development. The main advantage in favor of China is the low personnel costs, since the costs for the material and machines are almost the same all over the world. Today, mainly large tools are manufactured in China on the request from western employers, but, as know-how and technology will improve, it is most likely that the share of molds made in China will increase. Western mold makers still have an advantage in the production of complicated and small tools, since the cost and the time associated with the delivery of tools are still main drawbacks for the eastern companies. Delivery by airplane is expensive, due to the heavy weight of the molds, and shipping by boat takes a long time. If a mold re-construction is necessary, a great deal of the profits connected with ordering tools from Asia can be consumed. A part of a mold is depicted in Figure 3.

Hull's invention of stereolithography (SLA) in 1984 [4] cleared the way for a new technology called Rapid Prototyping (RP) or Free-Form Fabrication (FFF). As the name implies, this technology allowed designers and engineers to verify their designs early in the product design process by using three-dimensional representations manufactured in much less time than compared with traditional methods. Today, RP has evolved into several branches. One of them is called Rapid Tooling (RT). One reason for this development is the competitive pressures for the mold-making and injection-molding industries. As mentioned before, price competition is not viable due to the cost-efficient Asian companies, but speed is still a viable aspect for Western mold-makers to keep old and gain new market shares. RT can be an important tool in order to gain this competitive advantage, since cost reductions both for mold making and production of the parts can be achieved by using RT.

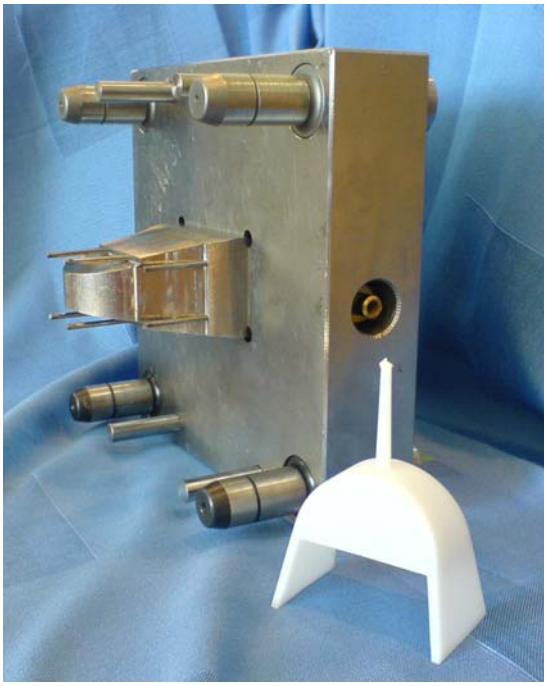

Figure 3. The core plate of a mold where the core insert, the ejector pins, and the inlet of the cooling system are visible. The molded part is also shown. The core was made using FFF.

The use of CAE alone does not ensure success, since the results gained from such a tool must be interpreted in some way. Mostly, this interpretation is made by an engineer, but the results can rather easily be presented in an illustrative way and can serve as a solid ground for discussions between the engineer and other persons involved in the project, such as salesmen, technicians, and other engineers. Injection-molding simulation has been a valuable tool for engineers ever since the introduction of the first commercial software in 1975, and, theoretically, the injection molding process is a three-dimensional, transient problem with a moving melt front where coupled heat transfer and non-Newtonian flow are present. An example of a simulation of the filling pattern for a mobile phone cover is depicted in Figure 4. One way of making the use of CAE software more efficient is to incorporate the use of optimization tools. By doing this, the steps to conceive the best product design possible can be automated and thereby more efficient. Optimization is a mathematical approach to tackle a design problem, and it can be defined as the act of obtaining the best result possible under certain circumstances. In other words, the aim is to maximize or minimize an objective function by altering a set of design variables without violating any given constraints. Today, optimization is widely used in many different areas and diverse algorithms can be found. Some have a true, mathematical approach, whereas others are mimic different phenomenon in nature.

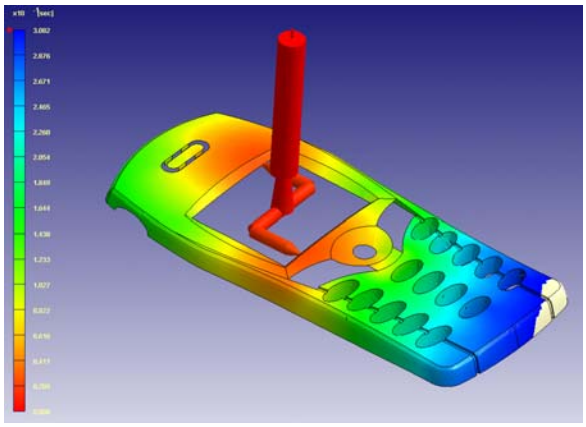

Figure 4. Simulation results from the software Moldex3D showing the filling pattern for a mobile phone cover. Courtesy of Coretech System.

The aim with this thesis is to contribute to the understanding of how the use of inserts manufactured by RT, and especially inserts manufactured by the Electron Beam Melting method, affects the process settings in injection molding and to compare the quality, in terms of dimensional accuracy, of injection-molded parts cooled by either a conventional cooling layout or an FFF cooling layout.

The purpose of this thesis is therefore to study:

- how different cooling channel layouts affect the cooling time and the dimensional accuracy of the product
- if the direct-metal FFF method Electron Beam Melting is a viable method for the manufacture of inserts to injection molding
- which process parameters affect the dimensional accuracy and to what degree
- the feasibility of optimization methods applied to injection-molding simulation and warpage minimization

2 Injection molding

The injection molding process can be divided into five separate steps: plastification, injection, holding, cooling, and finally ejection. The time used from the injection of the melt into the cavity to the ejection of the finished part is the most significant parameter in the calculation of the cost of manufacturing a plastic part. This is called the cycle time, see Figure 5.

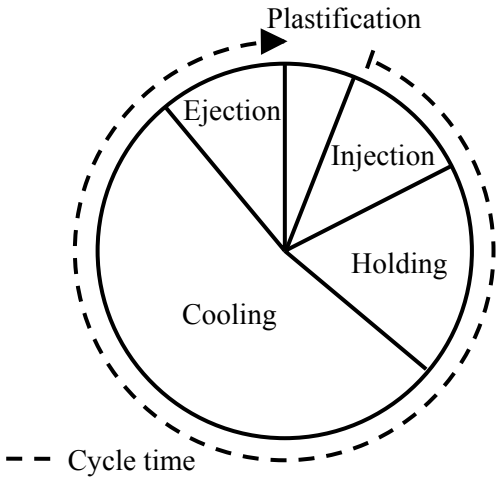

Figure 5. The injection molding cycle and the steps included in the cycle time.

The process starts with a selected plastic compound which is normally supplied as pellets. These pellets are put into a hopper on the injection molding machine, see Figure 6 and 7, and the pellets are then transferred to the electrically heated barrel. Inside the barrel, a screw is located and when the screw is rotating, the pellets are melted due to the heat generated by the friction between the barrel wall and the screw. The rotation of the screw feeds the partly molten pellets forward, and the screw is at the same time moved backwards by the accumulation of the melt in front of the screw tip. Up to 70% of the heat needed to melt the pellets is provided by this shear-induced heating, while the rest is provided by the heaters on the outside of the barrel.

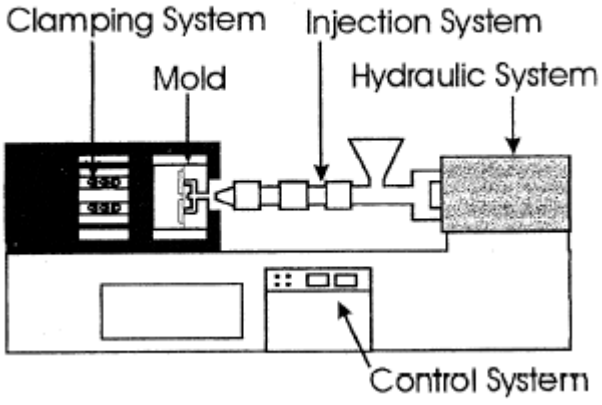

Figure 6. Injection molding machine. [5]

When the injection chamber is full with molten plastic, the rotation of the screw stops, and a valve is opened into the mold. The screw is pushed forward, and the melt flows through the nozzle, the sprue, and the runner system into the cavity. The cavity is the inverse of the desired shape of the part to be manufactured (Figure 7).

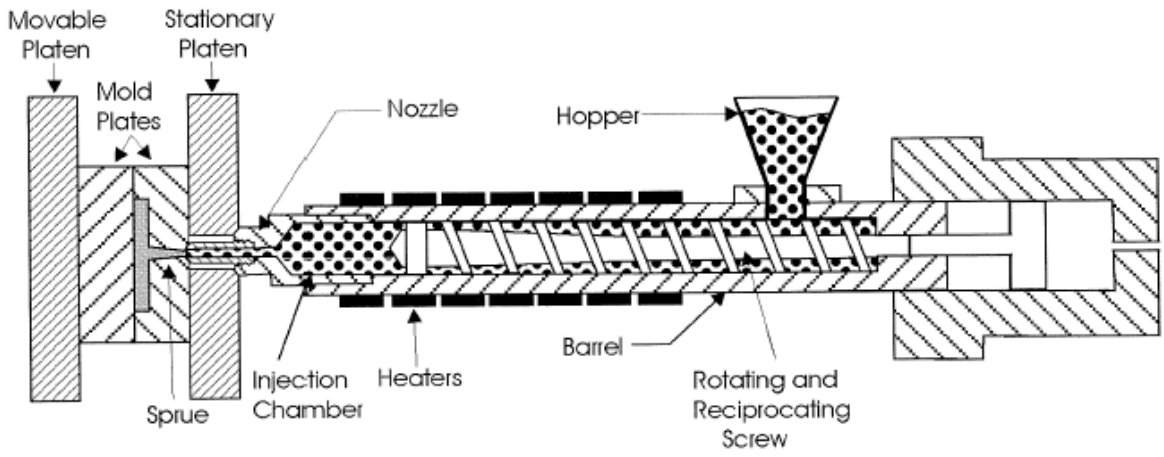

Figure 7. Injection molding cylinder. [5]

As soon as the melt comes into contact with the cold mold surface, it starts to cool down, and a frozen layer of plastic nearest the mold wall is shaped. This results in a narrower flow path, and the frozen layer on the cavity surface insulates the melt from the mold wall. The screw is still pushing the melt forward, but the force needed is gradually increasing due to the increasing flow resistance, as the flow path is getting narrower and longer.

When the cavity is completely filled, a hold pressure is applied. Plastics shrink from the melt temperature as they cool. The hold pressure applied by the screw compensates this loss of volume by pushing in more melt. The smallest passage into the cavity is called the gate, and when the gate has solidified, the entrance to the cavity is stopped, and no more melt can be pushed into the cavity. The cooling phase starts.

The metal mold cools the plastic. The cooling rate is highly dependent on the thickness of the part, but it can also to some extent be controlled by a mold temperature control unit where the flow rate and the temperature of the fluid in the cooling channels are controlled. These cooling channels are usually straight bored holes in the mold plates, and by letting a coolant, usually water or oil, flow through these channels, the cooling efficiency can be increased (Figure 8). When the part is stiff enough and has reached a temperature below the solidification point, the mold opens, and the part is ejected.

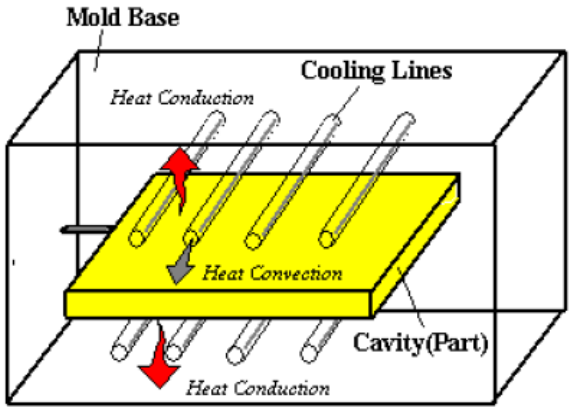

Figure 8. Schematic figure of the cooling channels and the mold cavity. Courtesy of Coretech System.

2.1 Mold cooling

Critical dimensions, surface finish, cycle time, etc., are all affected by mold cooling. Hence mold cooling is a decisive factor if a product will be manufactured with good quality and at a competitive cost. The mold has to be cooled, or heated if compared with the ambient temperature, with a heat exchange system, usually called temperature control unit, in order to remove the heat generated from the molten polymer, see Figure 9. The cooling process starts immediately upon the injection of the molten polymer, but the cooling time is referred to as the time from the solidification of the gate, when the holding step is finished, to the ejection of the part, when it has reached a temperature low enough to withstand the forces during ejection.

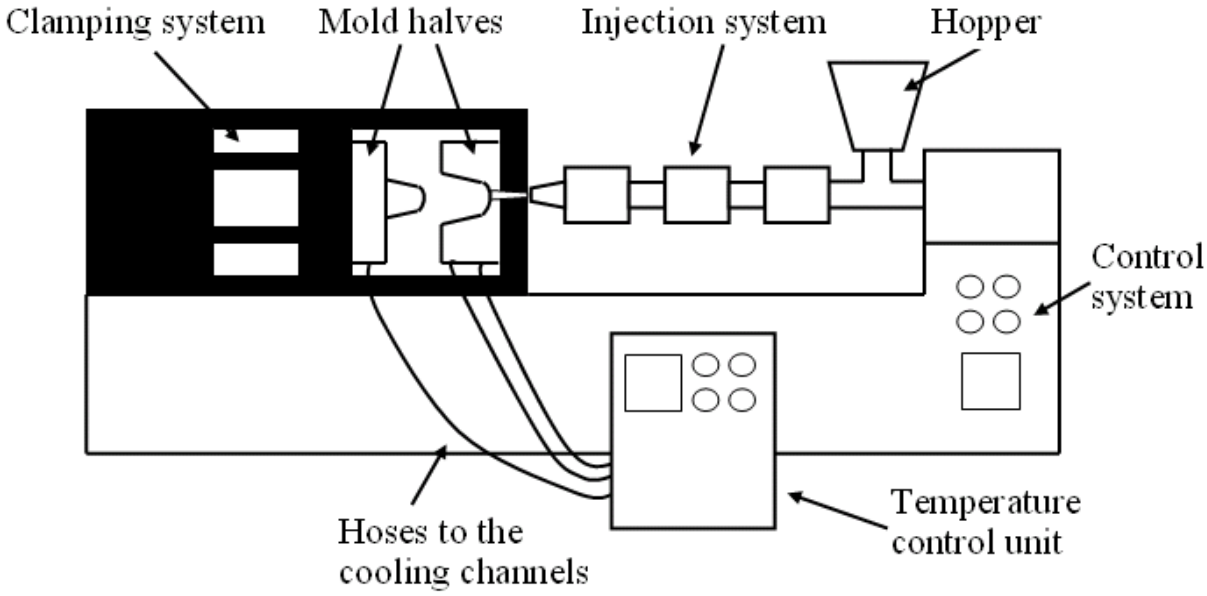

Figure 9. Schematic figure of the injection molding machine, the heat exchange system and the mold.

A classical example of a geometry for which it is hard to remove the heat effectively is the slender core. Insufficient cooling in the core will result in far too long cooling times and part distortions in form of sink marks and excessive warpage. Several options for conventional cooling of these kinds of cores are available, see Figure 10. Inserts made of high-conductivity materials such as beryllium-copper, improves the heat transfer. These inserts are usually press-fitted into the core and the cooling is improved by extending their base into a cooling channel (Figure 10a). A simple way of separating the inlet and outlet holes of a core hole is to use a baffle (Figure 10b). This method provides maximum cross-section for the coolant but it is hard to mount the divider plate exactly in the middle of the hole. Another drawback with this method is that the cooling effect for the two sides will differ due to the gradual heating of the coolant in the cooling channel. Alternative designs are baffles where the metal sheet forming the baffle is twist. Hence the more uniform temperature distribution is achieved. Another effective way of cooling the core is to use a bubbler (Figure 10c). An inlet tube conveys the coolant into the core hole and by choosing the relative diameter of the tube as half of the diameter of core hole, the flow resistance is kept equal in the both cross-sections. For cores with larger diameters (≥40 mm), helical cooling channels can be used (Figure 10d). The coolant passes a central hole and is led through a spiral to its circumference and between the core and insert helically to the outlet. By milling sections in the core which follow the geometry and increase the surface area, shorter cooling time and better dimensional accuracy

can be achieved. After the milling, the sections are joined together by high-temperature soldering under vacuum. [6]

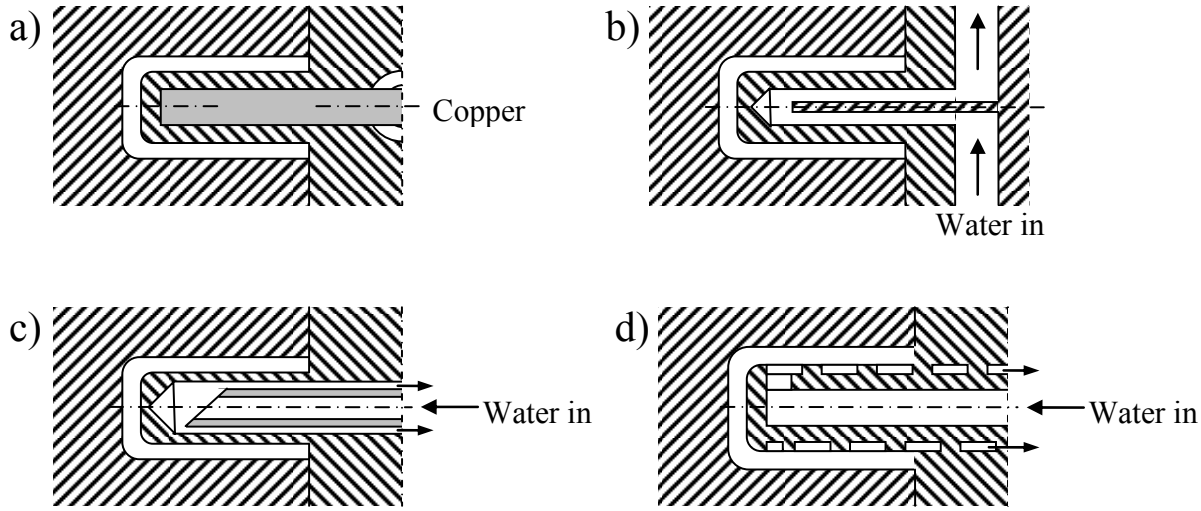

Figure 10. Different options of conventional core-cooling layouts.

2.2 Shrinkage and warpage

The ambitions for plastic manufacturers are to deliver parts at low costs, with a short delivery time, and with required quality. The quality can be defined differently depending on the usage of the product, but one important issue for the manufacturers today is the warpage of the final plastic products since they are often parts of a system assembled together. The warpage can be defined as the difference between the geometry of the CAD model created for manufacture of the mold and the dimensions of the molded part and the warpage are effects of variations in shrinkage. The shrinkage can be characterized by two broad classifications: volumetric and linearized. The volumetric shrinkage is the result of thermal contraction, which occurs in all polymers, and of crystallization which occurs in semi-crystalline polymers [5]. The following sub-chapters will discuss these effects and the warpage effect.

2.2.1 Volumetric shrinkage

All polymers exhibit shrinkage when cooled from the melting temperature to the solid state. The two classes of thermoplastics, amorphous and semi-crystalline, show a linear dependency of the specific volume on the temperature in the melted state. In the solid state, the specific volume of the semi-crystalline polymers decreases exponentially whereas the amorphous polymer keeps a linear dependency, although with a different slope. This can be visualized by the pvT diagram, see Figure 11, where the specific volume is plotted as a function of the temperature for different pressures.

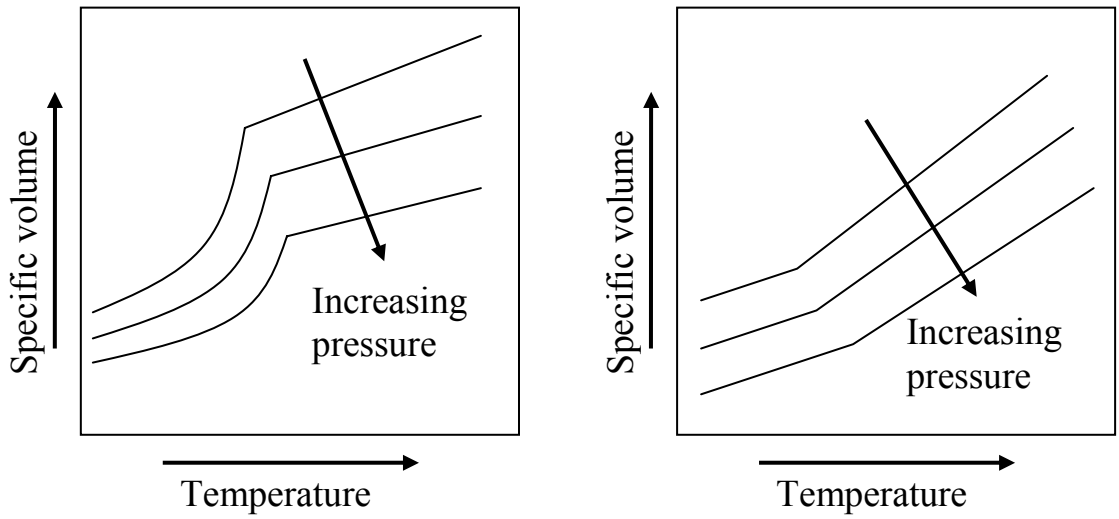

Figure 11. Example of pvT-diagram for semi-crystalline polymers (left) and amorphous polymers (right). The specific volume is plotted as a function of the temperature and for different pressures.

When an amorphous polymer is heated, it moves from a glassy state, where the molecules are frozen in crumpled formations, to a liquid state where segments of the molecules change places by thermally activated jumps. The transition between these two states is called the glass transition temperature, often abbreviated as T_g. The thermal expansion during the glassy state is due to the increasing separation between the crumpled, but still immobile, molecules. When reaching T_g, the mixture of increasing separation between the molecules and position changes by discrete jumps yields a smooth transition. Beyond T_g, the increase of the thermal expansion coefficient is due to the thermally activated jumps by the molecule segments. [2]

When cooling a semi-crystalline polymer below the melting temperature, crystallization is initiated at so called nuclei in the amorphous melt, on different locations. The crystallization proceeds by the growth of a spherulite around the nuclei and these spherulites are the result of the growth of many crystals which it comprises. More segments of the polymer chains disentangle from the melt and connect with the crystals until the spherulite impinges on its neighbors. During this process, some amorphous polymer is getting trapped between the crystals. Semi-crystalline grades suitable for injection molding often have a T_g below room temperature which implies that they exhibit toughness, as a result of the partial mobility of the amorphous parts, and strength, as a results of the crystalline portions. Crystals formed from the same polymer are rarely crystallized so that all the crystals are of precise equal thickness. Due to this variation, a melting range is observed instead of a melting temperature which a perfect crystalline material would exhibit. [2]

The pvT behavior is an important key to produce parts with low shrinkage. The injection molding process can be depicted as in Figure 12. The cavity is filled during an increased pressure (1→2) and at about the same temperature, the compression phase is started (2→3). The polymer is steadily cooled down while the holding pressure (3→4) partly compensates the volumetric shrinkage. When the gate is frozen (point 4), an isochoric pressure drop takes place until normal pressure is reached (point 5). This point establishes the volumetric shrinkage and the volume of the plastic part is the same as the volume of the cavity. The isobaric cooling stage takes place and at point 6, the part is ejected and the constraints from the surrounding mold are no longer there. At point 7, the part has reached a thermal equilibrium.

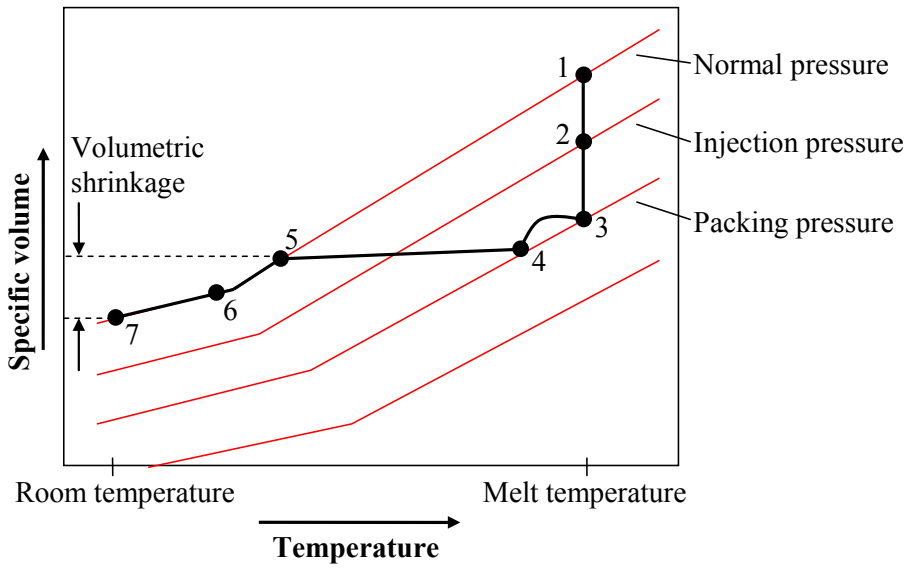

Figure 12. The different steps in injection molding depicted in the pvT diagram.

2.2.2 Linearized shrinkage

The linearized shrinkage is developed as the melt flows in the cavity. These flow-induced effects can be attributed to shear forces and extensional forces induced to the polymer during filling and packing.

The filling stage is characterized by a so-called fountain flow, see Figure 13. A shear field is developed due to the variations in the velocity field and the shear field makes the molecules oriented in the direction of the main strain direction. If there is time, and if the polymer would be kept in its molten state, this orientation is recovered. When the melt closest to the mold solidifies, the molecules keep their orientation in the flow direction as well as their molecular elongation. Hence this layer has a tendency to shrink in the direction of orientation. The molecules in the centre of the melt on the other hand, are insulated from the cold metal which allows them to relax from their stretched orientation. In this way, they will have more time to recover from the oriented state. They will therefore have less frozen in orientation and will also have less tendency to shrink relative to flow direction. This gradient of oriented molecules causes the skin to be in compression while the core is in tension and consequently a warpage effect arises. The variations of the cooling rate, the direction and the velocity of flow, part thicknesses, etc., over the part geometry make this shrinkage effect complex. The balance of the strains and their directions results in so called “residual stress” which in its turn can contribute to warpage.

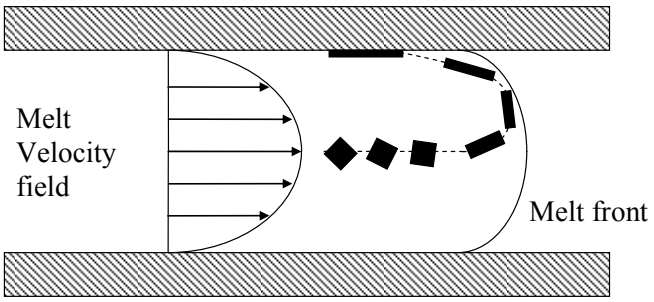

Figure 13. The fountain flow near the melt front. The deformation and orientation of a material element is depicted as it gets closer to the melt front.

As discussed above, the flow is almost linear in a long narrow part causing only shear forces but when diverging and converging flows are introduced, other components of strains are also present in the flow field. A typical example is the flow in a centered-gated disk where the flow expands outwards as it fills the cavity but at the same time, the flow also has a component in the perpendicular direction of the flow. This is referred to as extensional flow. In contrast to the shear-dominant flow, the outermost layer, the one closest to the mold, exhibits a random orientation of the molecules since the flow is not subjected to any shear forces. The next layer is subjected to high shear forces and will therefore have an orientation in the radial direction whereas the next layer is subjected to both shear and extensional flow effects and will show a random orientation. In the innermost layer, the shear forces are almost zero and the molecules will be subjected to high extensional forces and will be oriented in the perpendicular direction of the flow. The variations of the thicknesses of these layers as well as their magnitudes will affect the part differently and this is also a contributor to the residual stress.

Another important factor affecting the shrinkage is fibers. These fibers are used in the material in order to reinforce the part and like the molecules in the polymer, the fibers are oriented in the direction of the flow. The shrinkage in the direction of the fibers are counteracted since these fibers are very stiff and instead a fiber-reinforced polymer has a substantial shrinkage in the cross-flow direction. As before, the orientation of these fibers is varied in reference to flow direction, part thickness, and other process variations. Hence, it is a complex but important contributor to part stiffness and residual stresses.

2.2.3 Warpage and residual stress

Warpage occurs when the imbalance of the shrinkage exceeds the mechanical strength of the part. If the shrinkage is anisotropic, which is the case of all injection-molded parts, but too weak to overcome the structural strength, the result is residual stresses. These stresses can contribute to the premature failure of the part or they can relax over a period of time.

The volumetric and linearized shrinkages are dependent on many different process settings, where thermal distributions through the part thickness and over part areas are some of the most important. The previous sub-chapter discussed the main effects on the built-in stress due to volumetric and linearized shrinkages. The effect of theses shrinkages when the temperature distribution is imbalanced can be traced to two different sources: different temperature distributions through the part thickness and different temperature distributions over part areas.

Temperature gradients through the part thickness originate from different cooling rates for the opposing surfaces. The difference leads to a thicker frozen layer on the colder side at a higher pressure which results in a net bending moment towards the side with lower cooling rate, that is, the hotter side. Another example is the warpage of corners, see Figure 14. The inside corner is hard to cool, and, due to the local increase of thickness in the sharp corner, greater thickness shrinkage can be observed than for the rest of the part. Thus, a smaller angle is the result. This shrinkage can be decreased by changing the sharp corner to a radius.

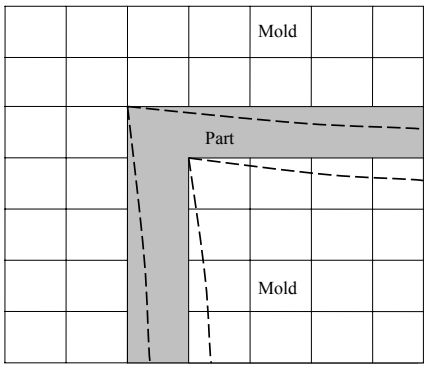

Figure 14. Poor cooling on the inside of a corner. Part geometry due to warpage is shown with dashed line.

Different area shrinkage refers to differences in thicknesses, in packing pressure or in mold wall temperatures. Thinner regions solidify more rapidly than thicker regions, if the cooling rate is constant. The frozen layer will represent a greater percentage of the thickness in the thin section than in the thick section. Consequently the thinner regions will solidify first at a higher pressure which results in lower shrinkage. Different mold wall temperatures will give the same effect: cooler areas will extract heat from the hotter areas, and they will solidify first at a higher pressure causing a lower shrinkage than for the hotter area.

Moreover, warpage is affected by variations in the process settings, that is, other variations than changing the material and the mold design. The main relationship between the different molding parameters and the shrinkage is depicted in Figure 15.

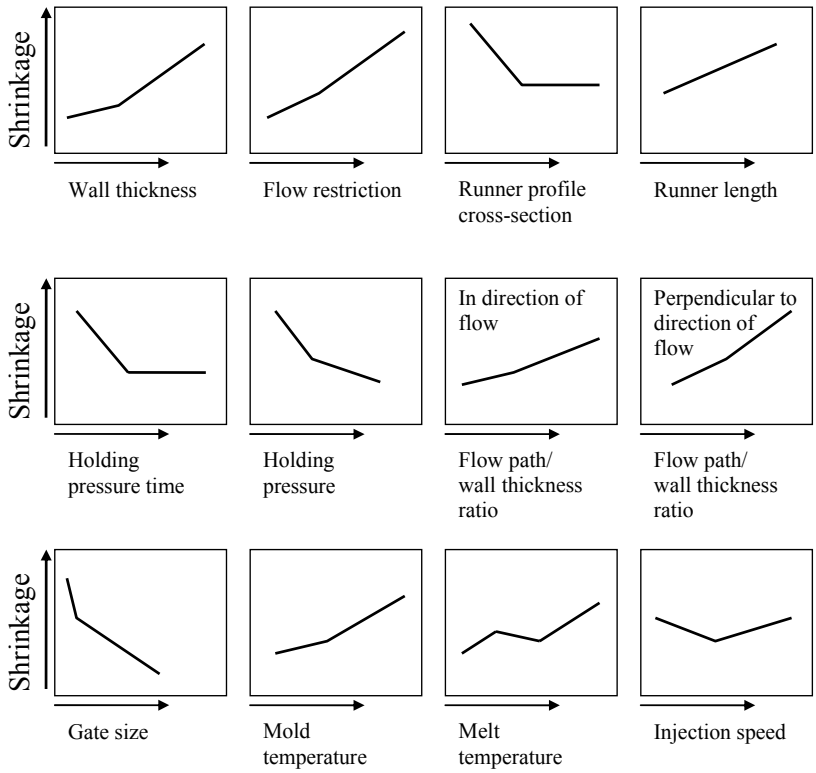

Figure 15. Relation between shrinkage and injection molding parameters. [7]

3 Analysis

One disadvantage with injection molding is that the mold tends to be very expensive and modifications of the mold and the design of the part that are to be produced is common and cost-consuming. Computer-Aided Engineering (CAE) is an essential tool for numerical simulation of the injection molding process. Its proper use will minimize the amount of redesign and retooling. By using numerical techniques, the process is simulated in a computational environment and mold alterations and process settings can be tested again and again before the actual production of the tool. Studies have shown that costs up to 50% can be cut for mold modifications and up to 15% for cycle time when using numerical process simulation [6].

Injection molding simulation has been a valuable tool for engineers since the introduction around 1975. The first commercial softwares could predict plastic flow in thin regions, based on 1D flow along lengths with various cross sections. In the eighties, so-called 2.5D flow analysis was developed where 2D flow analysis was applied to a 3D shell model. Later, shrinkage and warpage, fiber-filled materials were introduced and today, even if it is not used in this thesis, it is also possible to predict all the steps from flow to warpage in complicated 3D models where for example inertia and gravity effects are included.

Theoretically, the injection molding process is a three-dimensional, transient problem with a moving melt front, where coupled heat transfer and non-Newtonian fluid flow is present. Much effort has been put into the development of numerical simulations to model these physics. This chapter will describe the general idea of how numerical analysis can be carried out in order to simulate the different steps from the injection of the molten plastics to the ejection of the molded part.

3.1 Governing equations

3.1.1 Filling

The filling of a thin-walled thermoplastic part is a very complex process and in order to be able to analyze the process it can be simplified by a generalized Hele-Shaw (GHS) model with an incompressible, generalized, non-Newtonian fluid under non-isothermal conditions [8,9]. The GHS flow model refers to the flow between two plates close together, and hence the width of the gap is assumed to be much smaller than the other dimensions of the flow. This assumption yields that the flow at a given point is mostly influenced by the local geometry and therefore, the lubrication approximation can be applied, that is, the velocity in the gap-wise direction is neglected, and the pressure is a function of planar coordinates only.

The equations describing the Hele-Shaw polymer melt flow are:

Continuity equation:

$$\frac{\partial \rho}{\partial t} + \frac{\partial (\rho u)}{\partial x} + \frac{\partial (\rho v)}{\partial y} + \frac{\partial (\rho w)}{\partial z} = 0 \qquad (1)$$

Momentum equations:

$$\frac{\partial p}{\partial x} = \frac{\partial}{\partial z}\left(\eta \frac{\partial u}{\partial z} \right) \qquad (2)$$

$$\frac{\partial p}{\partial y} = \frac{\partial}{\partial z}\left(\eta \frac{\partial v}{\partial z}\right) \tag{3}$$

Energy equation:

$$\rho_p C_{pp}\left(\frac{\partial T}{\partial t} + u\frac{\partial T}{\partial x} + v\frac{\partial T}{\partial y}\right) = \eta\dot{\gamma}^2 + k_p \frac{\partial^2 T}{\partial z^2} \tag{4}$$

where (x, y, z) are the Cartesian coordinates, (u, v, w) - the velocity components, T - the temperature, p - the pressure, ρ_p - the density of the polymer, C_{pp} - the specific heat of the polymer, k_p - the thermal conductivity of the polymer, η - the viscosity, and $\dot{\gamma}$ is the shear rate. The thickness direction is represented by the z-coordinate and no flow will take place in the z-direction. The magnitude of the shear rate is governed by:

$$\dot{\gamma} = \sqrt{\left(\frac{\partial u}{\partial z}\right)^2 + \left(\frac{\partial v}{\partial z}\right)^2} \tag{5}$$

The model equations are based upon the following approximations: (i) the flow is inelastic, (ii) the fountain flow phenomena, the inertial forces and the body forces are disregarded, (iii) normal stresses are disregarded, (iv) thermal convection in the gap-wise direction and conduction in the flow direction are disregarded, (v) the conductivity and heat capacity are constant. The boundary and initial conditions are:

$$u = v = 0, \quad T = T_w \text{ at } z = h \tag{6}$$

$$\frac{\partial u}{\partial z} = \frac{\partial v}{\partial z} = \frac{\partial T}{\partial z} = 0 \text{ at } z = 0 \tag{7}$$

$$p = 0 \quad \text{along the flow front} \tag{8}$$

where T_w is a constant wall temperature, and $2h$ is the gap of the cavity (Figure 16).

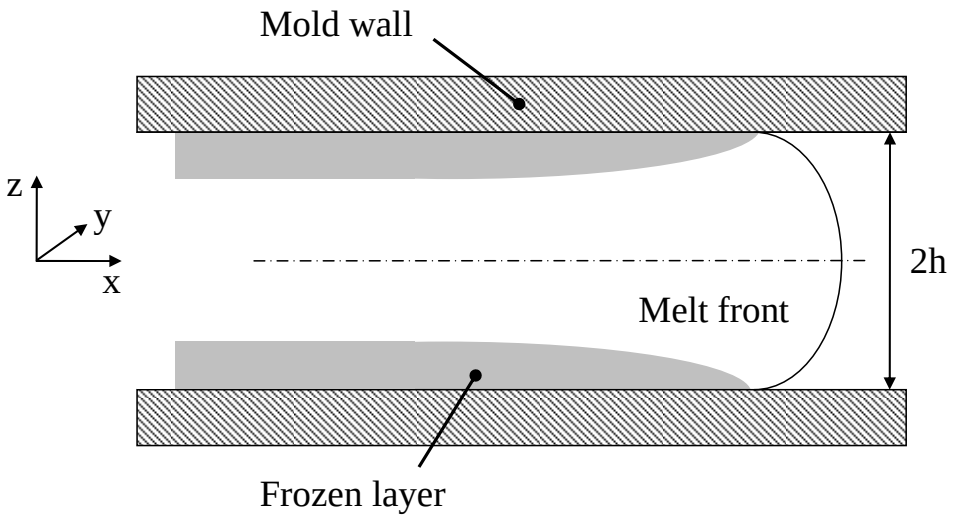

Figure 16. Cross-sectional view of the flow front.

Integration of Eq.2 and Eq.3 making use of Eq.8 results in:

$$\eta \frac{\partial u}{\partial z} = \frac{\partial p}{\partial x} z$$
$$\eta \frac{\partial v}{\partial z} = \frac{\partial p}{\partial y} z \tag{9}$$

Integrating once more together with Eq.6 results in:

$$u = -\frac{\partial p}{\partial x} \int_z^h \frac{z dz}{\eta} \tag{10}$$

$$v = -\frac{\partial p}{\partial y} \int_z^h \frac{z dz}{\eta} \tag{11}$$

Combining Eq.5 with Eq.10 and Eq.11 yields:

$$\dot{\gamma} = \frac{z}{\eta} \sqrt{\left(\frac{\partial p}{\partial x}\right)^2 + \left(\frac{\partial p}{\partial y}\right)^2} \tag{12}$$

Further, the gap-wise averaged velocities are obtained by integration of Eq.10 and Eq.11:

$$\bar{u} = \frac{-(\partial p/\partial x)}{h} S \tag{13}$$

$$\bar{v} = \frac{-(\partial p/\partial y)}{h} S \tag{14}$$

where S is called the flow conductance:

$$S = \int_0^h \frac{z^2}{\eta} dz \tag{15}$$

Substituting Eq.13 and Eq.14 into Eq.1 gives:

$$\frac{\partial}{\partial x}\left(S \frac{\partial p}{\partial x}\right) + \frac{\partial}{\partial y}\left(S \frac{\partial p}{\partial y}\right) = 0 \tag{16}$$

The viscosity can be described with different material models, and Figure 17 plots the viscosity according to three commonly used constitutive models: the Newtonian model (Eq.17), the power law model (Eq.18), and the Cross model (Eq.19).

$$\eta = \eta_0 \tag{17}$$

$$\eta = K \dot{\gamma}^{n-1} \tag{18}$$

$$\eta = \eta_\infty + \frac{\eta_0 - \eta_\infty}{1 + (C\dot{\gamma})^m} \tag{19}$$

where η_0 is the zero shear viscosity, K is the consistency coefficient, n is called the Power law index, η_∞ is the infinite shear viscosity, m is a parameter called the Cross rate constant/consistency constant, and C is a constant related to the material.

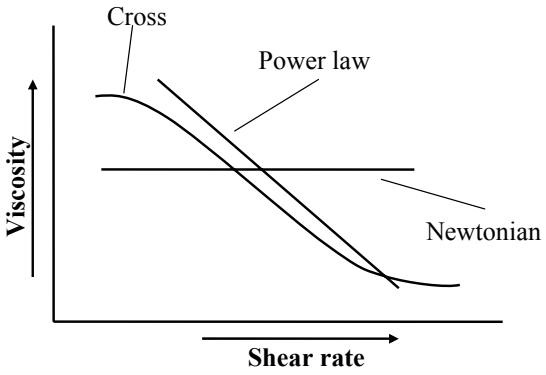

Figure 17. The viscosity as a function of the shear rate for three different material models.

3.1.2 Packing

In the packing phase, the mold is filled up by polymer melt. More melt is forced into the mold in order to compensate for the volumetric shrinkage and therefore, a compressible formulation is required to model this behavior. The governing equations for this phase are the same as for the filling phase and consideration is taken to the compressibility of the melt by using a dependency of the specific volume on pressure and temperature. This is called the pvT-relationship which can be modeled with different complexities. Commonly used models for the processing of polymers are the Spencer-Gilmore model, which is derived from the ideal gas law by adding a pressure and temperature correction term to the specific volume, and the Tait model [10]. For the simulations in this thesis, a modified Tait model with 13 parameters (Eq.20-26) is used. This model can predict the abrupt volumetric change for semi-crystalline polymers and it is also suitable for amorphous polymers. Figure 18 shows an example of the dependency of the specific volume on pressure and temperature for a semi-crystalline polymer.

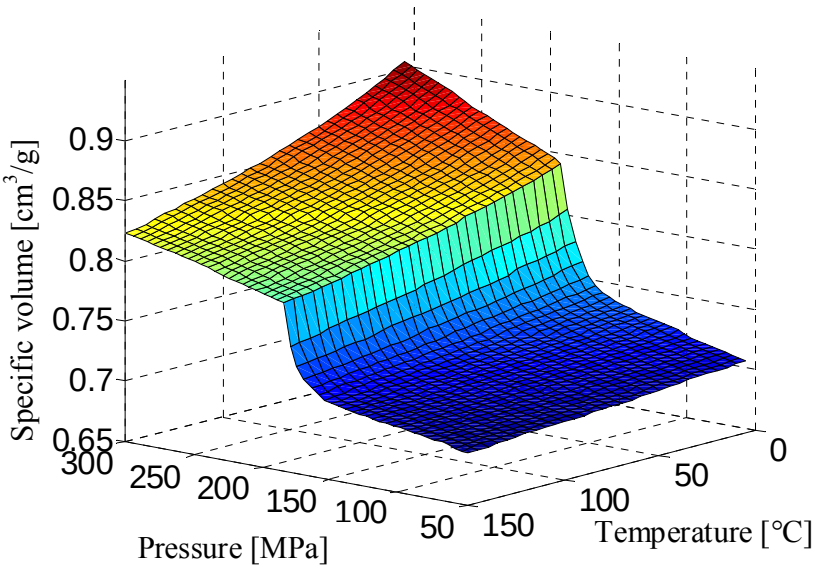

Figure 18. Example of the specific volume as a function of pressure and temperature for a semi-crystalline polymer.

$$\hat{V} = \hat{V}_0\left[1 - C\ln(1 + p/B)\right] + \hat{V}_t \tag{20}$$

$$\hat{V}_0 = \begin{cases} b_{1S} + b_{2S}\overline{T}\,, T \le T_t \text{ (solid state)} \\ b_{1L} + b_{2L}\overline{T}\,, T > T_t \text{ (melt state)} \end{cases} \tag{21}$$

$$B = \begin{cases} b_{3s}\exp(-b_{4S}\overline{T})\,, T \le T_t \text{ (solid state)} \\ b_{3L}\exp(-b_{4L}\overline{T})\,, T > T_t \text{ (melt state)} \end{cases} \tag{22}$$

$$\hat{V}_t = \begin{cases} b_7\exp(b_8\overline{T} - b_9 p)\,, T \le T_t \text{ (solid state)} \\ 0 \qquad\qquad\qquad\quad , T > T_t \text{ (melt state)} \end{cases} \tag{23}$$

$$\overline{T} = T - b_5 \tag{24}$$

$$T_t = b_5 + b_6 p \tag{25}$$

$$C = 0.0894 \tag{26}$$

where $\hat{V}$ is the specific volume, C is a universal constant [11], $b_{1\text{-}9}$ are material specific parameters, and where T_t is equal to the transition temperature.

The crystallization kinetics has an important effect on the shrinkage and warpage of the final part. Crystallization affects the volume and density, specific heat, conductivity, elastic modulus, etc. The model for crystallization is usually expressed as the rate of crystallization as a function of other terms such as crystallization rate, temperature, crystallinity, cooling rate etc. The behavior of polymer crystallization can be modeled with Malkin's kinetics model [12].

3.1.3 Cooling

The objective of the mold-cooling analysis is to solve the temperature profile at the cavity surface using boundary conditions of polymer melt during filling and packing analysis. When the injection molding process is in steady-state, the mold temperature will fluctuate periodically over time during the process due to the interaction between the hot melt and the cold mold, see Figure 19. In order to reduce the computation time for this transient process, a cycle averaged temperature, $\overline{T}$, that is invariant with time, is introduced for the mold but the transient state is still considered for the polymer [13].

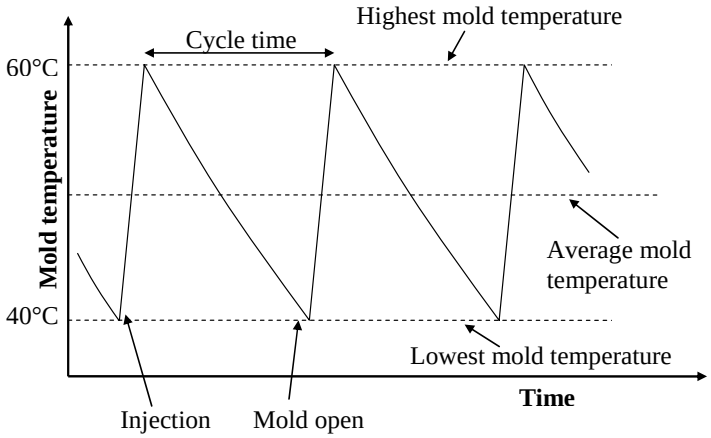

Figure 19. Typical mold temperature variations.

The overall heat conduction phenomenon is governed by the Fourier equation:

$$\rho_m C_{pm} \frac{\partial T}{\partial t} = k_m \left(\frac{\partial^2 \overline{T}}{\partial x^2} + \frac{\partial^2 \overline{T}}{\partial y^2} + \frac{\partial^2 \overline{T}}{\partial z^2} \right) \tag{27}$$

where ρ_m is the density of the mold, C_{pm} is the specific heat of the mold and k_m is the thermal conductivity of the mold. The cooling phase of the process is described by solving a steady-state Laplace equation for the cycle-averaged temperature distribution throughout the mold:

$$k_m \left(\frac{\partial^2 \overline{T}}{\partial x^2} + \frac{\partial^2 \overline{T}}{\partial y^2} + \frac{\partial^2 \overline{T}}{\partial z^2} \right) = 0 \tag{28}$$

where $\overline{T}$ is the cycle-average temperature of the mold. Eq.28 together with a simplified version of Eq.27, where only the gap-wise coordinate is considered, are both used to predict the mold and part temperature during cooling.

3.1.4 Shrinkage and warpage

The constitutive model used for warpage calculations should take both the flow- and temperature-induced residual stresses into account as well as the thermodynamic process when the part is cooled down outside the mold. An orthotropic, linear, thermal, elastic material that obeys the Duhamel-Neumann constitutive law [14] can be used for this purpose. The flow- and thermal induced residual stresses are then used as initial conditions for a solid mechanical analysis where the displacements of the nodes are calculated and, thereafter the shrinkage and warpage of the part are obtained.

3.2 Numerical solution using Moldex3D

This sub-chapter will describe how the software Moldex3D solves the equations described in chapter 3.1.1-3.1.4. The main steps to carry out an analysis in the software are described in Figure 20. The following sub-chapters are mainly influenced by the work of Tucker III et.al [9] and Chang et.al.[15,16]. To conclude, the temperature, pressure, velocity fields, etc. are obtained for each point in the cavity by using a hybrid finite element/finite difference method in order to simulate the injection molding filling, packing and cooling processes. A control volume method is applied to find the melt front position and also to calculate the temperature and pressure profile at any instant during the filling process. The boundary element and finite difference method are applied to carry out the mold cooling analysis where the temperature of the cavity surface is obtained and these are then used as boundary conditions for the filling and packing analysis. The flow- and thermal-induced stresses are then used as initial conditions for the solid mechanics analysis using a linear thermo-viscoelastic model. The final displacements, both in-plane and in thickness direction, are then solved using a three-dimensional finite element method.

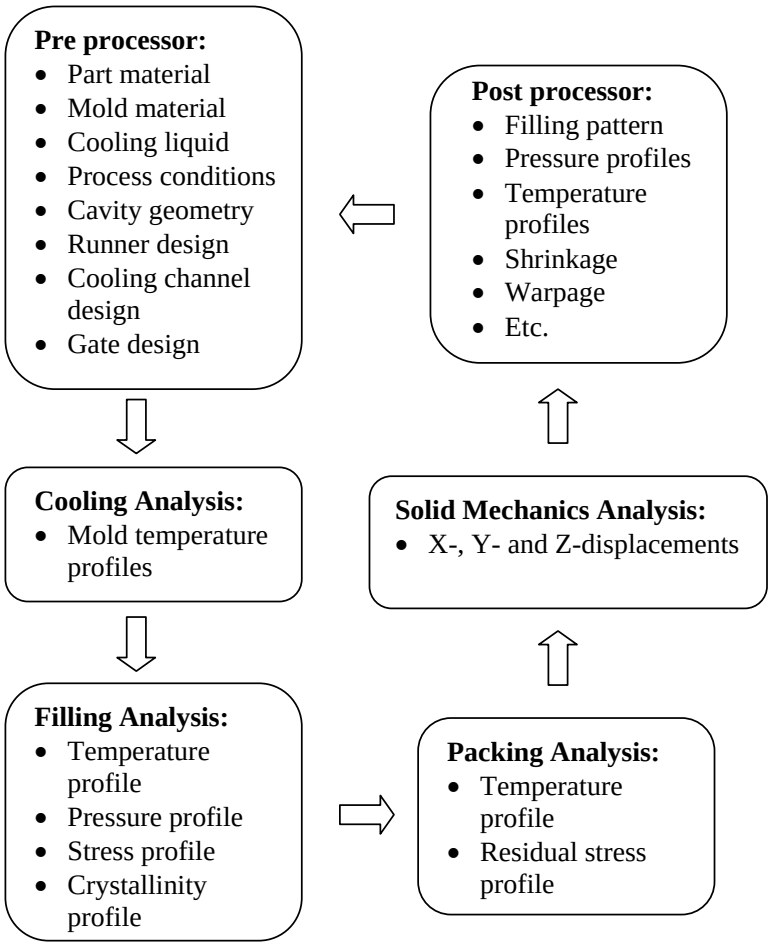

Figure 20. The steps to carry out an analysis.

3.2.1 Flow field

The flow field of each element in the part is treated as simple shear flow at each time step and the principle flow direction is based on the centeroid of each element. A combination of the control volume finite element method and finite-difference approach is employed to solve the governing equations. As shown in Figure 21, the nodal value of any variable at each center point represents the value over the entire control volume and by using the conservation principle:

$$\begin{aligned} &\textit{Net flux of F into CV by convection} \\ &+ \textit{net flux of F into CV by diffusion} \\ &+ \textit{generation of F in the CV} \\ &= \textit{increase of F in CV} \end{aligned} \qquad (29)$$

where F is any scalar specific property related to fluid motion and CV is the control volume.

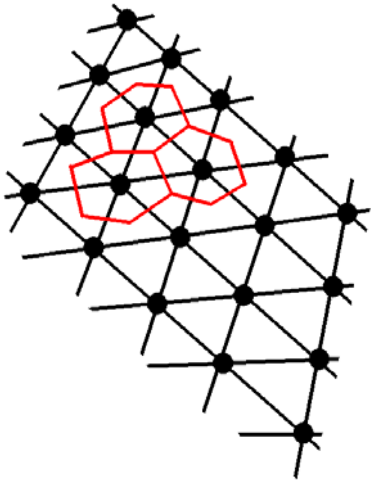

Figure 21. Nodes, triangular element,s and the associated polygonal control volume (in red).

The viscosity formulation used is the modified Cross model [17,18]:

$$\eta(T,\dot{\gamma}) = \frac{\eta_0(T)}{1+\left(\eta_0\dot{\gamma}/\tau^*\right)^{1-n}} \tag{30}$$

with

$$\eta_0(T) = Be^{T_b/T} \tag{31}$$

where n is the power law index, η_0 is the zero shear viscosity, τ^* is a parameter describing the transition region between zero shear rate and the power law region of the viscosity curve and B is a material specific parameter. Viscous flow is assumed during filling, i.e. no visco-elastic effects are considered, and the shear stress is calculated according to a non-Newtonian fluid:

$$\tau = \eta \cdot \dot{\gamma} \tag{32}$$

The governing equations in chapter 3.1.1 are solved in an iterative manner, where the finite element method is used in the planar direction, and where the finite difference method is used in the thickness direction and for the time steps. When both the pressures and temperatures have converged, the melt front advancement is obtained by the calculated flux at each front control volume and the flow front is updated until the cavity is filled with polymer melt.

3.2.2 Temperature field

The flow conductance S is temperature-dependent and hence, the temperature profile at each time step needs to be determined. The temperature profile is based on the center of each element, and it is obtained by solving the energy equation (Eq.4) where the convection term is expressed only in the principal flow direction. The energy equation is reformulated in finite differences where the temperature at the current time step is obtained in j number of layers in the element. By using an upwind procedure [9] to solve the equations, numerical stability is enhanced.

3.2.3 Thermally induced residual stress

As described in chapter 3.1.2, the compressibility of the polymer in the packing phase is taken into account by using the modified Tait equation to describe the pressure and temperature dependency of the specific volume (Eq.20-26).

The prediction of mold-wall temperatures on both the core and the cavity side during the process is based on the cycle-averaged principle where a steady state is assumed for the metal mold but a transient state for the polymer part. The simulations couple a three-dimensional boundary element method for the Laplace equation (Eq.28), used for obtaining the mold temperature, and a finite difference method for the Fourier equation (Eq.27), used for obtaining the polymer part. For Eq.27, only the gap-wise coordinate is considered yielding:

$$\rho C_p \frac{\partial T}{\partial t} = k \frac{\partial^2 T}{\partial \tilde{s}^2} \tag{33}$$

and

$$k_m \frac{\partial \overline{T}}{\partial n} = H^* \left(\overline{T}^* - T_a \right) \tag{34}$$

where $\overline{T}^*$ and T are the mold-wall temperature of the interface (involving mold surface, double side of cavity polymer, cooling channel surface) and the temperature of the polymer part, $\tilde{s}$ is the gap-wise coordinate of the polymer part, n is the outward normal direction of the interface. Eq.34 is a general form of boundary condition for the interface of metal/polymer, metal/cooling water and metal/air. H^* and T_a are the heat transfer coefficient of the interface and the ambient temperature of each interface (i.e. polymer melt, cooling water, or air temperature). The equations are solved in the following procedure:

(i) An initial estimation of the mold wall temperature $\overline{T}^*$ on both sides (cavity and core) of each element of the polymer part is made.
(ii) For Eq.33, a finite difference method is employed for each element and the time steps are increased until the average temperature for each element is below the ejection temperature, in other words, until the part is ejected. The cycle-averaged heat transfer coefficient of both sides of the mold can then be obtained.
(iii) A new mold-wall temperature distribution (cavity and core side of part) is obtained by coupling Eq.28 and Eq.34 and these equations are solved using the boundary element method.
(iv) Steps (ii) and (iii) are repeated until the mold-wall temperature profile of each element converges.

The coupling of the cooling analysis with packing phase is performed according to the following:

(i) The temperature profile of the part is assumed to be a uniform temperature, the same as the melt temperature.
(ii) During the cooling stage, the mold-wall temperature of the both sides of each element is subsequently obtained.
(iii) During the packing stage, the mold-wall temperatures from step (ii) are introduced and the temperature profile of the polymer part in each element and the pressure information of the packing phase are obtained. The temperature distribution of the polymer part at the end of filling is taken into step (ii) as a new cooling temperature.
(iv) Steps (ii) and (iii) are repeated until the temperature profile of the cavity surface reaches convergence.

3.2.4 Deformation field

The warpage analysis is separated into two processes. The first is the process where the part is subjected to in-mold constraints from end of packing to end of cooling. The second process is free deformation after the part is ejected. The part then cools down until it reaches thermal equilibrium with the surrounding air. The total warpage is the sum of these two processes. The molded part is assumed to be an orthotropic, linear, thermal, elastic material that obeys the Duhamel-Neumann constitutive law [14].The part deformation is assumed to be linear, elastic and static. $\boldsymbol{\sigma}$ is the stress tensor and **F** represents the body force and thermal loads in the equilibrium equation:

$$\nabla\boldsymbol{\sigma} + \mathbf{F} = 0 \tag{35}$$

and where the relation between the stress and strain is (assuming small deformations):

$$\boldsymbol{\sigma} = \mathbf{C}\left(\boldsymbol{\varepsilon} - \boldsymbol{\varepsilon}^{0} - \boldsymbol{\alpha}\Delta T\right) + \boldsymbol{\sigma}^{F} \tag{36}$$

$$\boldsymbol{\varepsilon} = \frac{1}{2}\left(\nabla\mathbf{u} + \nabla\mathbf{u}^{\mathrm{T}}\right) \tag{37}$$

where **C** is the forth-order constitutive stiffness tensor related to the elastic properties of the material, $\boldsymbol{\varepsilon}$ is the infinitesimal elastic strain tensor, $\boldsymbol{\varepsilon}^{\mathbf{0}}$ is the initial strain tensor due to volumetric shrinkage, $\boldsymbol{\alpha}$ is a tensor describing the linear thermal expansion, $\boldsymbol{\sigma}^{\mathrm{F}}$ is initial stress components induced by flow and **u** is the displacement vector. The data from the residual stress and temperature profile in the molded part serve as initial conditions for the Eq.35-37. The displacements of the nodes are obtained by a using a finite element method and finally, the displacements are used to calculate the shrinkage, warpage and sink marks of the part.

3.3 Literature survey

The shrinkage and warpage theory described in the previous subchapters is mainly influenced by textbooks in the area of injection molding but much research, which is not reported in these books, has been carried out in this area. This chapter will focus on literature discussing shrinkage and warpage related to injection molding.

Corner deformation is an important phenomenon to take in account when the warpage of e.g. a box-like product is evaluated. Figure 14 shows the result due to asymmetric cooling of a corner product but another important contributor to this phenomenon is the *spring forward effect*. This effect was first described for thin compression molding of sheet molding compounds (SMC). Due to long fiber length versus part thickness ratio, most fibers in SMC parts are oriented in the planar direction. The result is a higher thermal expansion coefficient in the thickness direction than compared with the in-plane direction and when the part cools down after polymer curing, the angle of a corner will decrease. Ammar et.al. [19] showed that the spring forward effect is generally the major source of corner deformation for injection-molded parts. They derived a spring forward indicator based on the shrinkage of a corner geometry where the in-plane shrinkage was assumed to be much lower than the shrinkage in the thickness direction due to geometry and friction between the polymer and mold wall which constrains the part during cooling and polymer solidification. Experiments using PP and variations in the mold temperature, packing pressure, and packing time, together with finite element analysis, showed that the thermal effect alone could not explain the angle deformation of the corner. As an example, predicted angle deformations due to asymmetric cooling using a viscoelastic model with isotropic expansion coefficients showed good correlation with measured variations of the angle deformation due to asymmetric cooling from the experiments. As the variations were accurately described, this was not the case for

the absolute value of the angel deformation and a difference of 3° compared with the experiments was shown and the conclusion was that this difference could be explained by the spring forward effect. The authors also used MOLDFLOW where only thermal effects could be modeled and the simulations confirmed the low influence of the asymmetric thermal effect in a corner on the warpage predictions.

Jansen et.al. [20] studied the effect of asymmetric cooling on the warpage of injection-molded products and especially, the effect of mold temperature difference and packing pressure on warpage for unfilled amorphous materials. They showed that the warpage increased linearly with applied temperature difference between the mold halves but more interesting, that a plate geometry curved towards the cold side of the mold when a high holding pressure was applied. At lower pressures, the plate curved towards the hot side which is generally known and accepted. Similarly, the study of a corner geometry with different radii showed that the angle deformation was dependent on the temperature difference as well as the packing pressure and an increased radius also implied an increased temperature sensitivity. They also compared the warpage predictions of the injection-molding software C-MOLD with their suggested model and the experiments and the model succeeded in predicting the direction of the warpage but the absolute values were only about half of the measured values. C-MOLD predicted that the warpage would always be directed towards the hotter side of the mold whereas the measurements showed that this was only the case for the lower packing pressures.

The influence of thermal parameters on the shrinkage and warpage has been discussed by many researches, and many of them conclude that warpage predictions are sensitive to small variations of these parameters. Denizart et.al. [21] reported a considerable effect on the warpage prediction of a polystyrene disc when changing the no-flow temperature by 10°. This variation was more important than anisotropic and heterogeneous values used in the three-dimensional thermo-elastic temperature-dependent model. Jansen et.al. [20] suggested that comparable effects are to be expected from variations in thermal conductivity.

Jansen et.al. [22] carried out another study where the effect of processing conditions on shrinkage for seven common thermoplastic polymers was investigated. The holding pressure was the key parameter, and the effect of melt temperature was slightly less important. The effects of injection speed and mold temperature on the warpage were smaller and differ for each material in the study. A thermo-elastic model was developed and their model accurately described the measured shrinkage for all experimental conditions for the amorphous materials. For semi-crystalline materials the correspondence was poor and shrinkages were overpredicted.

Cavity deformation is also a contributor to final part shape and size. Delauney et.al. [23] presented a method where local mold rigidities were determined based on the knowledge of cavity pressure history. The method together with experimental results showed that mold deformation analysis can improve the volumetric shrinkage estimation and they also showed that the mold deformation mainly influenced the cavity thickness during holding. Wu and Huang [24] estimated the cavity pressure, temperature distribution and clamping force by a mold-filling program and these were then applied as boundary conditions in a mold-deformation analysis. Molding experiments were carried out for a wedge-shaped part and the structural analysis was verified by strain gauge measurement on the mold. The measured warpage of the parts were smaller than the simulated warpage and the difference were considered to be due to cavity deformation. The study showed that the simulated cavity

deformation was close to this deviation and if this effect is taken into account, the simulation result was improved significantly.

The gradient of oriented molecules which cause the skin to be in compression while the core is in tension (ch. 2.2.2) is not always the case for injection-molded products. This type of stress profiles is observed in free-quenched products and the model describing this phenomenon is not sensitive to holding pressure settings. Sometimes the stress distribution is inverse, i.e. the skin is in tension and the core is in compression. Another model has been proposed where the stress distribution is dependent on the pressure. The idea is that layers frozen-in at elevated pressures will expand when released from the mold. Jansen et.al. [25] used a model where the free-quench model was assumed at low holding pressures and the pressure-induced model was assumed at high holding pressures. Measuring the residual stress is difficult and the authors used the principle of layer removal but instead of using mechanical milling, excimer laser milling was used. One of the big advantages using this method is that difficulties with excessive heating and stress relaxation during the milling are avoided.

Most of the pvT data are measured under rather slow cooling or heating rates, which is not the case for ordinary process conditions in polymer processing where high cooling rates are reached. This is a drawback with the Tait equation and will affect the prediction of the actual volumetric shrinkage and hence warpage. Chang et.al. [26] proposed a model where a new variable was introduced to the Tait model in order to include the cooling rate effect. The new variable was based on the dependence of the glass transition temperature on cooling rate and the study showed that the proposed model accurately represented volumetric behaviors of amorphous polymers. Chang and Hsieh [27] used this model and showed that for the cooling dynamics of a plastic lens, a better prediction of the volumetric shrinkage near the mold wall was achieved due to the formation of frozen layers which was taken into consideration in the cooling rate dependent Tait model.

4 Free-form fabrication

4.1 Background

Rapid Prototyping (RP) or Free-Form Fabrication (FFF) refers to a group of technologies which uses an additive approach when building physical models, tooling components or even production parts. The process is additive, that is, FFF joins liquid, powder, or sheets to form parts using plastics, metals, ceramics, cellulose or composites in contrast to CNC machines which subtract material in order to form a part. The models are based on the existence of a 3D computer model which can be obtained from computed-aided design data (CAD), computed tomography (CT) scans, magnetic resonance imaging (MRI) scans, or digitized data from 3D digitizing systems, see Figure 22. [28]

Figure 22. The figure shows a physical model of a knee, where the 3D computer model was obtained from a set of images acquired by a CT scan.

The objective is to streamline the product design process by reducing the time to market introduction, improve the product quality and reduce cost. By producing these "fit and feel" models, it also helps companies to reduce the likelihood of delivering the wrong product to the marketplace, since the models serve as excellent visualization tools to discuss design and function among the members in the product design team, but also to discuss with the customer or end user.

An FFF process starts by decomposing the 3D computer model into thin, parallel cross-sections, with a typical layer thickness of 0.05 to 0.3 mm. The part is then manufactured by building layer by layer, with each layer bonded together. Many variants of this process are available on the market today, but the first commercialized system for FFF was the Stereolithography (SLA) method from the company 3D Systems, and it was introduced to the market in 1987. This method uses a laser beam to solidify ultraviolet light-sensitive liquid polymer. Other competitive methods were established a few years later, like the Fused Deposition Method (FDM) from the company Stratasys where thermoplastic filaments are heated and extruded in order to produce parts layer by layer. Another pioneer in the area was the company Helisys which introduced a method called Laminated Object Manufacturing (LOM), where a digitally guided laser cuts sheet material of paper or plastic and then the

sheets are bonded together with heat-activated glue. Today, FFF has evolved into three market segments: Rapid Prototyping, Rapid Manufacturing (RM), and Rapid Tooling (RT). Rapid prototyping refers to the manufacturing of concept models or models for fit and functional testing, that is, the use that concurs to what RP was in its infancy. Thanks to the rapid development of materials and processes for FFF, many companies have utilized FFF as a method to produce finished manufactured parts, e.g. rapid manufacturing. The objective is to decrease the time to market introduction but some have also used RM to offer products uniquely manufactured for individual customers. Still, the production rate, available materials and accuracy limit the usage of RM. Nevertheless, RM is gaining more market shares, and some examples where RM is used are in the Formula One Grand Prix racing where panels, electrical boxes, and even sway bars in titanium are manufactured for the race cars. In recent years, several FFF methods where metal is used as a building material have appeared on the market. This has made it possible to manufacture tools for both low-volume and full-scale production and this market segment is called rapid tooling which is further described in the next chapter.

4.2 Rapid tooling

4.2.1 Direct and in-direct methods

The possibility of direct-metal rapid tooling from high quality steel is not commonly known in the injection molding industry today. Different RT technologies enable the production of inserts for injection molding tools, and a distinction between direct and in-direct RT is made where indirect methods usually involve more sequences than direct methods. Typically, an in-direct method uses a master pattern to produce a mold or die, while the direct methods build the actual tooling inserts directly in the prototyping machine. The different methods suitable for RT have been compared and discussed by Klocke [29], Karapatis [30], Radstock [31], Segal [32], Dormal [33], Kruth [34], and Wimpenny [35].

4.2.2 Improvement of the cooling efficiency

Sachs et. al. [36] showed that conformal cooling channels, that is, channels equidistant from the surface to be cooled, manufactured by the in-direct method Three-Dimensional Printing (3DP) improved the part quality and decreased the cycle time in comparison with traditionally manufactured cooling channels. No transient behavior was shown at the start of the molding whereas for the tool with straight channels, 10-15 cycles were needed in order to come to an equilibrium temperature. The conformal tool was also found to maintain a more uniform mold temperature during an individual molding cycle which in its turn improved the dimensional accuracy of the molded part. The DTM Rapid Steel process has also been proven to be suitable for conformal cooling channels but with limitations in terms of its ability to manufacture small features [37]. Rapid laminated tooling is also a viable method for conformal cooling and studies have shown a considerable reduction of cost and lead-times in the manufacturing process. At the same time, an improved part quality and reduced cycle time in comparison with conventional machined tool was reported [38]. A method which does not fall into to the category of additive processes is the Stratoconception process. It allows the manufacturing of aluminum or steel sheets for direct rapid tools. The cooling channels are manufactured by milling stratums which are then assembled using stiffeners and strengthening plugs to build a complete tool and the aim is to achieve a higher production rate but also to be able to control the temperature in the mold precisely during the cooling stage [39]. Donnchadha et. al. [40] showed a considerably reduced cost and lead-time for a core insert fabricated by Selective Laser Sintering (SLS), and also proposed a modular concept where parts of the tool are manufactured by traditional methods and inserts are manufactured

by SLS. This is done in order to ensure the viability of RT. High thermal conductivity is another way of cooling tools without having to manufacture complicated cooling channels. Direct Metal Deposition (DMD) is a method where a thin layer of tool steel is applied on a copper core to form a tool with high conductivity without sacrificing wear on the tool and the using the method reduces cycle times and improves part quality in terms of warpage [41]. Over et. al. [42] reported reduced lead-times up to 30% for the manufacturing of a complete tool when using Selective Laser Melting (SLM) as a manufacturing method for the tool insert. The Electron Beam Melting method differs from other direct-metal fabrication methods, since it makes use of a high energy electron beam, and Gibbons [43] showed that a significantly higher cooling efficiency was achieved resulting in reduced cooling times and a more homogenous temperature distribution in the mold.

As explained above, many processes have been proven suitable for RT, but few studies have been found where the direct-metal method EBM has been used to manufacture inserts for injection molding [43]. In Paper C, the aim was to investigate the advantages using inserts manufactured by EBM in comparison with conventional, machined inserts. A comparative study was carried out where the dimensional accuracy as a function of the cooling time was explored for the different layouts and the experimental results was compared with numerical results. In Paper D, the surface heat distribution of conventional and FFF inserts was investigated and the influence of the coolant temperature on the surface of the insert were studied.

5 Design of experiments

The first methods handling a systematic approach to the analysis of real data were proposed by Sir Ronald Fisher in the 1920s. He was an evolutionary biologist, geneticist, and statistician, and his work pioneered the principles of Design of Experiments (DOE). The methods were further developed by another statistician, Box [44], and later Taguchi [45,46] presented the planned experiments in a way more attractive to engineers, and since then, DOE is subject to an increased interest in manufacturing companies.

The basic idea of DOE is to perform well-planned experiments early in the product design process and by this increase the in-depth knowledge of the product, or process, to be developed. The aim can be to develop a product at the lowest cost level possible or to achieve the best possible product performance. Taguchi also introduced robustness, that is, insensitivity, against the environment. For many companies, this has been an important tool when developing manufacturing processes which are as insensitive as possible to so called noise factors. In other words, they minimize the effects of variations in the manufacturing process.

5.1 The design of experiment process

The basic procedure is to perform a series of well-planned experiments, according to a simulation plan which minimizes the numbers of experiments, with different settings of a set of variables, and then analyze the corresponding results to gain as much information as possible of how the changes in the variables affect the results of interest.

The procedure starts with the identification of a problem, and after that one must identify a suitable measurable response variable, or more than one, which can be continuous or discrete. The response is by definition a function of variables, or factors, and these factors can be selected by using for example Failure Mode and Effect Analysis (FMEA), or the Ishikawa diagram. The choice of levels for the factors is a crucial part of experimental design, and levels should be chosen so far away from each other that the scale is larger than the normal variation of the factor but not so far away that they become irrelevant. A general factorial design at two levels, i.e. a high (+) and a low level (-), is denoted 2^k where k is the number of factors and the required number of runs, or experiments, to carry out a general two-level experimental design will be 2^k. When k is getting bigger, the number of runs increases rapidly. The design space, that is, the set of all possible combinations of the factors, can be described by a design matrix where each row corresponds to one experiment and each column gives the settings of a factor. The design matrix contains nothing but ones, either with a plus sign or a minus sign. The signs give information whether or not the factor should be set on a low or high level in the experiment. With the information provided above, the response is measured, or calculated numerically if simulation is used for the experiments, with the levels for the factors in each run as described in the design matrix. Due to the general symmetry of the matrix, the effect or contrast, of each factor can be computed independently and the effect can be described as the average change in response when moving from the low to the high setting of the factor. For many applications, interaction effects can be found, that is, the response gained from changing one factor may be dependent on the level of another factor. For a 2^3 experimental design, 3 main effects can be calculated, one for each factor, but 3 two-factor interactions and 1 three-factor interaction can also be calculated. The possibility to calculate and analyze these interaction effects is one of the main advantages using DOE. It has been shown that the desired information often can be obtained by performing only a

fraction of the full design when more than a few factors are considered. This is known as fractional design. If assuming that high-order interactions are negligible, one or more factors can be assigned to the columns describing the high-order interaction effects and hence the numbers of experiments are reduced significantly.

The effects are then analyzed, for example by plotting the effects on a normal probability paper where a reference distribution is estimated from those effects that are assumed to be non-active. The effects that are larger than ±3 standard deviations are assumed to be significant, that is, they are more likely to have an influence on the response than the factors lying within ±3 standard deviations. From this, a predictive model of the response can be derived where the significant factors are used as variables and this model is then used in a residual analysis to verify the adequacy of the model against the observed values of the response. If the model assumption is correct, the model can be used to predict the response of the product or process when setting the factors at a specific level.

Another advantage using DOE is when a mathematical optimization is followed by the experimental design. Especially, when several variables and a computational expensive objective function are of interest it is wise to perform some kind of screening analysis before the optimization takes place. By identifying the most important variables before the optimization, the computer time can be reduced, since some of the less important variables can be discarded in the optimization. Within the area of optimization, the usual method to investigate the influence of the design variables on the objective function is to calculate gradients. This is done by altering the value of each design variable, one at a time, by a small finite step in the neighborhood of the nominal design. However, this only gives information about the sensitivity of the variables on the objective function around the present design point. The advantage of using DOE is that the experiments gives information about the sensitivity of the variables over the whole design space and possible interaction effects can also be identified.

5.2 Design of experiments in the injection molding process

The area of optimal injection molding control is an important area for research. DOE has been an important tool in these studies, for example when minimizing surface defects like shrinkage, sink mark, flash, diesel effect, etc. [47]. Another important quality criterion to take into account is the warpage of the finished molded part, especially if strict dimensional accuracy must be applied. The warpage is affected by many different process parameters and the most important parameters when using conventional design of the cooling system has been identified as packing pressure, mold and melt temperature, packing time, and to some extent, cooling time [48-51]. Studies not only considering simplified thin-walled parts but also a cellular phone cover showed that the packing pressure was the most important factor, and that interaction effects also were an important contributor to warpage [52]. Besides the process parameters, other factors contribute to the warpage, and Yen et. al. [53] successfully reduced the warpage by using the design of the gate and runner. Erzurumlu et. al. [54] used different rib design as factors in order to minimize the warpage. The use of Response Surface Methodology (RSM), that is, fitting a polynomial model to the experimental design, is also viable in order to minimize the warpage and Chiang et. al. [55] reported a 54% reduction of the warpage for a cellular phone cover when using mold temperature, packing time, packing pressure, and cooling time as factors.

The effects of different process parameters on the cycle time and the warpage are rather complicated, and it is often hard to balance the need for dimensional accuracy versus the cost-

consuming cooling time. Introducing new technologies like FFF makes these effects even harder to predict and until now, little effort has been put in order to investigate the settings of the process parameters in combination with FFF inserts. In Paper E, the effective factors to obtain dimensional accuracy of a test part were investigated using injection molding simulation and DOE. Two different cooling channel layouts were compared, a conventional cooling channel layout using straight holes and a baffle versus an FFF layout.

6 Optimization

When a new product is developed, quality, price, and time for market introduction are important factors determining whether or not the product will be successful. Simulation and optimization algorithms can be development tools that make the difference between success and failure. The progress in the efficiency versus the cost for the computers has been an important contributor to the growing interest for optimization within the engineering industry. Using simulation tools with which the physical behavior of a product is analyzed is indeed important when there are many different parameters influencing the behavior. However, it is hard to predict which parameter is the most important, and which value it should have in order to obtain the best result possible.

To use optimization methods in the product design process has several benefits. Before getting the answer to the question of how the product should be designed in order to improve a chosen characteristic, the engineer is forced to define the problem in a structured way like deciding which parameters should be used, how the design should be evaluated and what restrictions that should be used? Also, when the optimization has been carried out, information about the problem can be further analyzed by looking at the sensitivities and interval of the objective function, which gives the engineer a deeper understanding of the physical behavior of the product. Optimization is a mathematical approach to tackle a design problem and it can be defined as the act of obtaining the best result possible under certain circumstances. In other words, the aim is to maximize or minimize an objective function by altering a set of design variables without violating any given constraints. Today, optimization is widely used. In many different areas, a number of algorithms can be found, some have a true mathematical approach whereas some are mimicking different phenomena in nature. A good introduction to the area of engineering optimization is given by Arora [56].

6.1 Formulation of an optimization problem

An example of an optimization problem formulated in words is to minimize the weight of a beam subjected to a transversal load, by changing the cross-section of the beam without exceeding a certain stress limit. A standard formulation of an optimization problem is written as [56]:

$$\begin{aligned}
&\text{Find a vector} && \mathbf{x} = (x_1\ x_2\ \ldots\ x_n) && \\
&\text{which minimizes} && f(\mathbf{x}) && (38)\\
&\text{such that} && h_i(\mathbf{x}) = 0, \qquad i = 1, 2, \ldots I && (39)\\
& && g_j(\mathbf{x}) \le 0, \qquad j = 1, 2, \ldots J && (40)\\
& && x_k^l \le x_k \le x_k^u, \qquad k = 1, 2, \ldots n && (41)
\end{aligned}$$

where $\mathbf{x}$ is a vector of design variables which is bounded by side constraints x^l and x^u, $f(\mathbf{x})$ is the cost, or objective, function, and where $h(\mathbf{x})$ and $g(\mathbf{x})$ are the vectors describing the equality and inequality constraints respectively. This is called a constrained problem, but if no equality or inequality constraints exist, it is called an unconstrained problem.

6.1.1 Design variables

The design of a product can be changed by assigning different values to the so-called design variables. They should be independent of each other, and a given set of design variables gives

a certain point in the design space, that is, a design point. If proper design variables are not selected for a problem, the formulation will be incorrect or, maybe not even possible at all. In a first stage, it is wise to choose many design variables in order to have as many degrees of freedom as possible in the problem, even if it can be a disadvantage too, since the computational effort is increasing.

The design variables can be either continuous or discrete, and some typical design variables for a structural problem are dimensions like lengths, radii, thicknesses, material properties like Young's modulus and density. Not all optimization algorithms can handle discrete design variables. Nevertheless, many dimensions and properties are in fact discrete. For example, if Young's modulus is chosen as variable, one must see to that the optimized modulus is commercially available.

6.1.2 Constraints

A design point can either be feasible or infeasible. A feasible design meets all the requirements. One which fails to meet one or more of the requirements is called an infeasible design. The restrictions defined for a design are called constraints and they must also be influenced by one or more of the design variables. Some examples of constraints include: upper limit of the stress, a critical vibration frequency as well as upper and lower values for the design variables.

Figure 23 shows a typical design space with two variables and where three constraints are defined, the lower limit of x_1^l and the upper limit of x_2^u, which are called side constraints, and one inequality constraint $g_1(\mathbf{x})$.

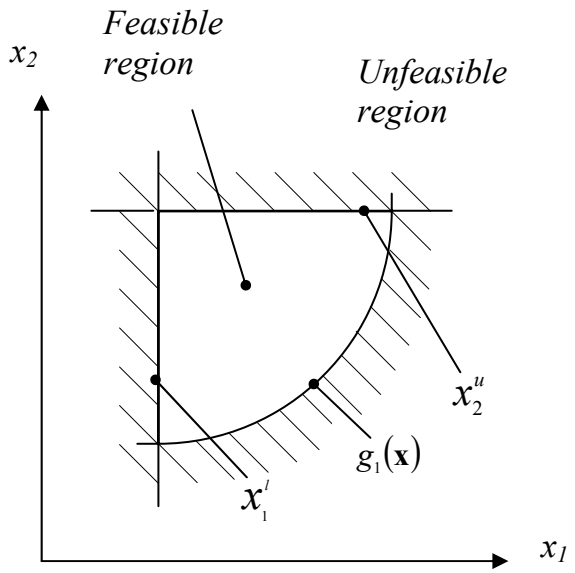

Figure 23. Constraint surfaces in a two-dimensional design space.

6.1.3 Objective function

In order to compare different designs, an objective function must be defined. This function must be dependent on the design variables. Otherwise it is not a meaningful objective function. This function can be either minimized or maximized. Some examples of objective

functions are the weight of a Formula One Grand Prix sway bar, which should be minimized, and the load capacity of a bearing, which should be maximized.

In Figure 24, an objective function is added to the design space, and it is plotted for constant values f_1, f_2, and f_3 where the objective function is descending as $f_1 > f_2 > f_3$. The optimal design is found at $\mathbf{x}=\mathbf{x}^*$.

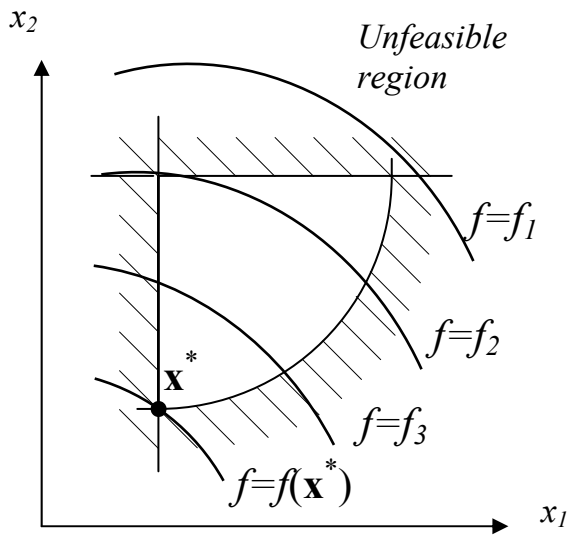

Figure 24. Contours of the objective function together with the constraint surfaces.

6.2 The solution process

Many methods with the purpose to find the optimum design have been developed over the years. So-called topology optimization uses the topology of the structure as design variables and by using this method, elements defining the structure are deleted or repositioned, and the optimized structure often appears as a framework. It could for example indicate where to put beam profiles in a vehicle in order to minimize the weight and to fulfill a certain stiffness criterion. Size optimization is another category of optimization methods. It is the most commonly used method in industry and in the literature. If this kind of method were used in the example above, the cross-section geometry of the beam profiles would be used as design variables.

The most common way to separate different optimization methods is to distinguish between optimality criteria methods (also known as indirect methods) and direct search methods. Optimality criteria methods are based on conditions that a function must satisfy at its optimum point, while the direct search methods are based on a chosen initial design and an iterative procedure is followed in order to find a better design.

6.2.1 Optimality criteria methods

For a general non-linear constrained optimization problem, the side constraints in Eq.41 are usually included in the inequality constraints in Eq.40. This constrained problem is usually transformed into an unconstrained problem by introducing a Lagrangian function, L, which is a scalar:

$$L(\mathbf{x},\mathbf{v},\mathbf{u}) = f(\mathbf{x}) + \mathbf{v}^T\mathbf{h}(\mathbf{x}) + \mathbf{u}^T\mathbf{g}(\mathbf{x}) \tag{42}$$

where v_j, j=1 to p, are Lagrange multipliers corresponding to the equality constraints, and u_i, i=1 to m, are Lagrange multipliers corresponding to the inequality constraints. In order to verify that an optimum design has been achieved, the candidate point must satisfy the Karush-Kuhn-Tucker (KKT) necessary conditions:

$$\frac{\partial L}{\partial x_j} = 0 \qquad j = 1 \text{ to } n \tag{43}$$

$$h_i(\mathbf{x}^*) = 0 \qquad i = 1 \text{ to } p \tag{44}$$

$$u_i^* g_i(\mathbf{x}^*) = 0 \qquad i = 1 \text{ to } m \tag{45}$$

$$g_i(\mathbf{x}^*) \le 0 \qquad i = 1 \text{ to } m \tag{46}$$

$$u_i^* \ge 0 \qquad i = 1 \text{ to } m \tag{47}$$

that is, for an optimum design point, Eq.43-45 must be equal to zero, the inequality constraint must be less than zero, and the Lagrange multipliers corresponding to the inequality constraints must be nonnegative [56].

6.2.2 Direct search methods

If the objective and constraint functions are non-linear and implicit, a numerical search algorithm must be used in order to find the optimum solution. Direct search methods are the most commonly used amongst these algorithms, and the basic procedure is that the design variables $\mathbf{x}_{(k)}$ are changed by increments to a better design $\mathbf{x}_{(k+1)}$ until the process has converged, see Eq.48. The last term in Eq.48 is referred to as the design change, and it consists of the step size $\alpha_{(k)}$ and the search direction vector $\mathbf{d}_{(k)}$.

$$\mathbf{x}_{(k+1)} = \mathbf{x}_{(k)} + \alpha_{(k)}\mathbf{d}_{(k)} \tag{48}$$

One way of deriving the search direction $\mathbf{d}_{(k)}$ is to use a generalization of Newton's method for unconstrained optimization, namely Sequential Quadratic Programming (SQP). The search direction is derived by solving a quadratic sub-problem approximation of the Lagrangian function where the constraints are linearized around the current design $\mathbf{x}_{(k)}$. SQP does not make use of the exact Hessian matrix $\mathbf{H}$ of the Lagrange function, but it is approximated for each iteration using the change in design and the gradients of the Lagrange function. This update is usually done by a modified Broyden-Fletcher-Goldfarb-Shanno (BFGS) procedure, although any quasi-Newton method can be used. The quadratic sub-problem can be solved using any Quadratic Programming (QP) algorithm, such as the Simplex method. [56]

After the search direction has been obtained, the step length $\alpha_{(k)}$ is determined by a line search procedure. This is carried out by a minimization of a one-dimensional descent function with α as the variable to be optimized. The descent function is defined by the objective function for unconstrained optimization, but if constraints exist, the descent function is defined by the

objective function and a penalty function. The penalty function is added in order to incorporate the influence of the constraints and when the constraints are getting violated, the value of the descent function is increased. [56]

Another viable method for solving non-linear problems is the Method of Moving Asymptotes (MMA) which was initially proposed by Svanberg [57]. This algorithm is based on a first-order Taylor expansion of the objective and constraint functions. With this method, the original implicit non-linear problem is approximated by an explicit convex sub-problem. This is done by linearizing the objective function in variables of type $1/(x_j - L_j)$ or $1/(U_j - x_j)$ dependent on the signs of the derivative of the objective function at the current iteration point. The values of the two parameters L_j and U_j are normally changed between the iterations. Hence, they are called Moving Asymptotes, and directions of how to set these parameters and some numerical tests can be found in [57]. One of the main advantages with MMA is its ability to converge to a solution which is fast and stable in comparison with other linear approximation methods.

The methods presented in this chapter have some weaknesses, and one of the most critical ones is that they can not distinguish between local and global optima, that is, the direct search methods can be trapped into a local minimum since they are based on the local information of the objective and constraint functions. Also, when using optimization in engineering design, numerical methods such as the Finite difference method must be used to calculate the gradients since the functions of interest often are both implicit and non-linear. This is time-consuming, and most of the computation time for these kinds of problems is devoted to function evaluations. One way to avoid the calculations of gradients and getting trapped in local minima is to use natural selection methods and this is further explained in the next section.

6.2.3 Natural optimization methods

Mathematically, a global optimum is defined as point $\mathbf{x}^g$ for which $f(\mathbf{x}^g) \leq f(\mathbf{x})$ for all feasible $\mathbf{x}$. An example of a function with several local optima is depicted in Figure 25.

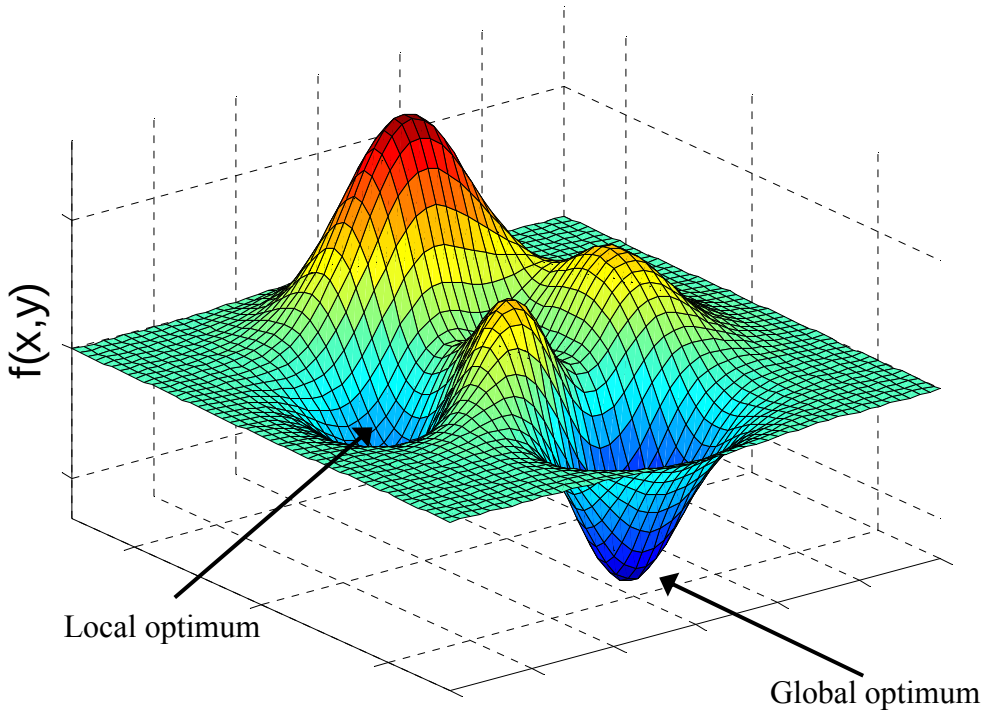

Figure 25. Two-dimensional function with both local and global optima.

As mentioned before, classical optimization methods are likely to get trapped in a local minimum depending on which initial design is chosen. Natural optimization methods, on the other hand, rely on the intelligent search of the whole design domain using statistical methods. Typically, a new design point is generated by applying operators to current points and statistically moving forward towards a better design point. As the name implies, the methods usually represent successful processes in nature. Since no gradients need to be calculated, they can easily handle discrete variables and non-continuous objective functions. One of the most commonly used methods is the Genetic Algorithm (GA) which was introduced by Holland in 1975 [58] and this method locates optima using processes similar to those in natural science and genetics. Other methods mimicking phenomena in nature are Particle Swarm Optimization (PSO), Ant Colony Optimization (ACO) and Simulated Annealing (SA).

SA was developed in the mid-eighties by Kirkpatrick et. al. [59], and it is an algorithm that is based on the simulation of finding the minimum energy state in the metal annealing process. The process starts with heating a substance above its melting point, and then it is gradually cooled downed to form a crystalline lattice. The atoms in the material have a high energy level when the temperature is high, but when the material is cooled down, the ability of the atoms to move is reduced. If the cooling rate is too high, defects in the crystalline lattice are formed by introducing amorphous parts and the energy state will be higher than for the optimal crystalline lattice. The optimum energy state can be seen as the optimum solution to the problem while the temperature decrease in analogy to a locally performed optimization.

The optimization is expressed by a sequence of iterations, and, in each iteration, the objective function is calculated by randomly modifying the design variables. If the value of the objective function is decreasing, the old variable set is replaced by a new one, but if the objective function is increasing, the new variable set can be either accepted or rejected. The acceptance of the new set is based on the value of the probability density function of the Bolzman distribution. This feature in SA gives it the possibility to climb out of local minima.

6.3 Optimization of the injection molding process

Optimization has been commonly used in studies concerning the injection molding process, since there are many variables to take into account when trying to achieve to best process, or product, possible. Pandelidis et. al. [60] used a combined method including both SA and a direct search method in order to minimize an indirect quality measure related to warpage and material degradation. The quality measure was a function of the temperature difference over the part at the end of filling, the percentage of overpacked elements, the percentage of overheated elements, and the maximum shear stress. The design variable was the position of the gate and the combined method was also compared using the direct search method and SA alone. In another study, Pandelidis et. al. [61] used the same quality measure to optimize fill time, mold, and melt temperature using a direct search method. Tang et. al. [62] used the cooling channel size, locations, and coolant flow rate as design variables when optimizing a function related to the average temperature of the part and the temperature gradients throughout the cavities in a multi-cavity mold. Another study considering the cooling of injection molds used the weighted sum of the temperature non-uniformity over the part surface and the cooling time using process parameters, coordinates and radii as design variables [63]. Qiao [64] presented a hybrid optimizer using a combined gradient-based and a stochastic optimization routine. In this work, the temperature distribution over the part surface for a rectangular plate was minimized using the location of the cooling channels as design variables. Li [65] proposed an approach where a plastic part was decomposed into simpler shapes, and the whole cooling system of the part was then developed based on the cooling systems obtained for the individual features.

Previous research in the area of optimization of the injection molding process, and specifically cooling time and warpage issues, has been focused on molds manufactured by traditional methods. No papers have been found where RT in combination with optimization has been used in order to optimize the injection molding process. Paper F describes how the warpage of a test part was minimized using the temperatures in the cavity and core, the melt temperature, and the cooling time as design variables. Two different cooling channel layouts were considered: one conventional using straight holes and a baffle, and one FFF design where the core cooling is conformal to the inner surface of the part. Also, three different optimization algorithms, SQP, MMA and SA, were used in order to investigate the efficiency of the different algorithms applied to this problem.

6.4 VerOpt – Versatile optimization

In Paper F, a Matlab-driven environment for applied optimization studies was used. This software was developed in order to serve the authors in Paper A as a tool for forthcoming optimization studies in different research areas, see Figure 26. The software is versatile in the sense that it is not restricted to injection molding optimization only. Several external solvers have been used such as Moldex3D and C-Mold (injection molding), Ansys (structural analysis), and Anybody (biomechanics). Currently four different optimization algorithms are implemented, SQP, MMA, SA, and GA. The procedure starts with defining the optimization

problem in the VerOpt software, as well as paths and names to input and output files for the external solver. After executing VerOpt, the optimization is conducted automatically: the external solver is started with the appropriate input file, after the analysis the results, that is, the objective and constraint functions, are read into VerOpt. The functions are analyzed in the chosen optimization algorithm which suggests a new design variable set, and the external solver starts again. This procedure is repeated until the user is satisfied with the solution or until a convergence criterion is reached.

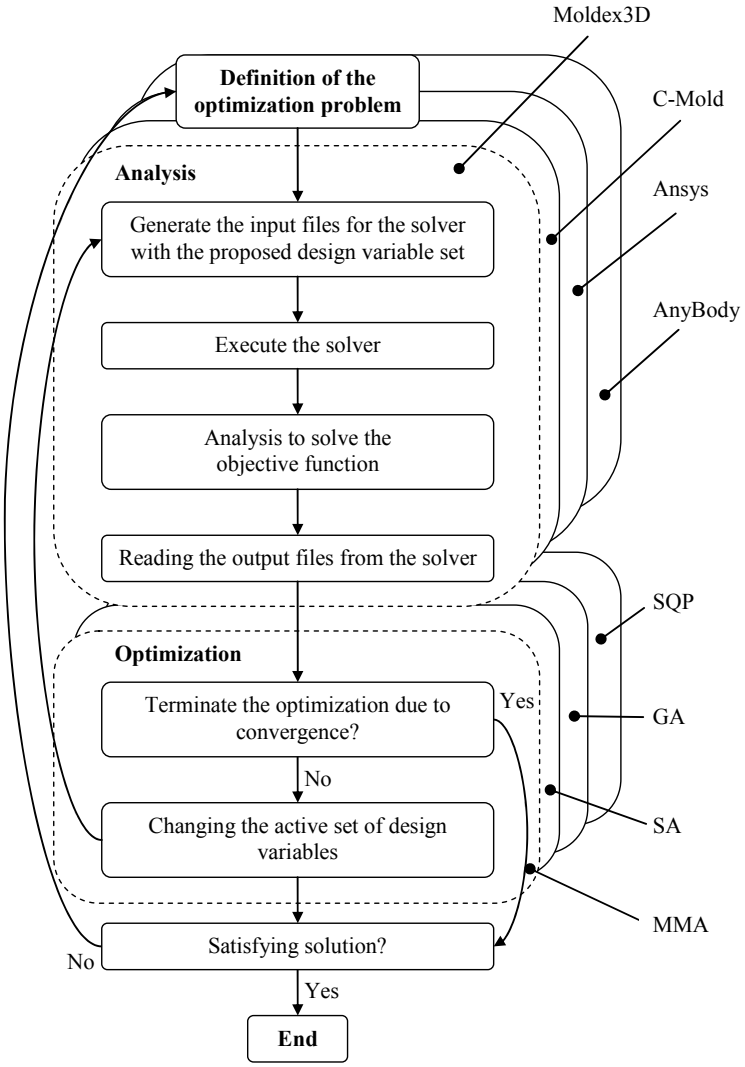

Figure 26. The VerOpt process.

VerOpt also enables the use of parallelization, but this has not been used in this thesis. Despite the rapid development of the computers efficiency and price, there is still and an increasing demand for shortening the lead-time of the product design process where simulation and optimization are important parts of the process.

The parallelization implementation is based on a TCP/IP toolbox developed for Matlab [66]. It is a client/server application where the client opens a connection through a TCP/IP network, to one or more computation servers. The connections are defined in Matlab, and with an open connection the client can request a function evaluation on a server. When the computation is

finished, the client receives the result. If there is an open connection to several servers, requests can be sent to each and every server, and consequently, the function evaluations of the servers can be made at the same time, i.e. in parallel.

If a direct search optimization method, like MMA for instance, is used for a problem, an effective and simple way of decreasing the computation time significantly is to parallelize the calculations of the gradients. Since these are independent, it is possible to compute them simultaneously but on different computers. Since most of the computer time is devoted to function evaluations when using optimization in the field of engineering, this kind of parallelization can reduce the computation time by almost a factor equaling the numbers of computers used in the parallelization.

Using a natural selection method, like SA, a different approach is needed. In this work, a simple form of domain decomposition is used where the design space is divided into a number of sub-spaces, which then are locally optimized by each computer in the system. When all the computations are made, the best result is chosen.

The methods used for parallelization in this software are easy to implement, but some drawbacks must be considered. Both Matlab and the TCP/IP toolbox must be installed on all the computers used, and, in addition to this, several files from the VerOpt package are needed. If you use SA, for example, all of the files from the package are needed on all of the servers, including the code for SA and the function to be evaluated. For a direct search method like MMA, only the client needs the whole package while the servers only need the function to be evaluated. In some cases, when using commercial software, licensing can be an issue since the software must be installed on all of the servers. For the studies conducted so far, the communication with the external solvers is solved by using the ASCII format, that is, input and output files are defined in text files, and, most probably, a better approach would be to use some kind of object request broker, although it would not be as easy to implement. The use of the ASCII format also implies a limited number of significant digits in the input and output files which must be considered when defining and evaluating an optimization in VerOpt.

7 Summary and conclusions

In this thesis, the dimensional accuracy of injection-molded parts manufactured by FFF has been investigated. Experimental and numerical tests have been conducted to study the difference between using conventional cooling channel layouts, with straight holes and baffle, or an FFF layout where the core cooling is conformal to the inner surface of the part. Design of experiments has been carried out in order to investigate the influence of different process parameters on the dimensional accuracy using the different cooling layouts. A software environment for applied optimization studies has been developed, and a comparison of different optimization algorithms applied to the minimization of the warpage of a part has been conducted.

Four main issues covered in this thesis were defined in the end of Section 1, and the corresponding conclusions are given below.

How different cooling channel layouts affect the cooling time and dimensional accuracy of the product

In Paper B, the warpage as a function of the cooling time for three different cooling channel layouts was studied. The results show that a considerable improvement of the dimensional accuracy can be achieved by using FFF cooling channels in comparison with conventional cooling channel layouts. In some cases, a significant reduction of the cooling time could be achieved as well as an improvement of the dimensional accuracy. Comparisons of numerical and experimental results in Paper C show that the experimental results correlate well with the numerical tests, albeit with some discrepancies. In Paper D, the surface heat distribution of conventional and FFF inserts was investigated and the influence of the coolant temperature on the surface of the insert was studied. The study showed that the cooling efficiency of the FFF cooling layout was higher than for the traditionally cooled insert, although not as high as other in situ studies have shown.

If the direct-metal FFF method Electron Beam Melting is a viable method for the manufacture of inserts to injection molding

An FFF insert manufactured by the Electron beam melting method was used in Paper C and Paper D, and the experiments showed that EBM is a viable method for the manufacture of inserts to injection molding, they also showed that no differences in machinability were detected for the EBM material in comparison with inserts manufactured from H13 steel plate.

Which process parameters affect the dimensional accuracy and to what degree

The parametric study in Paper B using the cooling time as a variable showed that the cooling time is an important factor influencing the warpage. In Paper E, design of experiments was used to investigate the influence of other process parameters, and the four most important factors influencing the warpage, for both a conventional cooling channel design and an FFF design, were the temperatures of the melt, the core, the cavity, and the cooling time.

The study showed that the FFF layout was more sensitive to the settings of the temperatures of the core and cavity in comparison with the conventional cooling channel design. So, plastic manufactures using FFF inserts should be aware that there are differences in how the process parameters should be set, and, especially, that it also differs which parameters are the most important ones, in comparison with traditional cooling channel designs. If this is not taken into consideration, the benefit of using inserts manufactured by RT is not fully utilized.

Feasability of optimization methods applied to injection molding simulation and warpage minimization

The influences of different process parameters on the dimensional accuracy for injection-molded parts are rather complicated, and using optimization can be a viable method of overcoming this difficulty. A Matlab-driven environment for applied optimization studies was presented in Paper A, where some test problems were analyzed using different optimization algorithms, and where the efficiency of using parallelization for both direct search methods and natural selection methods was studied. An external solver was also successfully used, and this work showed the benefits of using optimization. This software was also used in Paper F. The four parameters from Paper E were used as design variables in order to minimize the warpage for a part manufactured by both a conventional cooling channel layout and an FFF layout. The most efficient method for this problem was the gradient-based Method of moving asymptotes, although the stochastic method Simulated annealing and the built-in function in Matlab using Sequential quadratic programming was also applicable.

8 Future work

More than 3,500 parts were manufactured in the mold with the insert manufactured by the Electron Beam Melting method described in Paper C and Paper D. No visible signs of wear could be detected after the experiments, but in order to verify that the EBM material is suitable for long-term production, further experiments should be done to verify this.

FFF gives the possibility to create conformal cooling channels, but the possibility to create cooling channels with an effective cross section in reference to heat transfer has not been studied in this thesis. Future work will involve the optimization of the heat transfer between the mold and cooling channel using topology optimization. By doing this, the benefits of using FFF to manufacture inserts for injection molding can hopefully be even better than what has been proven until now.

In this thesis, both direct search and natural selection methods have been used, and future work will include the implementation of a combined method, where the effectiveness of the direct methods are combined with the ability to find the global minima of the natural methods. This will be an important feature when studying more complex optimization problems in the future.

References

[1] G. E. Dieter, *Engineering Design: A Materials and Processing Approach*, McGraw-Hill, Singapore, 2000.
[2] N. G. McCrum, C. P. Buckley, C. B. Bucknall, *Principles of Polymer Engineering*, Oxford University Press, 1997.
[3] W. Michaeli, *Plastic Processing, -An introduction*, Hanser Publishers, 1995.
[4] H. W. Hull, *Apparatus for production of three-dimensional objects by stereolithography*, patent, 457330, 1984.
[5] J. P. Beumont, R. Nagel, R. Sherman, *Successful Injection Molding: Process, Design and Simulation*, Carl Hanser Verlag, Munich, 2002.
[6] G. Menges, W. Michaeli, P. Mohren, *How to make injection molds*, Hanser Publishers, Munich, 2000.
[7] J. Frados, *Plastics Engineering Handbook*, Van Nostrand Reinhold, New York, 1976.
[8] H. Schlichting, *Boundary-Layer Theory*, Springer, Berlin Heidelberg, 2000.
[9] C. L. Tucker, (Ed.), *Fundamentals of Computer Modeling for Polymer Processing*; Hanser Publishers: Munich, 1989.
[10] H. H. Chiang, C. A. Hieber, K. K. Wang, *"A Unified Simulation of the Filling and Postfilling Stages in Injection Molding. I. Formulation"*, Polymer Engineering & Science, 31(2), (1991), 116-124.
[11] R. Simha, P. S. Wilson, O. Olabisi, *"Pressure-volume-temperature properties of amorphous polymers: empirical and theoretical predictions "*, Colloid and Polymer Science, 251(6), (1973), 402-408.
[12] A. Y. Malkin, V. P. Beghishev, I. A. Keapin, S. A. Bolgov, *"General treatment of polymer crystallization kinetics - Part 1. A new macrokinetic equation and its experimental verification"*, Polymer Engineering & Science, 24(18), (1984), 1396-1401.
[13] T. H. Kwon, *" Mold cooling system design using boundary element method"*, Journal of Engineering for Industry, 110(4), (1988), 384-394.
[14] Y. C. Fung, P. Tong, *Classical and Computational Solid Mechanics*, World Scientific Publishing, 2001.
[15] R.-Y. Chang, S.-Y. Chiou, *"A Unified K-BKZ Model for Residual Stress Analysis of Injection Molded Three-Dimensional Thin Shapes"*, Polymer Engineering & Science, 35(22), (1995), 1733-1747.
[16] R.-Y. Chang, S.-Y. Chiou, *"Integral Constitutive model (K-BKZ) to Describe Viscoelastic Flow in Injection Molding"*, International Journal of Polymer Processing, 9(4), (1994), 365-372.
[17] M. M. Cross, *"Relation between viscoelasticity and shear-thinning behaviour in liquids"*, Rheologica Acta, 18, (1979), 609-614.
[18] C. A. Hieber, H. H. Chiang, *"Shear-rate-dependence modeling of polymer melt viscosity"*, Polymer Engineering & Science, 32(14), (1992), 931-938.
[19] A. Ammar, V. Leo, G. Régnier, *"Corner Deformation of Injected Thermoplastic Parts"*, International Journal of Forming Processes, 6(1), (2003), 53-70.
[20] K. M. B. Jansen, D. J. Dijk, K. P. Keizer, *"Warpage of Injection Moulded Plates and Cormer Products"*, International Journal of Polymer Processing, 8(4), (1998), 417-424.
[21] O. Denizart, M. Vincent, J. F. Agassant, *"Thermal stresses and strains in injection molding: experiments and computations"*, Journal of Materials Science, 30, (1995), 552-560.
[22] K. M. B. Jansen, D. J. V. Dijk, M. H. Husselman, *"Effect of Processing Conditions on Shrinkage in Injection Molding"*, Polymer Engineering & Science, 38(5), (1998), 838-846.

[23] D. Delaunay, P. L. Bot, R. Fulchiron, J. F. Luye, G. Regnier, *"Nature of Contact Between polymer and Mold in Injection Molding. Part II; Influence of Mold Deflection on Pressure History and Shrinkage"*, Polymer Engineering & Science, 40(7), (2000), 1692-1700.
[24] C.-H. Wu, Y.-J. Huang, *"The influence of cavity deformation on the shrinkage and warpage of an injection-molded part"*, International Journal of Advanced Manufacturing Technology, 32(11-12), (2007), 1144-1154.
[25] K. M. B. Jansen, J. J. W. Orij, Z. Meijer, D. J. V. Dijk, *"Comparison of Residual Stress Predictions and Measurements using Excimer Laser Removal"*, Polymer Engineering & Science, 39(10), (1999), 2030-2041.
[26] R. Y. Chang, C. H. Chen, K. S. Su, *"Modifying the Tait Equation with Cooling-Rate Effects to Predict the Pressure-Volume-Temperature Behaviors of Amorphous Polymers: Modeling and Experiment"*, Polymer Engineering & Science, 36(13), (1996), 1789-1795.
[27] R. Y. Chang, Y. C. Hsieh, *"On the pvT and thermal Shrinkage for the Injection Molding of a Plastic Lens"*, Journal of Reinforced Plastics and Composites, 18(3), (1999), 261-270.
[28] T. T. Wohlers, *Wohlers Report 2005*, Wohlers Associates, Fort Collins, 2005.
[29] F. Klocke, T. Celiker, Y.-A. Song, *"Rapid metal tooling"*, Rapid Prototyping Journal, 1(3), (1995), 32-42.
[30] N. P. Karapatis, J. P. S. v. Griethuysen, R. Glardon, *"Direct rapid tooling: a review of current research"*, Rapid Prototyping Journal, 4(2), (1998), 77-89.
[31] E. Radstock, *"Rapid Tooling"*, Rapid Prototyping Journal, 5(4), (1999), 164-168.
[32] J. I. Segal, R. I. Campbell, *"A review of research into the effects of rapid tooling on part properties"*, Rapid Prototyping Journal, 7(2), (2001), 90-98.
[33] T. Dormal, *"Rapid tools for injection molding"*, in: 4:th National Conference on Rapid and Virtual Prototyping and Applications, Lancaster, U.K., 20 June, 2003, 139-151.
[34] J. P. Kruth, X. Wang, T. Laoui, L. Froyen, *"Lasers and materials in selective laser sintering"*, Assembly Automation, 23(4), (2003), 357-371.
[35] D. Wimpenny, *"Rapid tooling options compared"*, in: 4:th National Conference on Rapid and Virtual Prototyping and Applications, Lancaster, U.K., 20 June, 2003, 189-202.
[36] E. Sachs, E. Wylonis, S. Allen, M. Cima, H. Guo, *"Production of injection molding tooling with conformal cooling channels using the three dimensional printing process"*, Polymer Engineering and Science, 40(5), (2000), 1232-1247.
[37] K. Dalgarno, T. Stewart, *"Production tooling for polymer moulding using the RapidSteel process"*, Rapid Prototyping Journal, 7(3), (2001), 173-179.
[38] D. I. Wimpenny, B. Bryden, I. R. Pashby, *"Rapid laminated tooling"*, Journal of Materials Processing Technology, 138, (2003), 214-218.
[39] C. Pelaingre, L. Velnom, C. Barlier, C. Levaillant, *"A cooling channels innovative design method for rapid tooling in thermoplastic injection molding"*, in: 1:st International Conference on advanced Research in Virtual and Rapid Prototyping, VRAP 2003, Leiria, Portugal, 1-4 October, 2003, 439-445.
[40] B. Ó. Donnchadha, A. Tansey, *"Conformally cooled metal composite rapid tooling"*, in: 1:st International Conference on Advanced Research in Virtual and Rapid Prototyping, Leiria, Portugal, 1-4 October, 2003, 447-453.
[41] K. R. Davis, T. J. Gornet, J. W. Vicars, *"High thermal conductivity tooling from laser direct metal deposition"*, in: 1:st International Conference on Advanced Research in Virtual and Rapid Prototyping, Leiria, Portugal, 1-4 October, 2003, 503-507.
[42] C. Over, W. Meiners, K. Wissenbach, M. Lindemann, G. Hammann, *"Selective laser melting: a new approach for the direct manufacturing of metals parts and tools"*, in: 3:rd Conference on Laser Assisted Net Shape Engineering, Erlangen, Germany, 21-24 September, 2003, 391-398.

[43] G. J. Gibbons, R. G. Hansell, *"Direct tool steel injection mould inserts through the Arcam EBM free-form fabrication process"*, Assembly Automation, 25(4), (2005), 300-305.
[44] G. E. P. Box, W. G. Hunter, J. S. Hunter, *Statistics for Experimenters, -An introduction to design, data analysis and model building*, John Wiley & Sons, New York, 1978.
[45] G. Taguchi, *System of experimental design : engineering methods to optimize quality and minimize costs, vol.1*, UNIPUB, New York, 1987.
[46] G. Taguchi, *System of experimental design : engineering methods to optimize quality and minimize costs, vol. 2* UNIPUB, New York, 1987.
[47] K. H. Tan, M. M. F. Yuen, *"A fuzzy multiobjective approach for minimization of injection molding defects"*, Polymer Engineering and Science, 40(4), (2000), 956-971.
[48] M.-C. Huang, C.-C. Tai, *"The effective factors in the warpage problem of an injection-molded part with a thin shell feature"*, Journal of Materials Processing Technology, 110( ), (2001), 1-9.
[49] T. C. Chang, E. F. III, *"Shrinkage behavior and optimization of injection molded parts studied by the taguchi method"*, Polymer Engineering and Science, 41(5), (2001), 703-710.
[50] H. Kurtaran, B. Ozcelik, T. Erzurumlu, *"Warpage optimization of a bus ceiling lamp base using neural network model and genetic algorithm"*, Journal of Materials Processing Technology, 169(2), (2005), 314-319.
[51] B. Ozcelik, T. Erzurumlu, *"Comparison of the warpage optimization in the plastic injection molding using ANOVA, neural network model and genetic algorithm"*, Journal of Materials Processing Technology, 171(3), (2006), 437-445.
[52] S. J. Liao, D. Y. Chang, H. J. Chen, L. S. Tsou, J. R. Ho, H. T. Yau, W. H. Hsieh, *"Optimal Process Conditions of Shrinkage and Warpage of Thin-Wall Parts"*, Polymer Engineering and Science, 44(5), (2004), 917-928.
[53] C. Yen, J. C. Lin, W. Li, M. F. Huang, *"An abductive neural network approach to the design of runner dimensions for the minimization of warpage in injection mouldings"*, Journal of Materials Processing Technology, 174(1-3), (2006), 22-28.
[54] T. Erzurumlu, B. Ozcelik, *"Minimization of warpage and sink index in injection-molded thermoplastic parts using Taguchi optimization method"*, Materials & Design, 27(10), (2006), 853-861.
[55] K.-T. Chiang, F.-P. Chang, *"Analysis of shrinkage and warpage in an injection-molded part with a thin shell feature using the response surface methodology"*, International Journal of Advanced Manufacturing Technology, (2006),
[56] J. S. Arora, *Introduction to Optimum Design*, Elevier Academic Press, San Diego, 2004.
[57] K. Svanberg, *"The method of moving asymptotes - a new method for structural optimization"*, International Journal of Numerical Engineering, 24(2), (1987), 359-373.
[58] J. H. Holland, *Adaption in Natural and Artificial Systems*, University of Michigan Press, Ann Arbor, 1975.
[59] S. Kirkpatrick, C. D. Gelatti Jr, M. P. Vecchi, *"Optimization by simulated annealing"*, Science, 220(4598), (1983), 671-680.
[60] I. Pandelis, Q. Zou, *"Optmization of the Injection Molding Design. Part I: Gate Location Optimization"*, Polymer Engineering and Science, 30(15), (1990), 873-882.
[61] I. Pandelidis, Q. Zou, *"Optimization of Injection Molding Design. Part II: Molding Conditions Optimization"*, Polymer Engineering and Science, 30(15), (1990), 883-892.
[62] L. Q. Tang, C. Chassapis, S. Manoochehri, *"Optimal cooling system design for multi-cavity injection molding"*, Finite Elements in Analysis and Design, 26(3), (1997), 229-251.
[63] S. J. Park, T. H. Kwon, *"Optimal cooling system design for the injection molding process"*, Polymer Engineering and Science, 38(9), (1998), 1450-1462.

[64] H. Qiao, *"A systematic computer-aided approach to cooling system optimal design in plastic injection molding"*, International Journal of Mechanical Sciences, 48(4), (2006), 430-439.
[65] C. L. Li, *"A feature-based approach to injection mould cooling system design"*, Computer-Aided Design, 33(14), (2001), 1073-1090.
[66] P. Rydesäter, *TCP/IP Toolbox version 1.2.3*, www.mathworks.com, (March 2001), Toolbox to setup TCP/IP connection with Matlab.

Paper A

Versatile Optimization

J Holmberg and L-E Rännar

Nordic Matlab Conference

Oslo, Norway, 2001, pp.207-212

Versatile Optimization

Joakim Holmberg & Lars-Erik Rännar

Mid Sweden University
Dept. of Engineering, Physics and Mathematics
SE-831 25 ÖSTERSUND, SWEDEN

Joakim.Holmberg@mh.se & Lars-Erik.Rannar@mh.se

Abstract

VerOpt, a MATLAB driven versatile optimization environment, enables the choice of a suitable optimization routine, parallelization over TCP/IP and the use of external solvers. VerOpt is the result of working towards the creation of a versatile yet effective environment for applied optimization studies.

This paper presents the concepts behind VerOpt, including how and why we use parallelization, and the lessons learnt when using external solvers. The paper also gives a comparison of implemented optimization routines when applied to test problems.

Currently, links to three external solvers are implemented. Two of them come from the commercial software market for engineering solutions: ANSYS (version 5.6 University High), a general purpose FE-code and C-MOLD (version 2000.7.1), a code for injection molding. The third solver is from the academic world, AnyBody, a code for biomechanical studies. The implemented optimization routines referred to are Method of Moving Asymptotes (MMA), Simulated Annealing (SA) and a genetic algorithm (GA). The MMA is a gradient-based algorithm whereas the other two can be classified as stochastic. The results of the comparison of the implemented optimization routines, in which “fmincon” from the MATLAB Optimization Toolbox is also used, show that MMA is generally the fastest routine, but does not always find the best solution. However, in test cases when parallelization is used the comparison is not ideal, since the parallelization procedures for the algorithms are not equivalent. When optimization routines are based on numerically computed gradients, such as MMA, they are embarrassingly parallel. This is because the gradients are independent of each other, which makes it possible to compute them simultaneously, but on different processors. For a stochastic routine such as SA a different approach is needed. In our case we have used a simple form of domain decomposition. An interesting result is that, in the test case involving ANSYS, we found that using ANSYS alone, as solver as well as optimizer, did not give such a good solution as using VerOpt.

A clear future development is to add a greater number of different types of optimization routines. A possible future development is to transform VerOpt into something that is more akin to a regular style MATLAB Toolbox. Irrespective of this development, VerOpt will be a significant aid for education as well as research in applied optimization. It will also serve the authors as the environment for further research in the fields of injection molding and biomechanics.

Keywords: Biomechanics, CAE, Gradient methods, Injection molding, MATLAB, Optimization, Parallelization, Stochastic methods, TCP/IP, Versatility.

Introduction

Structural analysis answers the question about how a structure behaves. The analysis may concern strength, acoustics, weight, environmental cost, production cost etc. However, structural optimization answers the opposite question. How should a structure be designed to behave the way we want?

The use of Computer Aided Engineering (CAE) is today a key-factor for the industry in order to develop new products in an efficient way. In the conventional design process, the heuristics of the design engineer is a vital part in order to reach an adequate final design. This manual design process consists of several iterative steps where different assumptions are tested until the final accepted design is established.

The demands from the market are often higher than just to get to an "acceptable" design. Also, the time from idea to final product must be shortened to cut the costs. A way to fulfill these demands is to use modern optimization techniques in conjunction with numerical and computer based CAE tools incorporated in some kind of product development method [1].

There has been a rapid development of optimization techniques in the last four decades and these techniques are powerful tools in combination with modern computers. Typical applications are logistics, economics and structural engineering but there are still extensive fields in which optimization techniques haven't been implemented yet.

Choosing the right optimization technique and algorithm for a certain problem may not be an easy task. Therefore, a comparison of optimization routines when applied to different test problems is very interesting. MATLAB is a good environment for doing this comparison since it's easy to use and there are many free (at least for academic use) optimization routines available [2].

Why bother with parallelization? It's a relevant question since the computers of today are both fast and cheap. The question has several answers that make it interesting to explore the possibilities using MATLAB for parallel optimization. First, despite the rapid computer development, there's still an increasing demand to shorten the lead-time for product development and research in industry as well as in the academic world. Second, since MATLAB is practically platform independent the ability to make full use of existing computers, many often found dormant, is appealing. However, platform dependence may arise when external solvers are used, i.e. all computations are not performed within the MATLAB environment. Third, the method presented here is easy to implement.

There is a reason for all this; the authors need a versatile yet effective environment for applied optimization studies within their respective research areas, injection molding and biomechanics. The result is called VerOpt.

Optimization

Optimization is a mathematical method and can be defined as the act of obtaining the best result available under certain circumstances. A simple problem formulation can be to maximize the profits for transportation of goods between different locations or to minimize the weight of a structure without exceeding a stress limit. The general optimization formulation of a constrained problem can be stated as follows:

Find a vector	$\mathbf{x} = (x_1\ x_2\ \ldots\ x_N)$	
which minimizes	$f(\mathbf{x})$	
such that	$\mathbf{h}_i(\mathbf{x}) = 0,$	$i = 1, 2, \ldots I$
	$\mathbf{g}_j(\mathbf{x}) \le 0,$	$j = 1, 2, \ldots J$
	$x_k^l \le x_k \le x_k^u,$	$k = 1, 2, \ldots N$

where $f(\mathbf{x})$ is the cost function, $\mathbf{x}$ is a vector of the design variables that are bounded with side constraints x_k^l and x_k^u, $\mathbf{h}(\mathbf{x})$ and $\mathbf{g}(\mathbf{x})$ are vectors with equality and inequality constraints respectively. This is a constrained problem and if the formulation contains no $\mathbf{h}(\mathbf{x})$ or $\mathbf{g}(\mathbf{x})$, it is called an unconstrained problem. The vector $\mathbf{x}$ is called the design vector and includes the design variables. These variables have a freedom of movement in order to change, and hopefully improve, the objective function. Typical design variables in structural engineering are thickness, cross-sectional area and material properties.

A typical design space with two variables is shown in figure 1, where the objective function is plotted for three constant values. As seen, the problem has many feasible solutions but assuming that $f_1 > f_2 > f_3 > f(\mathbf{x}^*)$, the optimum design point is $\mathbf{x}^*$ [3].

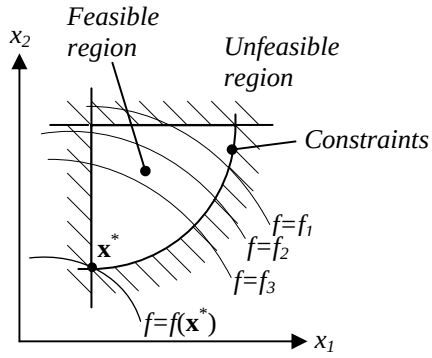

Fig. 1 - Constraint and objective function surfaces in two-dimensional space.

The implemented optimization routines are the Method of Moving of Asymptotes (MMA), Simulated Annealing (SA) and a genetic algorithm (GA). All three are standalone codes written in MATLAB. The built-in function *fmincon()* from the MATLAB Optimization Toolbox is also used. GA and SA are classified as "stochastic" or "intelligent" methods whereas the other two are classified as gradient-based [4].

GAs locates optima using processes similar to those in natural selections and genetics. SA, on the other hand, is an algorithm that is based on the simulation of finding the minimum energy state in the metal annealing process. These two methods only use the objective function, in contrast to the gradient-based methods that also need the derivatives. Both MMA and *fmincon()* are non-linear algorithms that approximate the original problem with a sub problem in each iteration [5,6,7,8].

Parallelization

This MATLAB implementation is based on a TCP/IP Toolbox created by Peter Rydesäter at Mid Sweden University in Östersund, Sweden [9]. Basically, it is a client/server application

where the client opens a connection, through a TCP/IP network, to one or several computation servers. The connection is from a MATLAB session on the client to a MATLAB session on the server. With an open connection the client can request a function evaluation on a server. When this computation is finished, the client can pick up the result. If there is an open connection to several servers, requests can be sent out to each and every server, using a loop for example, before the client picks up the results. Consequently, the function evaluations on the servers can be done at the same time, i.e. in parallel.

How to use this technique to an advantage when solving optimization problems? There are surely several ways and in this paper two are presented. Since the intention is to keep it very simple, parallelization is carried out at a high level. Thus, the approach taken strongly depends on the optimization algorithm.

When optimization routines are based on numerically computed gradients, such as MMA, they are embarrassingly parallel. This is because the gradients are independent of each other, which makes it possible to compute them simultaneously, but on different processors.

For example, if the optimization problem comprises of two design variables and there are two computation servers available the approach used is as the following simplified scheme.

On the client computer do the following.

1. Send vector $\mathbf{x} = (x_1+h, x_2)$ to server 1 for evaluation of $f(\mathbf{x})$, where h is a small number, typically 10^{-6}.
2. Send vector $\mathbf{x} = (x_1, x_2+h)$ to server 2 for evaluation of $f(\mathbf{x})$.
3. Evaluate $f(\mathbf{x})$ where $\mathbf{x} = (x_1, x_2)$.
4. Receive $f(\mathbf{x})$ from server 1 and calculate the gradient $\partial f/\partial x_1$ by forward differentiation.
5. Receive $f(\mathbf{x})$ from server 2 and calculate the gradient $\partial f/\partial x_2$ by forward differentiation.
6. Let the optimization algorithm calculate a new vector $\mathbf{x}$. If not convergence or maximum iterations are reached go back to step 1.

For a stochastic routine, such as SA, a different approach is needed. Here a simple form of domain decomposition is chosen. One of the design variables is used to split the design space. With the same conditions as in the example above the design space would be split up into three parts using x_1 for example. This generates three sub problems that can be optimized simultaneously. Two sub problems are distributed, i.e. different bounds for x_1 are sent, to the computation servers. When all computations are done and received the best result is chosen.

These two approaches seem fine when reasoning about them, but without performance analysis there is no way of knowing how well they work in practice. If there is no performance gain when using parallelization then why bother using it? To measure the eventual performance gain two measures are used, speed-up and efficiency, both based on execution time.

The speed-up of a p-node (in this paper p is the number of servers used plus the client, i.e. in the example above p would be 3) computation with execution time T_p is given by:

$$S_p = T_1^* / T_p ,$$

where T_1^* is the best sequential time obtained for the same problem on the same multicomputer (in this case the client) [10].

The efficiency of a p-node computation with speed-up S_p is given by:

$$\eta_p = S_p / p$$ [11].

There is one aspect that may be considered as a drawback. Both approaches always demand that MATLAB and the TCP/IP Toolbox are installed on all systems used. In addition to this, several other files from the VerOpt package is needed. For a stochastic routine, such as SA, most of the files from the whole package are needed on all systems, including SA and the function to be evaluated. For a gradient-based routine, such as MMA, only the client needs the whole package. The servers only need the function to be evaluated.

Test problems

Three different test problems were considered; *'Peaks'* – a function in MATLAB of two variables, obtained by translating and scaling Gaussian distributions, *'Bearing'* – a boundary value problem with two dimensions solved with a finite element code written in MATLAB by the authors and finally, *'Bearing cage'* – a simple but typical structural mechanics problem in two dimensions solved with finite element analysis in ANSYS [12].

The function *peaks()* in MATLAB is well suited for optimization studies since it has several extreme points, including two local and one global minimum, see figure 2. This function served as the first test problem since it is computationally cheap and all the extreme points are known.

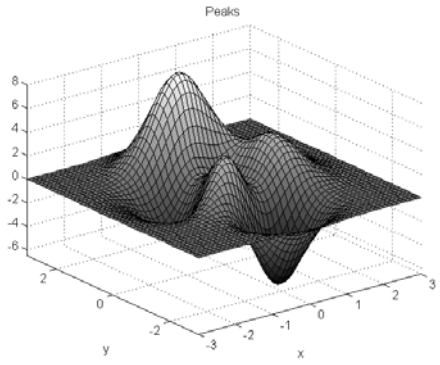

Fig. 2 - The function *peaks()* with two design variables, x and y.

The next problem is not as computationally cheap as the previous one but contains only one extreme point, a global maximum. The objective is to maximize the load capacity for a step pad bearing, see figure 3 & 4. The governing equation is Reynolds equation [13].

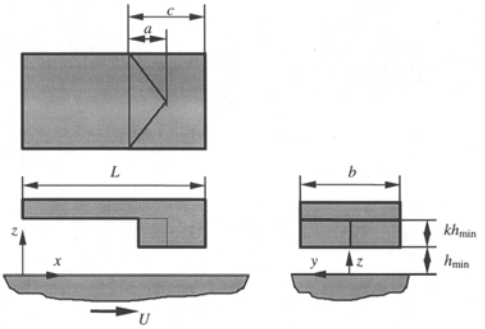

Fig. 3 - A step pad bearing with finite width. The dimension b and the constant k are chosen as design variables.

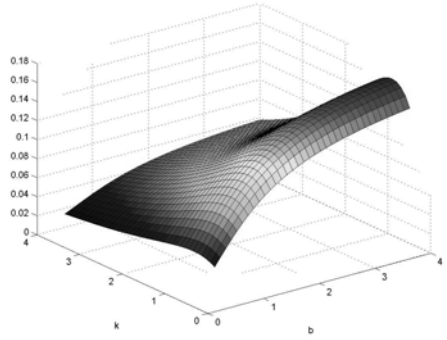

Fig. 4 - Objective function, non-dimensional load capacity, for step pad bearing.

The final problem requires a link to an external solver, ANSYS, and the objective is to minimize the weight of a bearing cage that is subjected to a bearing load, see figure 5. The original weight is 4.13 kg. This problem has been solved several times with the built-in optimization algorithms in ANSYS and it contains several local minima.

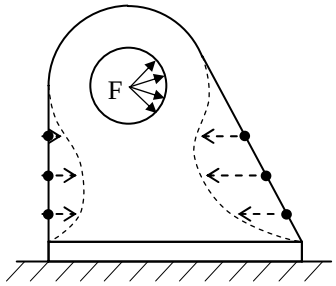

Fig. 5 - Bearing cage with 6 design variables, the preferred direction of movement in order to minimize the weight is presented with a dashed line.

Links to external solvers use text files in ASCII format for transferring information. With the read and write operations in MATLAB a shell script and an input file are created for starting the solver in batch. Results from the solver are through an output file read into MATLAB for evaluation.

The hardware used for getting the execution time results were PC's equipped with 256 MB RAM, 400 MHz CPU and Microsoft Windows NT 4.0 as operating system. Other setups, such as a mix of platforms have been tested and work fine but to get a correct comparison identical hardware is preferable.

Results

'Peaks' – Since MMA and *fmincon()* are constrained methods, an additional diagonal constraint was added to the test problem in order to divide the design space into two regions, one feasible and one unfeasible. The start point was chosen to [0 0] and the side constraints are [-3 3] for both variables. Convergence is calculated with respect to the change of the objective function. MMA is faster than *fmincon()* but as expected, both of them were caught in local minima when the start point was altered.

The additional constraint wasn't used for the stochastic methods. Both of them showed the same tendency, they did only find the global minima in two cases out of three. Convergence related to the objective function isn't presented for these methods, since it is more suitable to present the outcome towards local and global minimum, see table 1.

Method	Iter	F-evals	Conv	L/G**
MMA	10	45	1e-5	-
fmincon()	10	60	1e-6	-
GA	53	268	-	27/73
SA	8*	234	-	33/67

Table 1 - Results – *'Peaks'*.
Notes: * Number of initial temperature points.
** Outcome in percent towards local and global minimum.

'Bearing' – Two constraints were added for the gradient-based methods, giving the problem a slightly lower maximum value. Even so, these methods showed the best total performance with MMA as the fastest one. The stochastic methods came relatively close but required 2-5 times longer time to complete the optimization, see table 2. The time for one function evaluation is 15 seconds.

Method	Iter	F-evals	Obj	Time [s]
fmincon()	15	109	0.1629	1666
MMA	10	59	0.1629	1001
GA	15	118	0.1612	1847
SA	9*	288	0.1622	5150

Table 2 - Results – *'Bearing'*.
Note: * Number of initial temperature points.

'Bearing cage' – This test problem has two constraints, maximum stress in two different areas, with the lower stress limit at the bottom due to welding. The time for one function evaluation is 14 seconds. *fmincon()* was able to reduce the weight with 11% while SA managed to reduce the weight with 25%. As seen in table 3, GA used less function evaluations and was much faster than SA but it didn't reduce the weight as much. An interesting result is that using ANSYS alone, as solver as well as optimizer, only gave a weight reduction of 11%.

Method	Iter	F-evals	Obj	Time [s]
fmincon()	5	39	3.69	1040
MMA	4	66	3.39	1277
GA	5	50	3.41	803
SA	6*	325	3.10	4390

Table 3 - Results – *'Bearing cage'.*
Note: * Number of initial temperature points.

Since GA and SA are unconstrained algorithms, a penalty function was used in order to consider the constraints. The basic idea is to add a penalty to the objective function when the constraints are violated. The process is continued until there is no significant improvement in the estimate for the optimum point [14].

As seen in table 4, the speed-up and efficiency for SA in the *'Bearing'* problem are remarkable. The efficiency is higher than 1, i.e. 100%. This phenomenon is due to the stochastic nature of SA and its inefficiency for large domains, a small domain makes it more effective. A gradient-based method couldn't get any higher than 1.

Method	*Bearing*		*Bearing cage*	
	S_3	η_3	S_7	η_7
MMA	1.59	0.53	1.41	0.20
SA	5.00	1.67	4.02	0.57

Table 4 - Results – the speed-up and efficiency for MMA and SA in the problems *'Bearing'* and *'Bearing cage'*.

Discussion & Conclusion

When working with optimization studies, one must weigh the pros and cons between the different methods. Test problem number two clearly shows that gradient based methods, and especially MMA, finds the minimum in a convex problem faster than the stochastic methods. On the other hand, when the problem has several local minima, the stochastic methods shows their strength since they are capable of "climbing out" of local extreme points in complex multi-dimensional search spaces, but this quality costs in terms of function evaluations.

Results from the parallelization shows that there is time to be saved. In practice, where the evaluation of $f(\mathbf{x})$ may take a lot longer time than in these test problems, the gradient-based methods, such as MMA, should show better performance concerning speed-up and efficiency.

Using text files for transferring information from and to an external solver is most probably not the best method. Especially since it's difficult to get suitable output files from modern CAE tools. It would probably be a better approach to use some sort of object request broker, although more difficult to implement.

Future development, will involve the technique to combine stochastic and gradient-based methods in order to improve the convergence

for the global optimization problem. Since the stochastic methods are excellent in finding the areas of local minima's, it would be a great advantage to be able to "drop" a gradient method in each of these minima, while the stochastic method continues the search for other possible minima. In this way, a lot of time will be saved since the gradient-based methods would only work in areas where they have their benefits, convex subspaces.

A possible future development is to transform VerOpt into something that is more akin to a regular style MATLAB Toolbox, perhaps even with a GUI. This would be a great aid when using VerOpt for educational purposes in structural optimization.

The work presented in this paper has served as an instructive project in which a deeper understanding within the fields of optimization and parallelization has been gained. The result, VerOpt, will also serve the authors as the environment for further research in the fields of injection molding and biomechanics. C-MOLD [15], commercial software for simulation of the injection molding process, has already been implemented and tested to some extent as an external solver. The authors are currently working with the implementation of AnyBody [16], a code for biomechanical studies.

References

[1] Krause, Heimann & Kind, "An Approach towards a Design Process Language", Proceedings of the 2001 CIRP Design Seminar, KTH Stockholm, 7-12 (June 2001).

[2] MATLAB, Release 11, The Language of Technical Computing, http://www.mathworks.com.

[3] Arora J. S., Introduction to Optimum Design, McGraw-Hill Inc., Singapore, Ch. 2 (1989).

[4] Pham & Karaboga, Intelligent Optimisation Techniques, Springer-Verlag, London, (2000).

[5] Houck C., et al., "A Genetic Algorithm for Function Optimization: A Matlab Implementation", NCSU-IE Technical Report 95-09, North Carolina State University, USA, (1995). Code (including the paper) can be downloaded at http://www.ie.ncsu.edu/gaot.

[6] Kirkpatrick, Gelatt & Vecchi, "Optimization by Simulated Annealing", Science, 220, 670-680, (1983). Code can be downloaded at http://www.mathworks.com.

[7] Svanberg K., "The method of moving asymptotes – A new method for structural optimization", Int. J. Num. Methods in Eng., 24, 359-373 (1987). Code may be available from the author, krille@math.kth.se.

[8] Optimization Toolbox User's Guide, The MathWorks Inc, Natick, (1999).

[9] Rydesäter P., TCP/IP Toolbox version 1.2.3, http://www.mathworks.com, (March 2001). Toolbox to setup TCP/IP connection with MATLAB.

[10] Van de Velde E. F., Concurrent scientific computing, Springer-Verlag, New York, Ch. 1, 17 (1994).

[11] Ibid.

[12] ANSYS, version 5.6 University High, general purpose FE-code, http://www.ansys.com.

[13] Hamrock B. J., Fundementals of Fluid Film Lubrication, McGraw-Hill Inc., Singapore, Ch. 7 & 9 (1994).

[14] Arora J. S., Introduction to Optimum Design, McGraw-Hill Inc., Singapore, 337-339 (1989).

[15] C-MOLD, version 2000.7.1, code for injection molding, http://www.moldflow.com.

[16] AnyBody, code for biomechanical studies, developed by Rasmussen J., et al., http://anybody.auc.dk/.

Paper B

Efficient Cooling of FFF Injection Molding Tools with Conformal Cooling Channels, -An Introductory Analysis

L-E Rännar

1:st International Conference on Advanced Research in Virtual and Rapid Prototyping

Leiria, Portugal, 2003, pp.433-437

EFFICIENT COOLING OF FFF INJECTION MOLDING TOOLS WITH CONFORMAL COOLING CHANNELS, -AN INTRODUCTORY ANALYSIS

Lars-Erik Rännar

Mid Sweden University, Department of Engineering, Physics and Mathematics, Östersund, Sweden – lars-erik.rannar@mh.se
Norwegian University of Technology and Science, Department of Machine Design and Materials Technology, Trondheim, Norway

Abstract

Typically, the conventional machining techniques for the design of cooling layouts, in injection molding tools, are drilled straight bores placed around the tool cavity. Ejector pins, parting planes, cores, etc., make it impossible to gain an optimal cooling effect and the methods to improve the cooling, such as baffles and bubblers, are rather time-consuming and expensive.

A numerical comparison of the efficiency between conventional cooling channel layouts, using straight holes and a baffle, and a free-form fabricated (FFF) layout was carried out considering cooling time and dimensional stability.

The analyses showed a considerable improvement in both cooling time and dimensional stability in favor of FFF cooling channels. A reduction of the cycle time up to 67% was achieved with preserved, and even better tolerances on the dimensional stability.

Keywords

Free-form fabrication, Rapid tooling, Injection molding, Simulation, Cooling

Introduction

The injection molding process can be divided into four separate steps; plastification, injection, hold pressure and finally ejection. Pellets form a melt by heat transfer from the heated cylinder wall and to some extent by shear heating. The melt is then injected through a nozzle into a closed mold. The mold consists of two or three plates, pressed together by a clamping unit. During the injection, a pressure, which is counteracted by the clamping unit, is built up and maintained until the material in the gate has solidified. When the material in the cavity has solidified and reached a state where it is stiff enough, the mold opens and the part is ejected. The mold closes and the cycle is repeated. The time from the start of injection of the melt into the mold until the next start of injection is called the cycle time.

The cooling of the injection-molded part is a critical step in the process. It has a large impact on the profits, i.e. an efficient cooling reduces the cooling time, which increases the productivity. On the other hand, the quality can be affected in a negative way. A careless design of the cooling system can generate inaccurate products with too large a warpage and residual stresses. Today the cooling channels are typically drilled straight bores placed around the tool cavity. Ejector pins, parting planes, cores etc., make it impossible to gain the optimal cooling effect and the methods to improve the cooling, such as baffles and bubblers, are rather time-consuming and expensive. An even worse scenario is when complex parts may need extra post molding cooling in a custom-fit cooling jig. This operation is costly, both in lead time and man hours.

Rapid prototyping is nowadays an accepted technology. However, it is still in an expansive phase and new applications are evolving continuously. This technology will enable a completely new approach to the design of cooling channels for injection molding tools. The engineers have a vast number of options since they aren't any more restricted to conventional drilling and milling, but can focus on how to make the cooling as effective as possible, e.g. make cooling channels that follow the geometry. Such so-called conformal cooling channels have been subjected to extensive research in recent years and the two main benefits using them are improved productivity and process control [1]. Most of the research comprises methods which needs binding agents and/or sintering, such as Three Dimensional Printing (3DP) and Selective Laser Sintering (SLS). It has been shown that conformal cooling channels created with 3DP

process have several advantages, compared with conventional methods, such as the tool reaches steady state faster upon start of the process and a more uniform temperature distribution is achieved [2]. Another important issue is the cycle time and a reduction of the cycle time up to 15% is possible for a shallow part using SLS [3]. Other processes available for production of tools that have shown potential are laser generating [4] and the Electron Beam Melting Process (EBM).

EBM is utilized in a method called "*CAD to Metal®"*, developed by Arcam AB [5]. This technology is not based on sintering methods, as for example SLS, but it enables the creation of fully dense forms without certain binding agents. Electrons are emitted in the EBM canon, and at half the speed of light they are projected at the powdered metal on the building table. While in vacuum, the beam selectively joins the powder in the layer by the heat gained from the loss of the electrons kinetic energy as they hit the metal. More layers are added and finally the geometry created in a CAD environment is ready. The part is then cooled down and unbounded powder is taken away. After this, the part is ready for further processing such as drilling, milling, spark machining, etc. At this time, two materials are available, Arcam Low Alloy Steel 200 with a Brinell hardness of 200 and Arcam H13 Tool Steel with a Rockwell hardness of 48. Typical tensile strengths for the two materials are 290 MPa and 1400 MPa respectively.

The aim with this study was to investigate the possibility of decreasing the cycle time using conformal cooling channels, created with the *Cad to Metal®* method, with limitations in the dimensional stability. Two conventional cooling channel layouts are compared with the conformal layout for a detail with a deep core, a typical design for injection molded parts.

Numerical model

Moldex3D, the commercial injection molding analysis software, was used to determine the cooling time and the dimensional stability [6]. Thin shell elements and beam elements were used in order to simulate the part design, the cooling channels and the runner system. A total number of 6500 elements were used and a general shell element size of 1.5 mm was applied with further refinement in the gate area.

The cooling time is affected by several factors such as mold material, part material, injection temperature, cooling layout, cooling media temperature, etc. In this study, the cooling time is a variable and the dimensional accuracy is the quantity of interest.

The dimensional accuracy depends on the warpage, which is a result of differential shrinkage of the final part. There are several causes for the uneven shrinkage, and they can be divided into three major causes [7]:

1) Differential shrinkage through the part thickness.

2) Differential area shrinkage.

3) Differential shrinkage from orientation effects.

Different cooling rates for the opposing surfaces are the explanation for the first cause. This difference leads to a faster build up of the solidified layer on one side, which leads to an asymmetric shrinkage through the thickness. This in its turns causes the surface to bend towards the side with the lower cooling rate, i.e. the hotter mold side. A typical example is the cooling at the corners in a box.

The second cause refers to differences in packing pressures or in mold wall temperatures. Thinner regions solidify more rapidly than thicker regions, if the cooling rates are constant, and consequently they solidify at a higher pressure with less shrinkage. Different mold wall temperatures give the same effect: cooler areas will solidify first at a higher pressure causing a lower shrinkage than for the hotter area.

Finally, the orientation of the molecules also affects the warpage. When the melt next to the mold wall solidifies, the molecules keep their orientation in the flow direction as well as their molecular extension, due to the shear forces introduced during the flow. The centre part of the melt is insulated by the frozen layer and due to the fountain-flow effect, not as oriented as the outer layers and thus more relaxed. This difference in orientation leads to a core in compression and a skin in tension. Consequently a warpage effect ensues.

The warpage in this specific study is mainly caused by differential shrinkage through the part thickness.

Part Design

In cooperation with a plastics company, a design for the part was proposed. The purpose was to investigate a common and important issue: inadequate cooling in deep cores, see Figure 1. Deep cores lead to long cycle times, poor dimensional accuracy, and sometimes also additional cooling time in a custom-fit jig. In this case, the overall cooling time is of interest and the dimensional accuracy between the two braces, measured 66 mm in the original design.

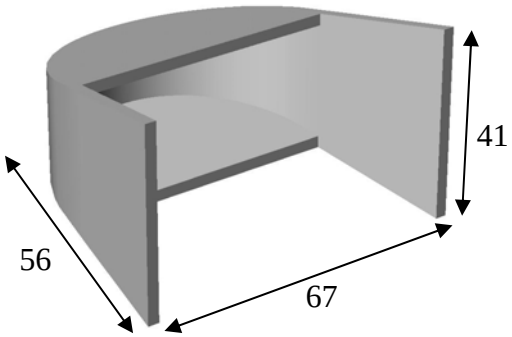

Figure 1 - Approximate part design, all dimensions in mm. Wall thickness is 3 mm and the draft angles are 10°.

Cooling Channel Layouts

Three different cooling channel layouts were analyzed, see Figures 2-4. The distance from the part wall to the cooling channels is approximately the same as the channel diameter, 10 mm.

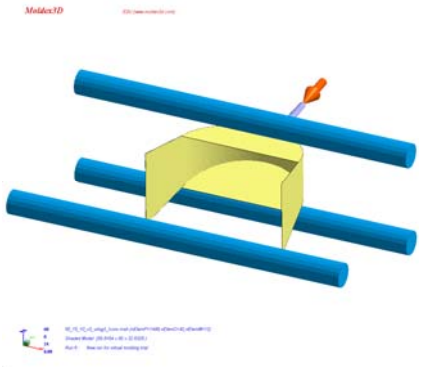

Figure 2 - Conventional cooling with straight bores around the cavity.

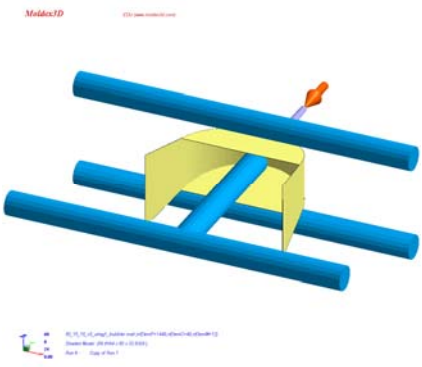

Figure 3 - Conventional cooling with straight bores in the A-plate (cavity plate) and a baffle in the B-plate (core plate).

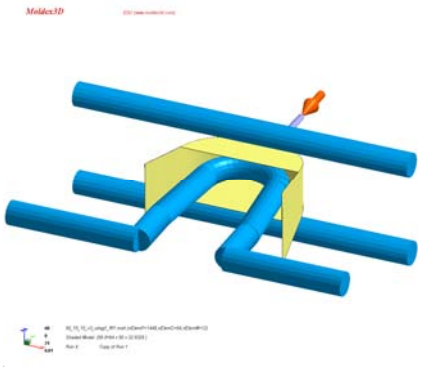

Figure 4 - Free-form fabricated cooling in the B-plate and straight bores in the A-plate.

Process Parameters

A commonly used plastic for technical goods was used in the simulation, POM Delrin 500 from DuPont. The gate is centered at the top of the part, with a diameter of 2.5/4 mm on the tapered runner.

Table 1 - Process parameters.

Part material	POM Delrin 500
Part volume	20.4 cm^3
Injection temperature	200°C
Ejection temperature	120°C
Filling time	1 sec
Packing time	3 sec
Packing pressure	30 MPa
Coolant temperature	56°C
Ambient temperature	25°C
Specific heat, mold	462 J/kgK
Conductivity, mold	47 W/mK
Density, mold	7852 kg/m^3

Results

In order to compare the efficiency of the different layouts, a sensitivity analysis was performed with the cooling time as a variable and the dimensional stability as object function. The cooling time was altered from zero seconds to 28 seconds for all three layouts. One should remember that the filling and packing time is also included in the total cycle time. The warpage, i.e. the difference in distance between the two braces in the original

model and the three cooling designs was determined. Figures 5 and 6 show the warpage between the two braces in millimeters and percentages.

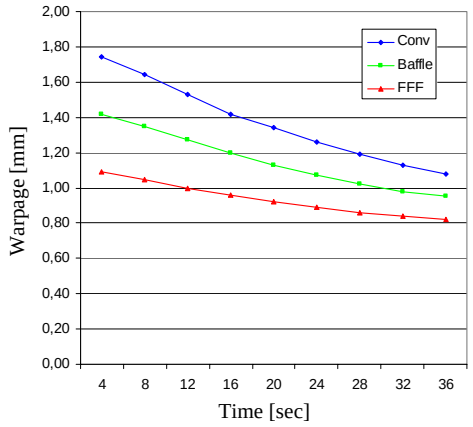

Figure 5 - Warpage, in mm, between the braces as a function of the cycle time.

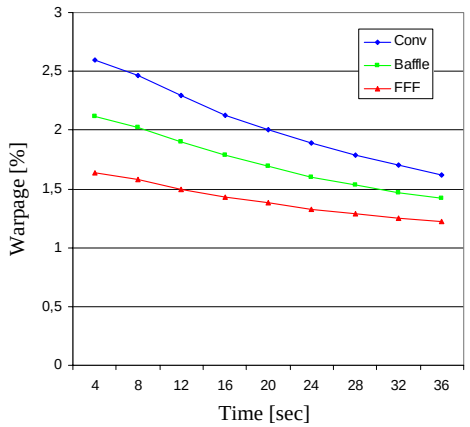

Figure 6 - Warpage, in percent, between the braces as a function of the cycle time.

As can be seen in the figures, conformal cooling channels can achieve less warpage with a shorter cycle time in comparison with conventional methods. With a limit of the dimensional stability of 1.5%, conformal channels reduce the cycle time with more than 67% in comparison with straight bores and with 60% in comparison with straight bores in combination with a baffle.

Discussion and Conclusions

A considerable improvement of the cycle time was obtained when using conformal cooling channels for the core in a typical part design. A 67% reduction of the cycle time was achieved with preserved, and even better dimensional stability.

Further work in this project will involve the production of the three core plate inserts using the *CAD to Metal*® method in order to experimentally verify the analytical results.

Since the warpage for this design is mainly caused by differential shrinkage through the part thickness, even better efficiency should be possible for more complex part designs where shrinkage due to other effects is also present.

Finally, introducing new methods in a complex production process like injection molding, makes it hard to set the process parameters and to anticipate the results. Simulation is a tool which will be even more needed in the future in order to ensure high quality but nevertheless, it will still be hard to achieve the optimal process conditions. Utilizing optimization techniques will be beneficial in order to learn more about the new opportunities and also to make it easier to find the optimal process conditions for specific needs.

Acknowledgments

The research presented in this paper is carried out in a project funded by the European Union Structural Fund, Objective 1, Södra Skogslänsregionen.

References

[1] K. Dalgarno, T. Stewart, Production tooling for polymer moulding using the RapidSteel process, Rapid Prototyping Journal, 2001, Vol. 7, No. 3, 173-179.
[2] Sachs, Wylonis, Allen, Cima, Guo, Production of Injection Molding Tooling with Conformal Cooling Channels Using the Three Dimensional Printing Process, Polymer Engineering and Science, 2000, Vol. 40, No. 5, 1232-1247.
[3] Ring, Dimla, Wimpenny, An Investigation of the Effectiveness of Conformal Cooling Channels and Selective Laser Sintering Material in Injection Moulding Tools, RPD 2002.
[4] Karapatis, van Griethuysen, Glardon, Direct rapid tooling: a review of current research, Rapid Prototyping Journal, 1998, Vol. 4, No. 2, 77-89.
[5] www.arcam.com
[6] www.moldex3d.com
[7] Beumont, Nagel, Sherman, Successful Injection Molding: Process, Design and Simulation, Carl Hanser Verlag, Munich, 2002.

Biography

Lars-Erik Rännar is a Ph.D. Student at the Norwegian University of Technology and Science. He is also employed as a teaching assistant at Mid Sweden University, where most of the research is carried out.

Paper C

Efficient Cooling with Tool Inserts Manufactured by Electron Beam Melting

L-E Rännar, A Glad, C-G Gustafson

Rapid Prototyping Journal

13(3), (2007), 128-135

Efficient cooling with tool inserts manufactured by electron beam melting

L-E. Rännar
Department of Engineering, Physics and Mathematics, Mid Sweden University, Östersund, Sweden, and
A. Glad and C-G. Gustafson
Department of Engineering Design and Materials, Norwegian University of Science and Technology, Trondheim, Norway

Abstract
Purpose – The purpose of this paper is to present a comparative study, regarding cooling time and dimensional accuracy, of conventional injection mold cooling channel layouts, using straight holes and a baffle, and free-form fabricated (FFF) layout, manufactured by the direct-metal rapid tooling (RT) method electron beam melting (EBM). Many other methods have been proven useful for RT, but the authors have not found any publications where EBM has been used to manufacture injection molding tools.
Design/methodology/approach – A test part was designed in order to replicate a common and important issue: inadequate cooling in deep cores. The part and the different cooling layouts were analyzed in an injection molding simulation software and the numerical results were compared with corresponding experimental results.
Findings – The analyses showed an improvement in both cooling time and dimensional accuracy in favor of conformal FFF cooling channels manufactured by EBM. The experimental results correlate well with the numerical tests, however with some discrepancies.
Research limitations/implications – The results presented are based on the direct-metal RT method EBM, and they were obtained using a specific test part.
Originality/value – This paper can be a useful aid when designing mold tools and especially when considering the usage of FFF cooling channels versus conventional cooling design. It can also serve as a reference when comparing the efficiency in terms of cooling time and dimensional accuracy between different layouts.

Keywords Rapid prototyping, Cooling, Cooling equipment, Simulation

Paper type Research paper

Introduction

Polymers have played an essential role for a long time in everyday life as well as in industry. The use of injection molding to manufacture engineering components has been growing rapidly during the recent decades, due to several factors such as the method efficiency when producing complex plastic parts, the lightness, the simplicity of processing plastics, etc. However, the use of analysis tools for the simulation of the molding process is a neglected area amongst many manufactures of plastic products. Mostly, the design and the choice of different process parameters are based on the experience of mold designers and other engineers. Sometimes the parts that are to be produced are redesigned on account of bad manufacturability of the injection molding tool. Especially, regarding complex parts, this iterative process between the designer and mold maker requires a lot of time and the reconstruction of both product and mold. The simulation facilities are vital in order to deliver tools in an efficient manner without unnecessary redesign and retooling. Studies have shown that costs up to 50 percent can be cut for mold modifications and up to 15 percent for cycle time when using simulation (Menges *et al.*, 2000).

The injection molding process can be divided into five separate steps: plasticization, injection, hold pressure, cooling, and finally ejection. Pellets form a melt by heat transfer from the heated cylinder wall, but mainly by shear-induced heating. The melt is then injected through a nozzle into a closed mold. The mold consists of two or three plates, pressed together by a clamping unit. During the injection, a pressure, which is counteracted by the clamping unit, is built up and maintained until the material inside the gate has solidified. When the material in the cavity has solidified and reached a state where it is stiff enough to withstand the ejector pins, the mold opens and the part is ejected. The mold closes, and the cycle is repeated. The time from the start of the injection of the melt into the mold until the next shot is started is called the cycle time.

The cooling of the injection molded parts is a critical step in the process. It has a large impact on the profits, i.e. an efficient cooling reduces the cooling time, which increases the productivity. On the other hand, the quality can be affected in a negative way. A careless design of the cooling system can generate inaccurate products with too large a warpage and

The current issue and full text archive of this journal is available at
www.emeraldinsight.com/1355-2546.htm

Rapid Prototyping Journal
13/3 (2007) 128–135
 [ISSN 1355-2546]
[DOI 10.1108/13552540710750870]

Received: 1 June 2005
Revised: 1 January 2007
Accepted: 5 March 2007

Rapid Prototyping Journal
Volume 13 · Number 3 · 2007 · 128–135

residual stresses. Today, the cooling channels are typically drilled straight bores around the tool cavity. Ejector pins, parting planes, cores, etc. make it impossible to gain the optimal cooling effect, and the methods to improve the cooling, such as baffles and bubblers, are rather time-consuming and expensive. The worst scenario is when complex parts may need extra post-molding cooling in a custom-fit jig. This operation is costly, both in lead-time and man-hours.

The possibility of direct-metal rapid tooling (RT) from high quality steel is not commonly known in the injection molding industry today. However, the RT industry is in an expansive phase and new applications are evolving continuously. Different RT technologies enable the production of inserts for injection molding tools. They can be divided into different types and Menges *et al.* (2000) suggest a classification of RT as follows:

- conventional removal and coating processes;
- material additive processes;
- master mold processes; and
- hybrid processes.

Also, a distinction between direct and in-direct RT is made, where indirect methods generally involve more sequences than direct methods. The different methods have been discussed and compared (Klocke *et al.*, 1995; Karapatis *et al.*, 1998; Radstock, 1999; Segal and Campbell, 2001; Dormal, 2003; Kruth *et al.*, 2003; Wimpenny, 2003), and some competitive methods in the RT market are presented:

- 3D Keltool, by 3D systems.
- EBM, electron beam melting, by Arcam.
- DLF, direct laser forming by Trumpf.
- DMD, direct metal deposition, by the POM Group.
- DMLS, direct metal laser sintering, by EOS.
- LAM, laser additive manufacturing, by Aeromet.
- LaserCusing, by concept laser.
- Laser consolidation, by Accufusion.
- LENS, laser engineered net shaping, by Optomec.
- ProMetal, by ProMetal RCT.
- RSP, rapid solidification process, by RSP tooling.
- SLM, selective laser melting, by MCP Group.
- SLS, selective laser sintering, by 3D Systems.
- Solid phase laser sintering, by Phenix systems.
- Stratoconception by CIRTES.

Inserts made by free-form fabrication (FFF) has been subjected to extensive research in recent years. It has already been stated that conformal cooling channels, i.e. channels equidistant from the surface to be cooled, have an impact on the quality of the product as well as on the cycle time. Sachs *et al.* (2000) showed that conformal cooling channels produced by 3DP exhibited no transient behavior at the start of the molding, at the same time that it maintained a more uniform temperature in the tool during a individual molding cycle. Rapid laminated tooling is also a viable method for conformal cooling, and studies have shown a considerable reduction of cost and time saving in comparison with a conventional machined tool (Wimpenny *et al.*, 2003). Dalgarno and Stewert (2001) used the DTM RapidSteel process (formerly DTM Corp., nowadays 3D Systems) to manufacture conformal cooling channels and also presented some results regarding the manufacturability of small features for the process. Pelaingre *et al.* (2003) studied the possibility to create complicated cooling channels by milling stratums which then were assembled using stiffeners and strengthening plugs to build a complete tool. The aim was to achieve a higher production rate and to be able to control the temperature in the mold precisely during the cooling stage. ÓDonnchadha and Tansey (2003) showed considerable reduced cost and lead-time for a core insert fabricated by SLS and also proposed a modular concept where parts of the tool are manufactured by traditional methods and inserts by SLS, this in order to ensure the viability of RT. SLM is also a viable method for RT. Over *et al.* (2003) reported time-savings up to 30 percent when using SLM to manufacture inserts in steel. Another way to optimize the cooling effect without fabricating complicated cooling channels is to use high thermal conductivity tooling. Davis *et al.* (2003) showed that reduced cycle time without sacrificing wear on the tool or part quality can be achieved by using DMD. Spray-deposited metal is another method suitable for RT, and Knirsch (2003) showed that this method is able to spray high-conductivity aluminum alloy onto a H13 insert. This will allow a simple water line, machined by conventional methods, to cool the entire surface of the mold.

Motive and aim

Many processes have been proven useful for RT. However, few studies have been published where the direct-metal freeform technique of electron beam melting (EBM), developed and commercialized by the company Arcam AB (www.arcam.com), has been used to manufacture injection molding tools. The aim with this study is to investigate the advantages of using inserts manufactured by EBM in comparison with conventional, machined inserts. A comparative study, regarding cooling time and dimensional accuracy, was carried out both experimentally and numerically. Two conventional cooling channel layouts are compared with the conformal layout for a detail with a deep core, a typical design for injection molded parts where the geometry of the part prevents short cooling times, due to heat concentration in the core.

Electron beam melting

The actual usage of the EBM process in the present study was motivated by the fact that it is not based on fusion or the sintering of metal particles such as utilized in selective laser sintering. The EBM process is capable of creating fully dense forms without any binding agents, see Figure 1. By heating a Tungsten filament (1) to more than 2,500°C, electrons are emitted. The electrons are then accelerated with the aid of a high voltage difference up to about half the speed of light in the electron beam gun (2) and forming a beam (3). Two magnetic fields (4, 5) bring the beam into focus and control the movement of the beam. Actually, this is basically the same principle as the one at work for a cathode ray tube used in conventional TV-sets. While having the entire machinery kept in high vacuum, the beam selectively welds the powder in the layer by the heat generated from the loss of the electrons kinetic energy as it hits the metal. The diameter of the focused beam is 0.6 mm, and some of the surrounding material will melt or sinter due to the heat. The powder is deposited in powder containers (6) and distributed by a movable powder vessel (7) with a thickness of each layer from 0.05 to 0.2 mm, depending on which material quality is used. Successive layers

Figure 1 EBM process overview

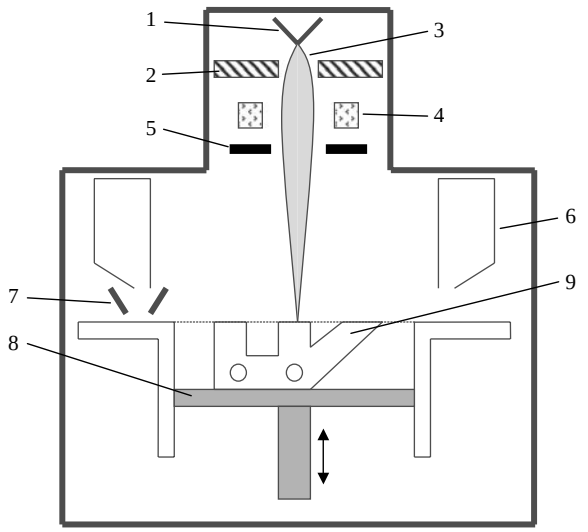

are added while lowering the building table (8), and finally the geometry (9), as it was originally created in a CAD environment, is finished. The part is then cooled from the building temperature of approximately 900°C, and unbound powder is removed. Thereafter, if necessary, the part is ready for further processing such as drilling, high-speed milling, electric discharge machining, etc. Presently, two different steels suitable for injection molds are available, Arcam Low Alloy Steel and Arcam H13 Tool Steel (Table I). The EBM method is well suited for a variety of materials, and Taminger and Hafley (2002) studied the possibility to use electron-beam freeform fabrication (EB F^3) to high reflective materials like aluminum, but instead of using powder, a metal wire is fed into the molten pool on the metallic substrate.

Few studies have been found regarding Arcam EBM process, but the mechanical properties of the Arcam H13 Tool Steel have been investigated and compared with materials manufactured by competitive methods and the Arcam H13 steel showed a consistent modulus when compressing it up to a level of 1,100 MPa (Dalgarno and Goodridge, 2004). The part properties are rather sensitive of the processing conditions, but studies using standard recommended processing conditions have shown that the method is able to create parts with virtually no porosities and with full interlayer bonding (Cormier *et al.*, 2004).

Experiment

Part design

In cooperation with a very capable injection molding company, which also designs and manufactures molds, the researchers conceived a design for a suitable part. The purpose of the investigation was to find out more about a common and important issue: inadequate cooling in deep cores. The part geometry is shown in Figure 2. The draft angle was set rather high in order to facilitate the ejection of parts when using short cooling times. The thickness of 3.0 mm was chosen to generate a rather large amount of heat for the cooling systems to remove. Owing to insufficient cooling capacity, deep cores lead to long cycle times, poor dimensional accuracy, and therefore even additional out-of-cavity cooling in a custom-fit jig. In this study, the overall cooling time was of prime interest together with the dimensional accuracy as measured between the two braces (Figure 3 and equation (1)). Also, preliminary analyses were conducted in order to get an idea of how to set the process parameters for the experimental tests. The injection molding analysis software Moldex3D from Coretech System (www.moldex3d.com) was used for this purpose and for the numerical verification to be presented later:

$$\text{Warpage} = \frac{L_0 - L_w}{L_0} 100 \quad (1)$$

Mold design

Three different cooling-channel layouts were chosen for this study: a conformal layout using freeform fabrication by EBM and two conventional layouts with straight bores and a baffle (Figures 4-6). The gate is located at the center of the part (marked with an arrow in the figures), with a diameter of 2.5/4 mm on the tapered runner. The distance from the part wall to the cooling channels is approximately the same as the channel diameter, 10 mm.

A modular tool concept was chosen for the injection molding experiments where the cooling with straight bores in the cavity plate is the same for all three layouts. The cavity and the inserts for the core were made from H13 steel plate using traditional machining methods. The insert for conformal cooling was manufactured by EBM using the Arcam H13 Tool Steel, and 1 mm was added for machining allowance (Figures 7 and 8). Furthermore, eight ejector pins with a diameter of 2.5 mm were used in order to facilitate an even pressure on the part while ejecting, see Figure 9 for a part example and the core plate with ejector pins.

Table I EBM injection mold materials

	Arcam low alloy steel	Arcam H13 tool steel
Particle size (μm)	<106	<106
Layer thickness (μm)	0.1	0.1
Tensile strength (MPa)	290	1,400
Impact resistance (J (KU))	7	8-10
Hardness	180-220 HB	46-50 HRC
Thermal expansion coefficient (× 10^{-6})	14.0	14.0
Density (percent)	>99.9	>99.9 (7.905 g/cm^3)[a]

Note: [a]Swedish Ceramic Institute, November 2005
Source: Arcam AB

Figure 2 Approximate part design

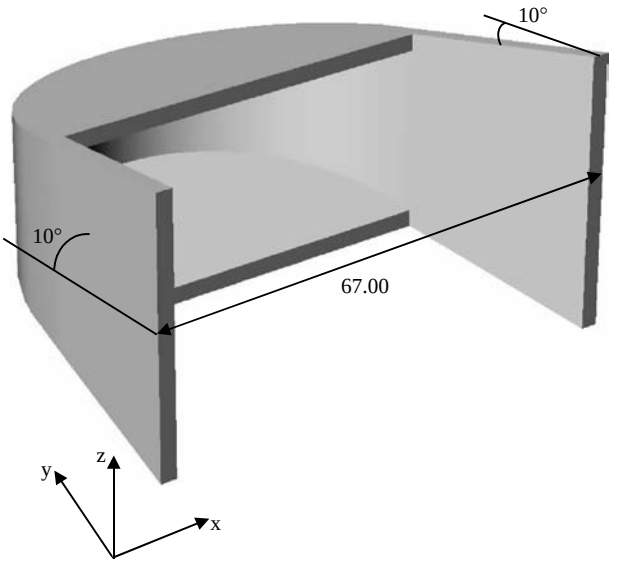

Note: Wall thickness is 3.0 mm and the draft angle indicated is 10˚. The target dimension between the two braces is 67.00 mm

Figure 3 Undeformed part (solid line) designed in the CAD system and deformed part (dashed line) after manufacturing

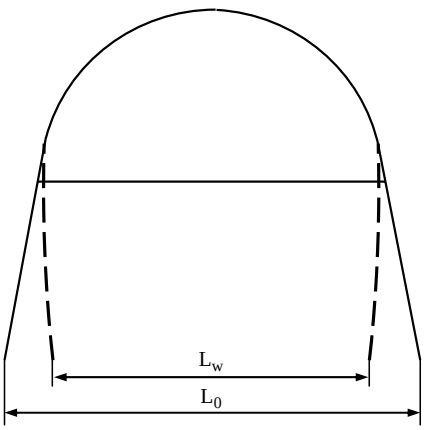

Note: The warpage is calculated as a percentage of the undeformed distance, L_0, versus the deformed distance L_w

Figure 4 Conventional cooling with straight bores around the cavity

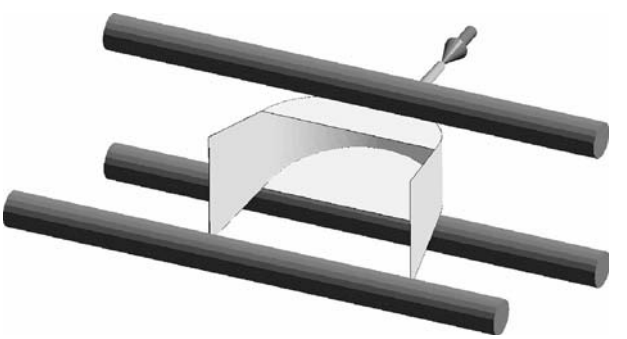

Figure 5 Conventional cooling with straight bores in the A-plate (cavity plate) and a baffle in the B-plate (core plate)

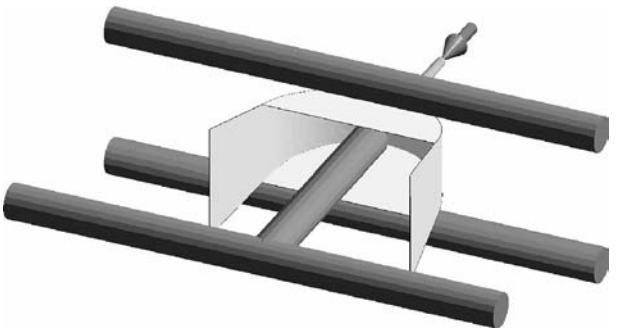

Figure 6 Freeform fabricated cooling in the B-plate and straight bores in the A-plate

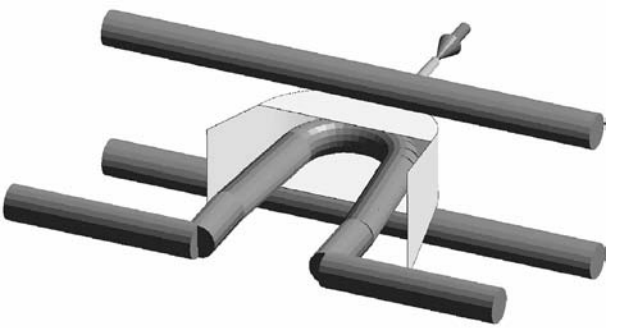

Figure 7 Insert fabricated by EBM with 1 mm machinery allowance

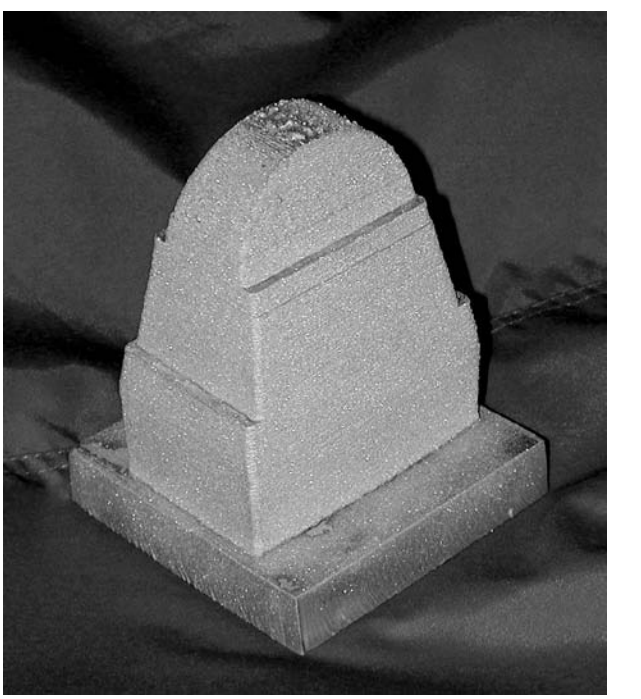

Figure 8 Machined insert, with conformal cooling, used in the modular tool

Mold trial

The injection molding experiments were carried out using an Arburg machine with a clamp force of 85 metric tons. Before the actual test parts were manufactured, the machine was running a while in order to get the tool temperature and machine configuration in steady-state condition. A temperature controller was set to keep the coolant temperature constant at 60°C.

The cooling time was altered one second at a time from 1 to 18 s. For every time step, ten scrap parts were manufactured before another five examples were manufactured with the purpose to determine the dimensional accuracy as a function of cooling time. After ejection, every part was given a unique identification, and the parts were set aside for post-cooling for 36 h, before they were measured with a sliding caliper. In order to confirm the measurement by the sliding caliper, some of the parts were measured with a non-contact 3D digitizing equipment, ATOS III from GOM (www.gom.com). The measurements were then analyzed in geomagic qualify from raindrop geomagic (www.geomagic.com), and the results from this study showed good agreement with the caliper measurements.

More than 3,000 parts were produced with the insert manufactured by EBM, and no visual signs of wear could be detected after the experiments.

Numerical model

In order to assure the unanimity between the actual tool and the model used for the simulations, the dimensions of the tool

Figure 9 Core plate with ejector pins, insert fabricated by EBM with a molded part placed in front

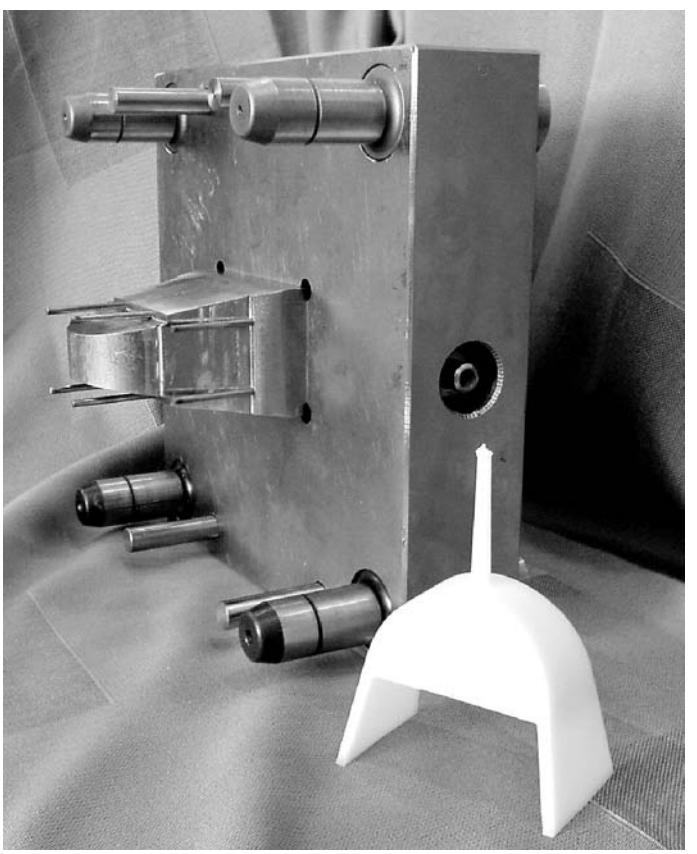

cavity were measured with conventional measuring instruments as well as a the 3D digitizing equipment described above. The measured dimensions were then used for the model created using the injection molding analysis software. The process parameters in the model were set as for the experiments (Table II). The shear viscosity versus shear rate is shown in Figure 10. The pvT diagram representative for the grade POM used is shown in Figure 11.

A total number of 6,500 elements, both shell and beam elements, were used with a nominal value of 1.5 mm for the edge length and with further refinement at the gate area.

As for the experiments, the three cooling-channel layouts were analyzed for the entire experimental cooling-time range, from one to 18 s. The warpage in the *x*-direction, see Figure 3 and equation (1), for the center of the braces was extracted from the simulation results, and the warpage values for both the experimental and numerical tests are shown in Figure 12.

Results and discussion

As seen in Figure 12, using conformal cooling channels created by EBM gives less warpage with the same or even shorter cycle time in comparison with conventional methods. However, it should be noted that the experimental results with the local minima are not recognized in the numerical tests. The dispersion of the results from the mold trials is presented in Table III, and it shows an acceptable statistical behavior.

In contrast for the numerical tests, the baffle cooling channel design is approximately as efficient as the FFF cooling channel design when using cooling times shorter than 7 s in the mold experiments. This discrepancy could be due to the visco-elastic effect in the part when ejecting and for some test parts, penetration marks from the ejector pins were recognized when using a short cooling time. In the numerical tests however, ideal ejection is presumed with no friction or sticking in the mold.

The correlation between the numerical and experimental results is not perfect. The experimental tests imply that there are local minima for the cooling time at 7 and 8 s for the three designs. This is indeed interesting, since on the shop floor, the experience is that a longer cooling time usually implies a better dimensional accuracy. Nevertheless, the simulations do not capture these minima, and the discrepancy is not yet fully understood.

A possible contributor to the difference could be the material model used in the software. For the heat capacity over the temperature range, a constant value is proposed and used in the software. POM materials typically show a discontinuity at the crystallite melting temperature due to the phase transformation between the liquid and solid states, since they contain both amorphous and crystalline portions, i.e. they are semi-crystalline polymers (Michaeli, 1995). A differential scanning calorimetry (DSC) study of the POM would reveal that the heat capacity is highly temperature-dependent, and since the heat capacity directly influences the temperature distribution in the polymer, it is of the highest importance to have a proper model for the heat capacity.

Another possible cause for the minima at cooling times around 7-8 s could be due to extra-ordinary balanced residual stresses through the part thickness at ejection at a cooling time of 7-8 s. However, this could not be confirmed by analyzing the frozen layer in the simulations, or the mold and part temperature differences. They showed a typically

Table II Process parameters

Part material	POM copolymer
Part volume	20.4 cm^3
Injection temperature	220°C
Ejection temperature	120°C
Filling time	1 s
Packing time	3 s
Packing pressure	20 MPa
Coolant temperature	60°C
Ambient temperature	25°C
Specific heat, mold	460 J/kg°C[a]
Conductivity, mold	25 W/m°C[a]
Density, mold	7,905 kg/m^3

Source: [a]Arcam AB

Figure 10 The viscosity as a function of the shear rate for different temperatures

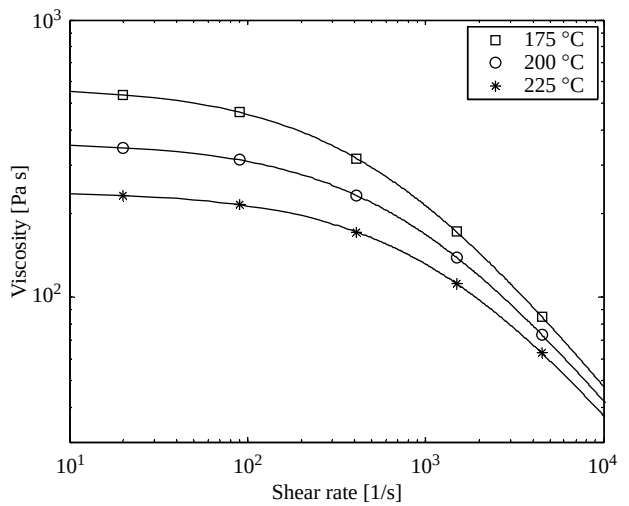

Note: Data from Coretech System

Figure 11 The specific volume as a function of the temperature for different pressures (pvT diagram)

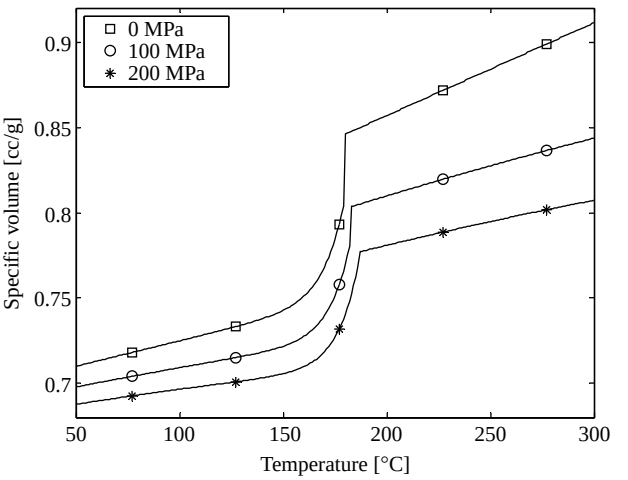

Note: Data from Coretech System

Figure 12 Numerical and experimental values of the warpage, here shown in percentage, between the braces for the three layouts. (**Note:** The experimental values are the arithmetic mean of the warpage at each time step)

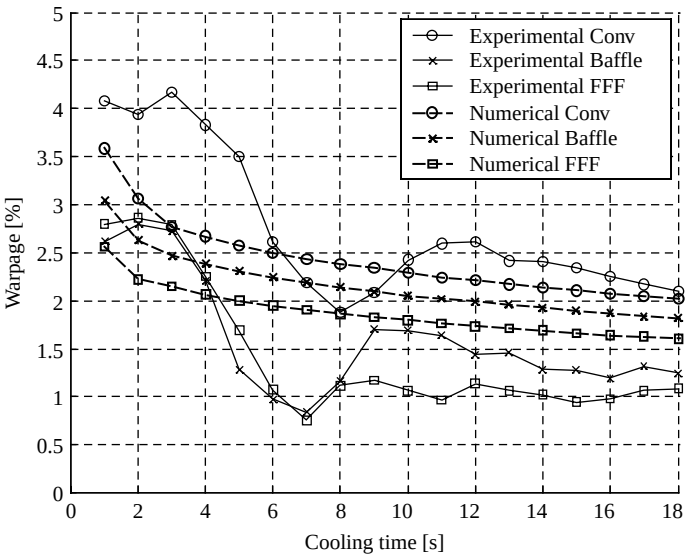

Table III Arithmetic mean of the warpage for the different mold trials, the standard deviation and the ratios

		Cooling time setting																	
		1	2	3	4	5	6	7	8	9	10	11	12	13	14	15	16	17	18
Conv	Mean	4.08	3.93	4.16	3.82	3.50	2.61	2.19	1.88	2.08	2.41	2.59	2.61	2.41	2.40	2.34	2.25	2.17	2.09
	SD	0.20	0.39	0.09	0.13	0.08	0.09	0.11	0.08	0.06	0.07	0.09	0.05	0.04	0.07	0.05	0.05	0.05	0.10
	SD/mean	0.05	0.10	0.02	0.03	0.02	0.04	0.05	0.05	0.03	0.03	0.03	0.02	0.01	0.03	0.02	0.02	0.02	0.05
Baffle	Mean	2.61	2.79	2.72	2.20	1.28	0.98	0.84	1.15	1.70	1.68	1.64	1.43	1.46	1.28	1.27	1.19	1.31	1.24
	SD	0.24	0.11	0.19	0.15	0.12	0.09	0.13	0.02	0.10	0.09	0.15	0.08	0.07	0.05	0.08	0.09	0.07	0.09
	SD/mean	0.09	0.04	0.07	0.07	0.10	0.09	0.15	0.02	0.06	0.05	0.09	0.06	0.05	0.04	0.07	0.08	0.05	0.07
FFF	Mean	2.80	2.86	2.79	2.25	1.68	1.07	0.75	1.11	1.17	1.06	0.97	1.14	1.06	1.02	0.94	0.98	1.06	1.07
	SD	0.13	0.09	0.18	0.10	0.13	0.13	0.09	0.10	0.10	0.05	0.12	0.10	0.07	0.12	0.04	0.04	0.07	0.06
	SD/mean	0.05	0.03	0.07	0.04	0.08	0.12	0.12	0.09	0.09	0.04	0.13	0.09	0.07	0.12	0.04	0.05	0.06	0.06

asymptotic behavior, like the one presented for the simulations in Figure 12. The software calculates shrinkage and warpage until post-shrinkage has occurred, i.e. until the part has reached thermal equilibrium with the surrounding air, and all the stresses are fully released and this implies that the kind of balanced cooling described above should be recognized in the software.

The specific heat capacity and the conductivity of the mold are set as for conventional H13 steel, but these values have not been experimentally verified. However, the density and thermal diffusivity have been tested for the Arcam H13 Tool Steel, and these tests show that the density and thermal diffusivity correspond to those of conventional H13 tool steel (Larsson, 2003). A slight difference in actual values for this insert will most probably have only a small influence and will not explain the minimum points.

Conclusions and future work

The results show that conformal FFF cooling channels manufactured by EBM constitute a viable method to improve the dimensional accuracy and cooling time in comparison with cooling layouts manufactured by conventional machining. No difference in machinability was detected for the EBM H13 insert in comparison with the inserts manufactured from H13 steel plate.

However, further research in this area should comprise new analysis with an improved heat capacity model for the polymer. At this time, the software does not have the possibility to fully describe the complex nature of the heat capacity, but developments are being conducted in order to release a version with this function as soon as possible.

In this study, a parametric study was done with the cooling time as variable and the warpage as objective function. Further, research should include design of experiments (DOE) in order to investigate the influence of more parameters, e.g. melt temperature, coolant temperature, packing pressure, etc. and possible interaction effects.

FFF gives the opportunity to create conformal cooling channels, but in this paper, the possibility to create innovative cooling channel cross sections has not been studied. The EBM process has limitations regarding small features such as diameters, radii, etc. but most possibly, further improvement

of the cooling efficiency could be achieved with new types of cross sections. The circular hole is indeed much less efficient regarding heat transfer in comparison for example with a crumpled cross section, due to the larger area for the latter.

References

Cormier, D., Harrysson, O. and West, H. (2004), "Characterization of H13 steel produced via electron beam melting", *Rapid Prototyping Journal*, Vol. 10 No. 1, pp. 35-41.

Dalgarno, K.W. and Goodridge, R.D. (2004), "Compression testing of layer manufactured metal parts: the RAPTIA compression benchmark", *Rapid Prototyping Journal*, Vol. 10 No. 4, pp. 261-4.

Dalgarno, K. and Stewert, T. (2001), "Production tooling for polymer moulding using the RapidSteel process", *Rapid Prototyping Journal*, Vol. 7 No. 3, pp. 173-9.

Davis, K.R., Gornet, T.J. and Vicars, J.W. (2003), "High thermal conductivity tooling from laser direct metal deposition", *Proceedings of the 1st International Conference on Advanced Research in Virtual and Rapid Prototyping, VRAP 2003, Portugal*, pp. 503-7.

Dormal, T. (2003), "Rapid tools for injection molding", *Proceedings of the 4th National Conference on Rapid and Virtual Prototyping and Applications, UK*, pp. 139-51.

Karapatis, N.P., van Griethuysen, J-P.S. and Glardon, R. (1998), "Direct rapid tooling: a review of current research", *Rapid Prototyping Journal*, Vol. 4 No. 2, pp. 77-89.

Klocke, F., Celiker, T. and Song, Y-A. (1995), "Rapid metal tooling", *Rapid Prototyping Journal*, Vol. 1 No. 3, pp. 32-42.

Knirsch, J. (2003), "RSP tooling – rapid production tooling", *Proceedings of the 1st International Conference on Advanced Research in Virtual and Rapid Prototyping, VRAP 2003, Portugal*, pp. 553-9.

Kruth, J.P., Wang, X., Laoui, T. and Froyen, L. (2003), "Lasers and materials in selective laser sintering", *Assembly Automation*, Vol. 23 No. 4, pp. 357-71.

Larsson, M. (2003), *Arcam H13 Tool Steel Specification Sheet*, Arcam AB, Gothenburg.

Menges, G., Michaeli, W. and Mohren, P. (2000), *How to make Injection Molds*, Hanser Publishers, Munich.

Michaeli, W. (1995), *Plastic Processing – An Introduction*, Hanser Publishers, Munich.

Over, C., Meiners, W., Wissenbach, K., Lindemann, M. and Hammann, G. (2003), "Selective laser melting: a new approach for the direct manufacturing of metals parts and tools", *Proceedings of the 3rd Conference on Laser Assisted Net Shape Engineering, LANE 2003, Germany*, pp. 391-8.

ÓDonnchadha, B. and Tansey, A. (2003), "Conformally cooled metal composite rapid tooling", *Proceedings of the 1st International Conference on Advanced Research in Virtual and Rapid Prototyping, VRAP 2003 Portugal*, pp. 447-53.

Pelaingre, C., Velnom, L., Barlier, C. and Levaillant, C. (2003), "A cooling channels innovative design method for rapid tooling in thermoplastic injection molding", *Proceedings of the 1st International Conference on Advanced Research in Virtual and Rapid Prototyping, VRAP 2003, Portugal*, pp. 439-45.

Radstock, E. (1999), "Rapid tooling", *Rapid Prototyping Journal*, Vol. 5 No. 4, pp. 164-8.

Sachs, E., Wylonis, E., Allen, S., Cima, M. and Guo, H. (2000), "Production of injection molding tooling with conformal cooling channels using the three dimensional printing process", *Polymer Engineering and Science*, Vol. 40 No. 5, pp. 1232-47.

Segal, J.I. and Campbell, R.I. (2001), "A review of research into the effects of rapid tooling on part properties", *Rapid Prototyping Journal*, Vol. 7 No. 2, pp. 90-8.

Taminger, K.M.B. and Hafley, R.A. (2002), "Characterization of 2219 aluminum produced by electron beam freeform fabrication", *Proceedings of the 13th Solid Freeform Fabrication Symposium, USA*, pp. 482-9.

Wimpenny, D. (2003), "Rapid tooling options compared", *Proceedings of the 4th National Conference on Rapid and Virtual Prototyping and Applications, UK*, pp. 189-202.

Wimpenny, D.I., Bryden, B. and Pashby, I.R. (2003), "Rapid laminated tooling", *Journal of Materials Processing Technology*, Vol. 138, pp. 214-8.

About the authors

L-E. Rännar obtained an MSc degree at Blekinge Institute of Technology, Karlskrona, Sweden. He is currently a PhD student at the Norwegian University of Science and Technology where he is a part of the research group within the area of polymers and composites. He is also employed as an instructor at Mid Sweden University, where most of the research is carried out. L-E. Rännar is the corresponding author and can be contacted at: lars-erik.rannar@miun.se

A. Glad obtained an MSc degree at the Norwegian University of Science and Technology, Trondheim, Norway. He is currently a PhD student at the Norwegian University of Science and Technology where he is a part of the research group within the area of polymers and composites, in which most of his research is carried out. E-mail: anders.glad@ntnu.no

C-G. Gustafson is a Professor at the Norwegian University of Science and Technology and heading the research group in polymers and composites, since 1989. Professor Gustafson obtained an MSc at the Chalmers University of Technology, Gothenburg, Sweden, in 1969 and a PhD at the Royal Institute of Technology, Stockholm, Sweden, in 1988. His main research is focused on composites and the processing of filled polymers. E-mail: claes.g.gustafson@ntnu.no

Paper D

Improvement in Surface Heat Distribution of Injection Molding Tooling using Conformal Cooling Channels

L-E Rännar and C-G Gustafson

submitted to the Journal of Materials Processing Technology

Improvement in Surface Heat Distribution of Injection Molding Tooling using Conformal Cooling Channels

LARS-ERIK RÄNNAR[1,2]

CLAES-GÖRAN GUSTAFSON[2]

[1)] *Mid Sweden University, Dept. of Engineering, Physics and Mathematics, Akademigatan 1, SE-831 25 Östersund, Sweden*

[2)] *Norwegian University of Science and Technology, Dept. of Engineering Design and Materials, Richard Birkelandsvei 2B, N-7491, Trondheim, Norway)*

Abstract

Heat distribution of a free-form fabricated (FFF) insert, with conformal cooling channels, has been compared with a baffle insert, machined by conventional methods. The inserts, used for injection molding, has been compared by using thermal imaging of the surfaces of the inserts after the ejection of the part and the study also includes numerical simulations. The effect on changing the coolant temperature in the inserts was investigated. The direct-metal rapid tooling (RT) method electron beam melting (EBM) was used for the manufacture of the FFF insert. Many other methods have been proven suitable for RT but few publications have been found where EBM has been used to manufacture injection molds. Using FFF inserts for injection molding can lead to reduced costs concerning the production time but also products with a better quality due to a better dimensional accuracy of the product. The study shows that the cooling efficiency of the FFF cooling layout is higher than for the traditionally cooled insert, although not as high as other in situ studies have shown.

Keywords

Injection molding, rapid tooling (RT), heat distribution, cooling efficiency, thermal imaging

1. Introduction

Injection molding is a process where a molten polymer is injected through a nozzle, sprue and gate into a cavity whereafter a hold pressure is applied in order to compensate for the volumetric shrinkage. The solidification starts immediately upon the injection of the melt into the cavity and due to polymer relaxation, differences in pressures and temperatures, the part exhibits shrinkage and warpage. Mold cooling is an important issue in order to minimize the warpage. The cooling channels are typically drilled straight bores and where core cooling can be achieved by using baffles, bubblers or high thermal conductivity inserts [1]. These methods can not achieve an optimal cooling effect due to restrictions imposed to the design of the cooling systems by means of ejector pins, parting planes and also by the geometric limitations from straight holes.

The invention of the stereolithography process (SLA) by Hull [2] cleared the way for a new technology called rapid prototyping (RP), or free-form fabrication (FFF). The process is additive, i.e. FFF joins together liquid, powder or sheets to form parts in different materials such as plastics, ceramics or metal alloys. The component is built by adding layer upon layer. The main benefits using FFF is the process ability to manufacture highly complex structures and features. In the recent years, several FFF methods have appeared in the market where metal alloys are used as building material and this has made it possible to manufacture tools for both low-volume production and full-scale production. This market segment is called rapid tooling (RT) [3]. A distinction between direct and indirect methods is made and usually indirect methods involve more sequences during manufacturing in comparison with direct methods. Many processes have been tried in order to manufacture injection molding tools and Sachs et.al. [4] showed that the indirect method 3D printing improved the part quality and decreased the cycle time in comparison with traditionally manufactured cooling channels. The transient behavior at the start of the molding was also decreased when using FFF cooling channels. Dalgarno and Stewart [5] showed that the RapidSteel process was able to manufacture conformal cooling channels and they reported limitations in terms of its ability to manufacture small features. Wimpenny et.al. [6] used rapid laminated tooling and showed improved part quality and reduced cycle times as well as reductions of costs and lead-times in the manufacturing process in comparison with conventional machined tools. In order to ensure the viability of RT, Donnchadha [7] proposed a modular concept where parts of the tool was manufactured by traditional methods and inserts was made by selective laser sintering (SLS).

The electron beam melting method (EBM) is well suited for a variety of materials and Taminger and Hafley [8] used aluminium wire which was fed into the pool on the metallic substrate. It differs from other direct-metal fabrication methods since it makes use of an electron beam and Gibbons and Hamsell [9] showed that a significantly higher cooling efficiency was achieved by using a flood cooled insert manufactured by EBM. This resulted in reduced cooling times and a more homogenous temperature distribution in the mold but the effect of changing the coolant temperature was not investigated. EBM is capable of creating fully dense forms without any binding agents and the mechanical properties have been investigated and compared with competitive methods. Dalgarno and Goodridge [10] found that the H13 tool steel manufactured by EBM showed a consistent modulus when compressing it up to a level of 1100 MPa and Cormier et.al. [11] showed that standard recommended process conditions made it possible to create parts with virtually no porosities and with full interlayer bonding.

Few studies have been found in the literature were EBM have been used for the manufacture of inserts for injection molding. The aim with the present study is to compare the surface heat distribution of inserts manufactured by EBM with inserts manufactured by traditional methods. The inserts have been compared by using thermal imaging of the surfaces, after the ejection of the part, and the study also includes numerical simulations. The impact of changing the coolant temperature in the inserts has been investigated. Two different channel designs are considered, one conventional using straight holes and a baffle (MD1) and one FFF design where the core cooling is conformal to the inner surface of the part (MD2).

2. Experimental

2.1. Mold design and manufacture

The geometry of the part for this study is shown in Fig. 1. The part thickness of 3 mm was chosen to generate a higher thermal load for the cooling system to remove. A modular tool concept was chosen where the cooling channels in the cavity plate are the same for both layouts but where the core insert is interchangeable between the two layouts MD1 and MD2. Fig. 2 shows the geometry of the inserts. The distance between the surface of the insert and the conformal cooling channel is approximately the same as the cooling channel diameter for both layouts, 10 mm. The tapered runner has a diameter of 2.5/4 mm and eight ejector pins with a diameter of 2.5 mm are used in order to facilitate an even edge pressure on the part while ejecting. The MD2 insert was manufactured by the Arcam S12 EBM system using the Arcam H13 tool steel and 1 mm was added for machining allowance while the MD 1 insert was manufactured from a H13 tool steel plate using conventional methods. The insert as fabricated by EBM is shown in Fig. 3 and the core plate with the MD2 insert is shown in Fig. 4. EBM is able of creating fully dense forms without any binding agents using electron beam melting of metal powder. The beam is formed by emitting electrons from a Tungsten filament heated up to 2,500°C using a voltage difference up to 60 kV. The focus and position of the beam on the building table is adjusted by two different magnetic fields and the beam then selectively welds the powder in the layer by heat generated from the loss of the electrons kinetic energy as these hits the powder. The building table is kept in vacuum and surrounding powder is sintered and acts as support for the successive layers. When the building is complete, the part is cooled down and unbound powder is removed by sand blowing and the part is then ready for further processing such as drilling, high-speed milling, electric discharge machining etc.

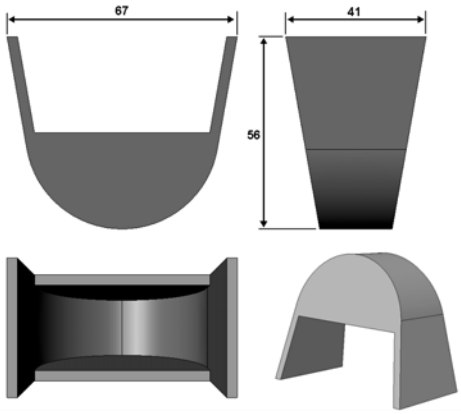

Fig. 1 Approximate part design. Draft angles are 10° and wall thickness is 3 mm.

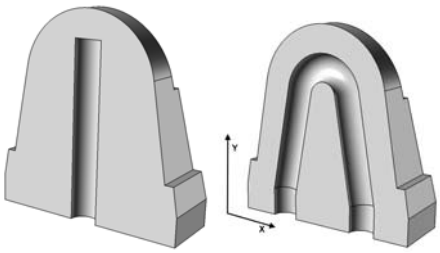

Fig. 2 Geometry of the two inserts. MD1 with the baffle is to the left and MD2 with the conformal channel is to the right.

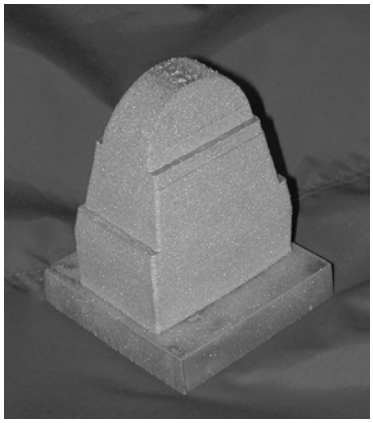

Fig. 3 The MD2 insert as fabricated by EBM with 1mm machining allowance.

Fig. 4 The core plate with the MD2 insert.

2.2. Molding trials

The trials were performed on an Arburg machine with a clamp force of 85 metric tons and the process parameters used in the experiment are shown in Table I. The coolant temperature for the core was increased from 33°C to 70°C and for each temperature setting, 30 parts were manufactured in order to attain steady-state. Thereafter the molding trial was performed, imaging the insert in the xy-plane (Fig. 2) after each ejection. Five images were taken for each temperature setting and the images were recorded five seconds after the ejection of the part since this time was needed for the opening of the safety gate of the Arburg machine.

Table I - Process parameters.

Part material	POM (BASF Ultraform N2320 003)
Melt temperature	220 [°C]
Cavity temperature	70 [°C]
Core temperature	33-70 [°C]
Coolant flow rate	133 [cm^3/s]
Cooling time	7 [s]
Filling time	1 [s]
Filling pressure	110 [MPa]
Packing time	3 [s]
Packing pressure	40 [MPa]

2.3. Experimental set-up

The inlet temperature of the coolant was measured continuously (registering minimum, maximum and mean temperature) using a thermocouple of type K (Ahlborn, Therm2280-3) and this thermocouple was also used in order to calibrate the emissivity of the inserts. A ThermaCAM E2 from FLIR Systems with a 160x120 pixel detector and an accuracy of ±2°C was used for the thermal imaging. The experimental set-up is shown in Fig. 5.

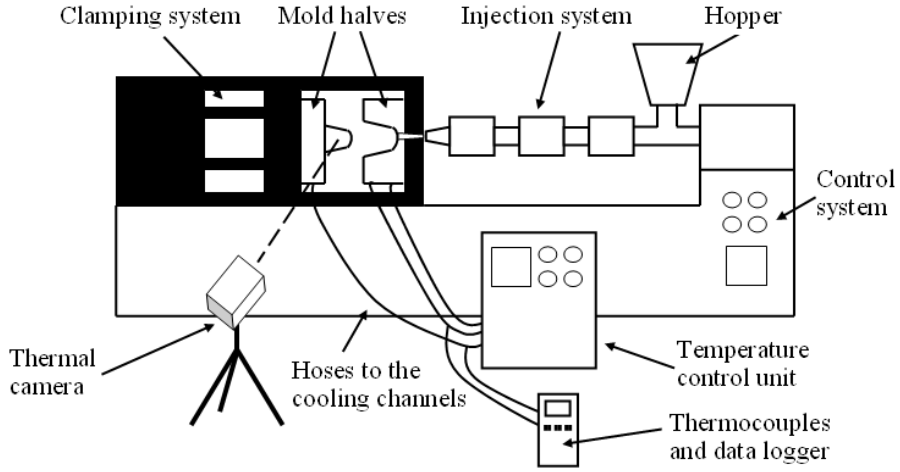

Fig. 5 Experimental set-up.

3. Numerical model

Moldex3D, the commercial software for injection molding simulation, was used to determine the temperature distribution of the inserts. The process parameters in the numerical trial were set as for the experiments (Table I) and the material data used is shown in Table II. A total number of 6,500 elements, both shell and beam elements, were used with a nominal edge length of 1.5 mm. The dimensions of the inserts and the cavity were measured using a 3D digitizing equipment (ATOS III, GOM) as well as conventional measuring equipments and these measurements were then used for creating the model in the injection molding simulation software.

Table II –Material data.

Part material	POM (BASF Ultraform N2320 003)
Volume	20.4 [cm^3]
Melt flow index	7.5 [g/10min][a]
Ejection temperature	118 [°C][a]
Freeze temperature	160 [°C][a]
Thermal conductivity	2 [kJ/kg°C][a]
Specific heat	0.2 [W/m°C][a]
Mold material	H13
Specific heat	460 [J/kg°C][b]
Thermal conductivity	25 [W/m°C][b]
Density	7905 [kg/m^3][b]
Cooling channel diameter	10 [mm]
Cooling channel offset	10 [mm]
Runner dimension	2.5/4 [mm]
Source:	[a]Moldex3D, [b]Arcam AB

The theory behind the process of injection molding can be described as a three-dimensional, transient problem with a moving melt front where non-Newtonian flow and coupled heat transfer are also involved. In Moldex3D, the temperature, pressure, velocity fields etc. (the filling, packing and cooling processes) are obtained for each point in the cavity by using a hybrid finite element/finite difference method. A control volume method is applied to find the melt front position and also to calculate the temperature and pressure profile at any instant during the filling process. The boundary element and finite difference method are applied to carry out the mold cooling analysis where the temperature of the cavity surface is obtained and these are then used as boundary conditions for the filling and packing analysis. The flow and thermal induced stresses are then used as initial conditions for the solid mechanics analysis using a linear thermo-viscoelastic model. The final displacements, both in-plane and in thickness direction, are then solved using a three-dimensional finite element method. [12-15]

The pressure and temperature dependency of the specific volume is modeled by a modified Tait equation (Eq 1-7) with 13 parameters:

$$\hat{V} = \hat{V}_0\left[1 - C\ln(1 + p/B)\right] + \hat{V}_t \tag{1}$$

$$\hat{V}_0 = \begin{cases} b_{1S} + b_{2S}\overline{T}\,, T \le T_t \text{ (solid state)} \\ b_{1L} + b_{2L}\overline{T}\,, T > T_t \text{ (melt state)} \end{cases} \tag{2}$$

$$B = \begin{cases} b_{3s}\exp(-b_{4S}\overline{T})\,, T \le T_t \text{ (solid state)} \\ b_{3L}\exp(-b_{4L}\overline{T})\,, T > T_t \text{ (melt state)} \end{cases} \tag{3}$$

$$\hat{V}_t = \begin{cases} b_7\exp(b_8\overline{T} - b_9 p)\,, T \le T_t \text{ (solid state)} \\ 0 \qquad\qquad\qquad\quad , T > T_t \text{ (melt state)} \end{cases} \tag{4}$$

$$\overline{T} = T - b_5 \tag{5}$$

$$T_t = b_5 + b_6 p \tag{6}$$

$$C = 0.0894 \tag{7}$$

where $\hat{V}$ is the specific volume, C is a universal constant [16], p is the pressure, T is the temperature, $b_{1\text{-}9}$ are material specific parameters and where T_t is equal to the transitions temperature. The values used in the analysis are shown in Table III. The shear rate and temperature dependency on the viscosity is modeled by a modified Cross model [17,18]:

$$\eta(T,\dot{\gamma}) = \frac{\eta_0(T)}{1+\left(\eta_0\dot{\gamma}/\tau^*\right)^{1-n}} \tag{8}$$

with

$$\eta_0(T) = Be^{T_b/T} \tag{9}$$

Where $\dot{\gamma}$ is the shear rate, n is the power law index, η_0 is the zero shear viscosity, τ^* is a parameter describing the transition region between zero shear rate and the power law region of the viscosity curve and B is a constant related to the material. The values used in the analysis are shown in Table IV.

Table III – Constants used in the modified Tait model.

Constant	Value
$\mathbf{b_{1S}}$	7.49e-4 [m^3/kg]
$\mathbf{b_{2S}}$	2.98e-7 [m^3/kg K]
$\mathbf{b_{3S}}$	2.37e8 [Pa]
$\mathbf{b_{4S}}$	5.36e-3 [K^{-1}]
$\mathbf{b_{1L}}$	8.46e-4 [m^3/kg]
$\mathbf{b_{2L}}$	5.44e-7 [m^3/kg K]
$\mathbf{b_{3L}}$	1.28e8 [Pa]
$\mathbf{b_{4L}}$	4.21e-3 [K^{-1}]
$\mathbf{b_5}$	4.53e2[K]
$\mathbf{b_6}$	3.13e-8 [K/Pa]
$\mathbf{b_7}$	6.5e-5 [m^3/kg]
$\mathbf{b_8}$	1e-1 [K^{-1}]
$\mathbf{b_9}$	3.13e-9 [Pa^{-1}]
Source:	Moldex3D

Table IV – Constants used in the modified Cross model.

Constant	Value
n	1.49e-1 [-]
τ^*	3.28e5 [Pa]
B	1.88e-1 [Pa s]
$\mathbf{T_b}$	4.12e3 [K]
Source:	Moldex3D

4. Results

4.1. Molding trial results

The inserts were sand blown in order to get a smooth surface and thus a reliable value of the emissivity. The surface temperature of the inserts was measured by the thermocouple and at a temperature of 64°C, the emissivity of the surfaces was calibrated to 0.52. This value was then used for the thermal imaging of the inserts in the mold trials. The coolant temperature was continuously measured for each temperature setting and the measurements showed a ±1°C deviation around the target temperature.

The surface heat distribution from the trial is shown in Fig. 6. The arithmetic mean value of the maximum surface temperatures in the target circle from the thermal images (five images for each coolant temperature setting) is plotted against the coolant temperature. The 95% confidence interval is also plotted for each coolant temperature setting. Some of the heat distribution images are shown in Figs. 7-8 and in these figures, the highest temperature in the target circle for each image is shown in the upper right corner of each image.

In order to ensure that the temperature differences between the layouts MD1 and MD2 are statistically significant, an Analysis of Variance (ANOVA) was carried out. Table V shows the arithmetic mean difference and the 95% confidence interval for the different coolant temperature settings.

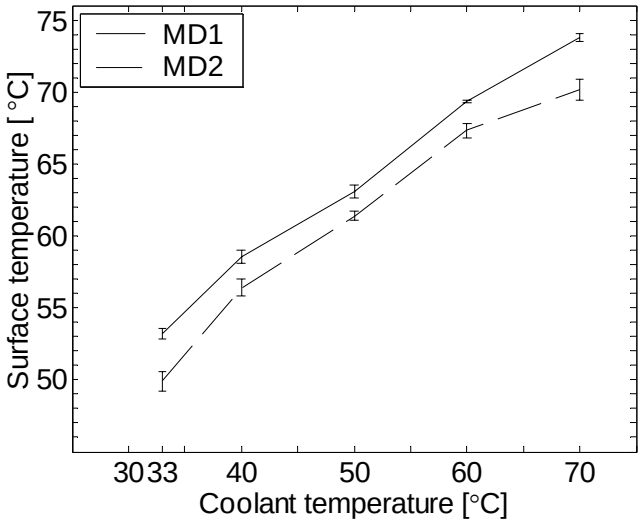

Fig. 6 The arithmetic mean value of the maximum surface temperatures obtained from the mold trials plotted against coolant temperature.

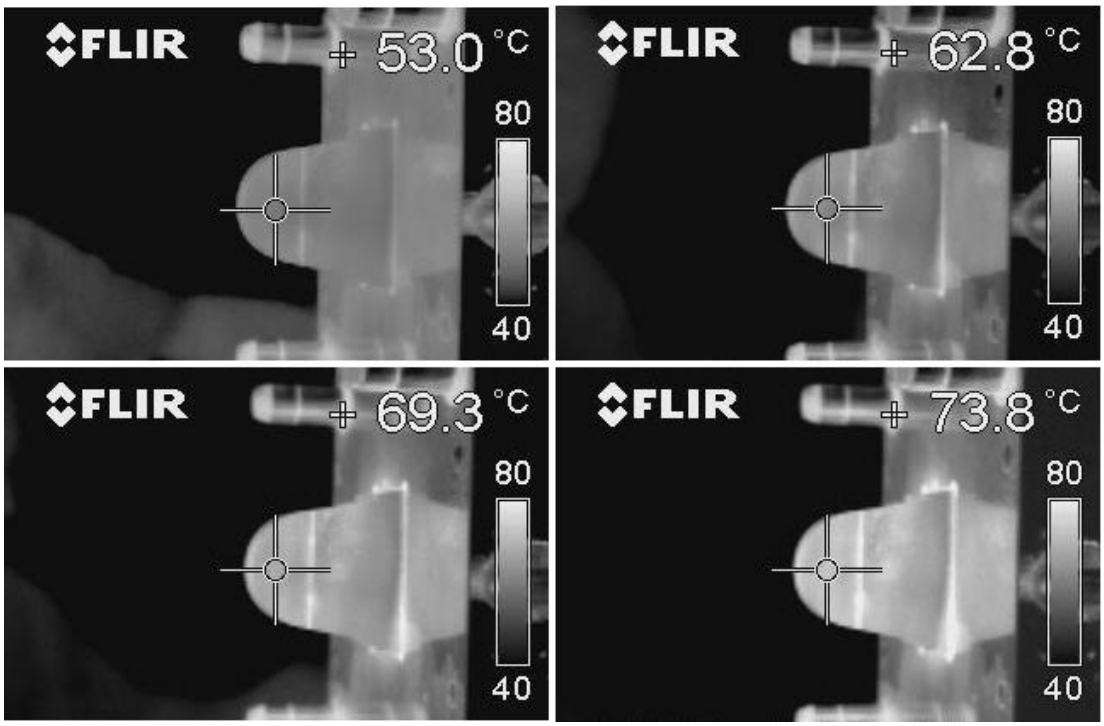

Fig. 7 Surface heat distribution for MD1 obtained from the mold trial, coolant temperature 33, 50, 60 and 70°C.

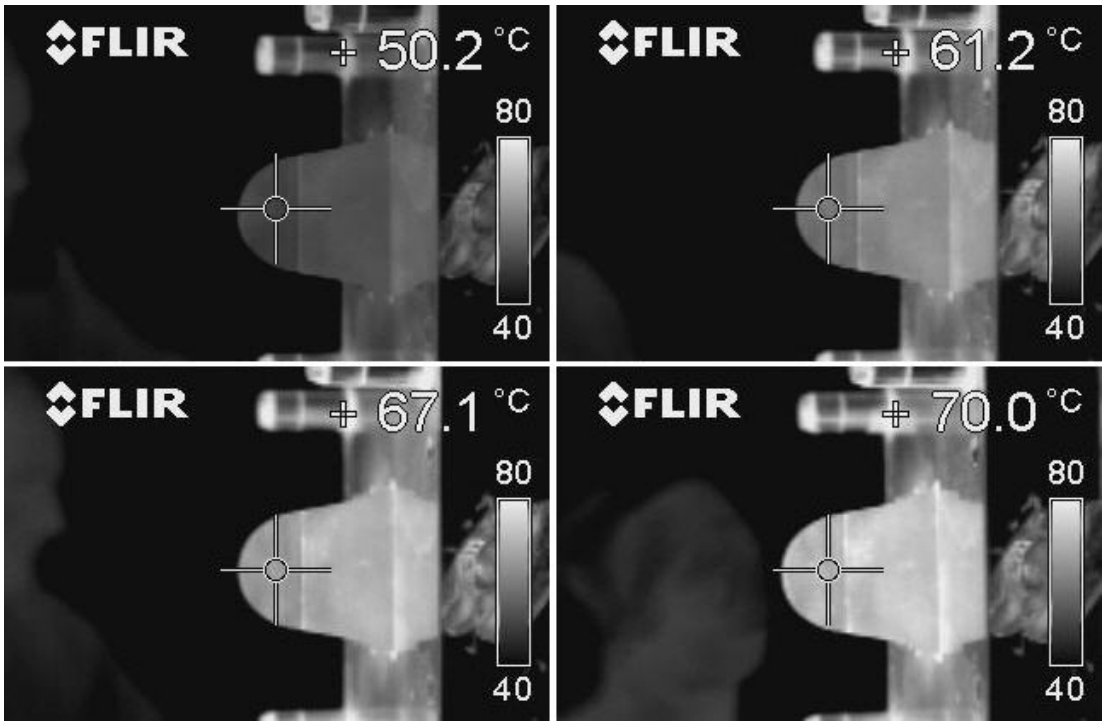

Fig. 8 Surface heat distribution for MD2 obtained from the mold trial, coolant temperature 33, 50, 60 and 70°C.

Table V – Statistical data for the mold trial showing the arithmetic mean difference and the 95% confidence interval for the different coolant temperature settings.

Coolant temperature	**33°C**	**40°C**	**50°C**	**60°C**	**70°C**
$\overline{MD1} - \overline{MD2}$	3.32	2.14	1.70	2.02	3.60
95% Confidence Interval	[2.66 3.98]	[1.50 2.78]	[1.23 2.17]	[1.61 2.43]	[2.96 4.24]

4.2. Numerical results

The surface temperature of the inserts was analyzed by extracting the highest element temperature in a circle of the same size as the target circle in the thermal images, see Fig. 9. This in order to compare the results obtained from the thermal images where the maximum temperature plotted in the images is the maximum temperature of a single pixel within the target circle in the image. In the simulations, the part is modeled and not the actual cavity so in Fig. 9, the cavity and core mold surfaces are represented by the front and back surface of the part.

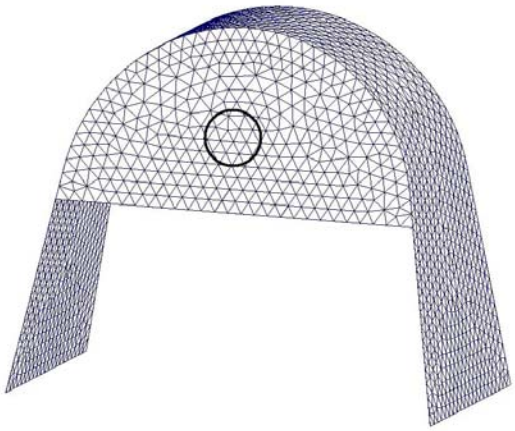

Fig. 9 Target circle for the analysis of maximum temperature for the simulations.

The surface heat distribution from the simulations is shown in Fig. 10 by plotting the maximum surface temperature against the coolant temperature. Table VI shows the difference between the maximum surface temperatures for different coolant temperature settings obtained from the simulations.

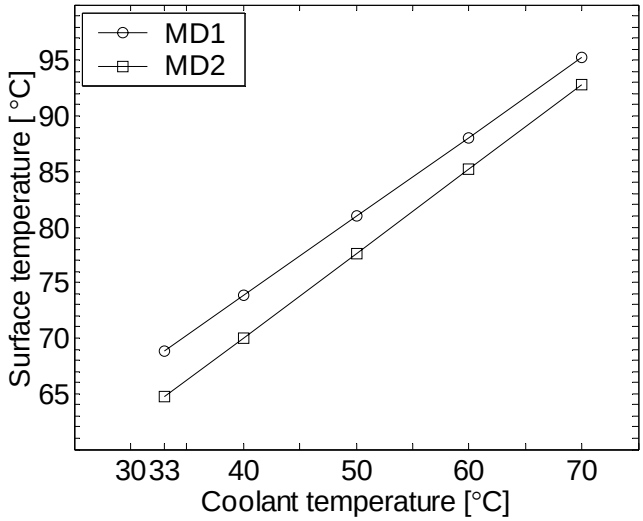

Fig. 10 The maximum surface temperatures obtained from the simulations plotted against coolant temperature.

Table VI – The difference between the maximum surface temperatures for different coolant temperature settings obtained from the simulations.

Coolant temperature	**33°C**	**40°C**	**50°C**	**60°C**	**70°C**
$MD1_{max}$-$MD2_{max}$	4.11	3.78	3.30	2.84	2.38

As seen in Figs. 6 and 10, the offset between the simulated results and the results obtained from the experiments are ~15-21°C for cooling design MD1 and ~14-23°C for cooling design MD2.

5. Discussion

As seen from Figs. 6-8 the free-form fabricated insert is more efficient than the baffle cooling design. The mean values of the maximum temperatures are between 1.70-3.60°C less for cooling layout MD2 than for cooling layout MD1. The surface temperature of MD2 is more even than that of MD1. The difference between the layouts is statistically significant as shown in Table III but it is not as considerable as other in situ studies have shown. Most likely the geometry chosen for this experiment is not as sensitive to the mold cooling and the results from the other studies are all based on geometries where it is not as easy to remove the heat from the core. Sachs et.al. [4] showed a 40°C difference between a conventional layout and a conformal layout using a ring-shaped geometry and Wimpenny et.al. [6] studied a beaker tool and showed a 10-15°C decrease of the average insert temperature in favor of a free-form fabricated spiral cooling design. Gibbons and Hansell [9] also studied a beaker geometry and found a 20°C difference between the core temperatures of a baffle and a free-form fabricated layout. The influence of emissivity is minimized since both inserts were sand blown and the calibration using the thermocouple resulted in the same emissivity value for both inserts.

As for the experiments, the free-form fabricated design is more efficient than the baffle cooling design but the maximum temperatures obtained from the simulations are higher than those obtained from the experiment. One reason for this offset is the cycle averaged principle used by the software [19]. When the injection molding process is in steady-state, the mold surface temperature will fluctuate periodically over time during the process due to the interaction between the hot melt and the cold mold, see Fig. 11. In order to reduce the computation time for this transient process, a cycle averaged temperature that is invariant with time is introduced for the mold but the transient state is still considered for the polymer. Hence, the temperatures of the mold surface obtained from the simulations are the cycle averaged temperatures while the results from the experiments correspond to the lowest temperature in Fig. 11.

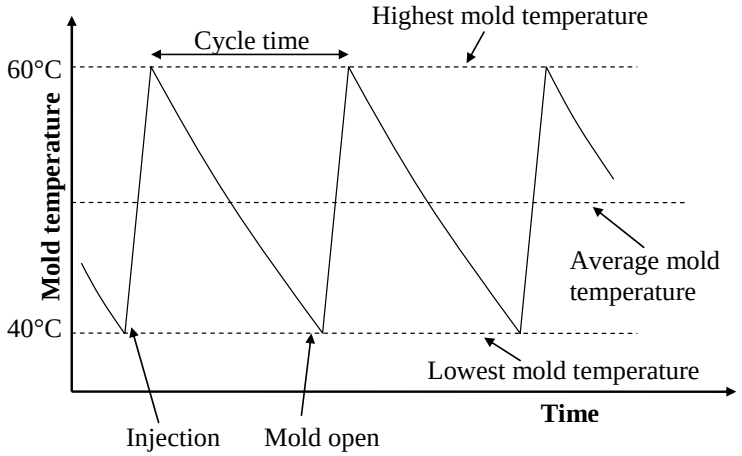

Fig. 11 Typical mold temperature variations.

As seen in Table V and VI, the difference of the surface temperatures at the same cooling time is higher in the simulations than for the experiments. Most likely this is due to the uncertainty in the values of the material properties and the process parameters used in the simulations. Thermal conductivity and heat capacity of mold and polymer, coolant flow rate, melt temperature etc. all influences the temperature profile obtained in the simulations and hence they will also contribute to an inaccurate result if they are not properly related to the materials used in the experiment.

6. Conclusions

There are many opportunities to affect the core temperature on the shop floor and in this work, the influence of changing the coolant temperature was investigated. Changing melt temperature, injection speed, cooling time etc. all affects the core temperature but as for the coolant temperature, these changes can affect the part quality as well. Lower melt temperature generates a higher degree of orientation of the molecules which can cause the part to warp more easily and increasing the cooling time leads to a longer cycle time which has a negative impact on the productivity. In this experiment, no visual surface defects on the manufactured parts was detected and consequently, decreasing the mold temperature from the recommended interval of 60-100°C is one viable way of decreasing the core temperature. The effect of how the core temperature affects the warpage has however not been investigated and this will be one of the studies that the authors will continue with.

References

[1] G. Menges, W. Michaeli, P. Mohren, How to make injection molds, Hanser Publishers, Munich, 2000
[2] H. W. Hull, Apparatus for production of three-dimensional objects by stereolithography, patent, 457330, 1984
[3] T. T. Wohlers, Wohlers Report 2005, Wohlers Associates, Fort Collins, 2005
[4] E. Sachs, E. Wylonis, S. Allen, M. Cima, H. Guo, "Production of injection molding tooling with conformal cooling channels using the three dimensional printing process", Polymer Engineering and Science, 40(5), (2000), 1232-1247
[5] K. Dalgarno, T. Stewart, "Production tooling for polymer moulding using the RapidSteel process", Rapid Prototyping Journal, 7(3), (2001), 173-179
[6] D. I. Wimpenny, B. Bryden, I. R. Pashby, "Rapid laminated tooling", Journal of Materials Processing Technology, 138, (2003), 214-218
[7] B. Ó. Donnchadha, A. Tansey, "Conformally cooled metal composite rapid tooling", in: 1:st International Conference on Advanced Research in Virtual and Rapid Prototyping, Leiria, Portugal, 1-4 October, 2003, 447-453
[8] K. M. B. Taminger, R. A. Hafley, "Characterization of 2219 aluminum produced by electron beam freeform fabrication", in: 13:th Solid Freeform Fabrication Symposium, U.S.A., 2002, 482-489
[9] G. J. Gibbons, R. G. Hansell, "Direct tool steel injection mould inserts through the Arcam EBM free-form fabrication process", Assembly Automation, 25(4), (2005), 300-305
[10] K. W. Dalgarno, R. D. Goodridge, "Compression testing of layer manufactured metal parts: the RAPTIA compression benchmark ", Rapid Prototyping Journal, 10(4), (2004), 261-264
[11] D. Cormier, O. Harrysson, H. West, "Characterization of H13 steel produced via electron beam melting", Rapid Prototyping Journal, 10(1), (2004), 35-41
[12] R.-Y. Chang, S.-Y. Chiou, "Integral Constitutive model (K-BKZ) to Describe Viscoelastic Flow in Injection Molding", International Journal of Polymer Processing, 9(4), (1994), 365-372
[13] C. L. Tucker, (Ed.), Fundamentals of Computer Modeling for Polymer Processing; Hanser Publishers: Munich, 1989.
[14] R.-Y. Chang, S.-Y. Chiou, "A Unified K-BKZ Model for Residual Stress Analysis of Injection Molded Three-Dimensional Thin Shapes", Polymer Engineering & Science, 35(22), (1995), 1733-1747
[15] H. Schlichting, Boundary-Layer Theory, Springer, Berlin Heidelberg, 2000
[16] R. Simha, P. S. Wilson, O. Olabisi, "Pressure-volume-temperature properties of amorphous polymers: empirical and theoretical predictions ", Colloid and Polymer Science, 251(6), (1973), 402-408
[17] M. M. Cross, "Relation between viscoelasticity and shear-thinning behaviour in liquids", Rheologica Acta, 18, (1979), 609-614
[18] C. A. Hieber, H. H. Chiang, "Shear-rate-dependence modeling of polymer melt viscosity", Polymer Engineering & Science, 32(14), (1992), 931-938
[19] T. H. Kwon, " Mold cooling system design using boundary element method", Journal of Engineering for Industry, 110(4), (1988), 384-394

Paper E

An Investigation of Optimal Process Settings in Injection Molding Using Inserts Manufactured by Rapid Tooling

L-E Rännar and C-G Gustafson

submitted to the Journal of Manufacturing Science and Engineering

An Investigation of Optimal Process Settings in Injection Molding Using Inserts Manufactured by Rapid Tooling

LARS-ERIK RÄNNAR[1,2]

CLAES-GÖRAN GUSTAFSON[2]

[1)] *Mid Sweden University, Dept. of Engineering, Physics and Mathematics, Akademigatan 1, SE-831 25 Östersund, Sweden*

[2)] *Norwegian University of Science and Technology, Dept. of Engineering Design and Materials, Richard Birkelandsvei 2B, N-7491, Trondheim, Norway)*

Abstract

Background. The effects on cycle time and warpage of different processing parameters in injection molding are rather complicated, and, typically, it is hard to balance the need for dimensional accuracy versus the cost-consuming cooling time. These effects are even harder to predict when new technologies in the injection-molding process are introduced. One such improvement is the use of conformal cooling channels preferably for inserts made by direct-metal rapid tooling (RT) of tool steel. Little effort has been put to investigating the settings of the process parameters in combination with inserts made by RT.
Method of approach. In this paper, a design of experiments (DOE) with a numerical model is carried out in order to investigate the influence of different process parameters and cooling channel designs on the dimensional accuracy of a test part. The test part was designed in order to replicate a common and important issue: inadequate cooling in deep cores. A conventional cooling channel layout, using straight holes and a baffle, was compared with a conformal layout in a fractional 2-factor analysis using seven process parameters.
Results. The four most important parameters in reference to both layouts influencing the dimensional accuracy of this test part were the cooling time and the temperatures of the melt, the cavity and the core.
Conclusions. The study shows the importance of choosing the right settings of different process parameters in order to use the effectiveness provided by free-form fabricated cooling channels. The results presented can be beneficial for manufacturers and producers using injection molding when they develop new mold tools and especially when they make parts where strict dimensional accuracy has to be applied.

Keywords

Rapid tooling (RT), injection molding, simulation, cooling, DOE

1. Introduction

Plastic manufacturers' ambition is to minimize the cycle time and maximize the quality of the part. The quality can be defined differently depending on the usage of the plastic part, but one common issue is the warpage which is a result of differential shrinkage of the final part. This shrinkage can be traced to several causes such as orientation effects, different temperature distributions through the part thickness and also across part areas [1]. The two last causes are highly dependant on the cooling channel layout in the same way that cycle time is. Ejector pins, parting lines, cores, etc., make it hard to design an efficient cooling system. In this paper a common and important issue for the mold industry is addressed: inadequate cooling in deep cores. Injection molding simulation has been a valuable tool for engineers since its introduction around 1975, and, theoretically, the injection-molding process is a three-dimensional, transient problem with a moving melt front where coupled heat transfer and non-Newtonian fluid flow are present. The software used to solve the equations describing the injection molding process in this study is Moldex3D from the Coretech System company (www.moldex3d.com).

The software simulates the injection molding filling, packing and cooling processes by obtaining the temperature, pressure, velocity fields etc. for each point in the cavity by using a hybrid finite element/finite difference method. A control volume method is applied to find the melt front position and also to calculate the temperature and pressure profile at any instant during the filling process. The boundary element and finite difference method are applied to carry out the mold cooling analysis where the temperature of the cavity surface is obtained and these are then used as boundary conditions for the filling and packing analysis. The flow and thermally induced stresses are then used as initial conditions for the solid mechanics analysis using a linear thermo-viscoelastic model. The final displacements, both in-plane and in thickness direction, are then solved using a three-dimensional finite element method. Studies related to warpage have shown that commercial softwares have some limitations in describing the true physics in the injection molding process. Ammar et.al. [2] studied the deformation of corner geometries and showed that the *spring forward effect* generally is the main contributor of corner deformation of injection molded parts and that asymmetric thermal effect not alone could explain the deformation. Jansen et.al [3] studied the effect of asymmetric cooling on part warpage and especially, the effect of mold temperature difference and packing pressure on warpage for unfilled amorphous materials. They showed that the warpage increased linearly with applied temperature difference between the mold halves but more interesting, that a plate geometry curved towards the cold side of the mold when a high holding pressures was applied. At lower pressures, the plate curved towards the hot side which is generally known and accepted. The influence of thermal parameters on the shrinkage and warpage has been discussed by many researches and Denizart et.al. [4] concludes that warpage predictions are sensitive the no-flow temperature. A small variation of 10°C was more important than anisotropic and heterogeneous values used in the three-dimensional thermo-elastic temperature-dependent model. Delauney et.al. [5] and Wu & Huang [6] studied the effect of mold deformation on the warpage prediction and the studies showed that packing pressure history applied to mold deformation analysis could improve the warpage predictions of the molded part.

For almost two decades, the possibility to manufacture physical models by rapid prototyping (RP), or free-form fabrication (FFF) has been used by industry in order to make the product development process more efficient. As the name RP implies, the initial use was to visualize

an idea or a product with a tactile model, and this model was often built by a rather simple material like plastic or paper. The method relies on the existence of a three-dimensional computer model which is sliced up into thin layers, and, by using an additive approach, the RP machine reproduces the model. Lately, the RP market has been extended and involves methods like rapid tooling (RT) and rapid manufacturing (RM), where the building material is restricted not only to paper and plastic, but where ceramics, composites, and metals can be used to produce fully functional "prototypes", or, in other words, RP has evolved and it is now possible to make small batch manufacture with it. Inserts for injection molding manufactured by RT has been subjected to extensive research, and Sachs [7] showed that conformal cooling channels, i.e. channels equidistant from the surface to be cooled, and manufactured by the indirect method called Three-dimensional printing (3DP), improved the part quality and decreased the cycle time in comparison with traditionally manufactured cooling channels. Dalgarno et. al. [8] showed that the RapidSteel process had limitations in terms of its ability to manufacture small features, but conformal cooling channels could be made without difficulties. Donnchadha [9] proposed a modular concept where parts of the tool are manufactured by traditional methods, and where inserts are fabricated by Selective laser sintering (SLS). Reduced cost and lead-times were reported from the use of this method. Selective laser melting (SLM) is another viable method for RT, and Over et.al. [10] reported time savings up to 30% when using SLM for manufacturing inserts. High thermal conductivity cooling is another way of cooling tools without having to manufacture complicated cooling channels. Davis et.al. [11] used Direct metal deposition (DMD) to reduce the cycle time without sacrificing any part quality or wear of the tool. Gibbons & Hull [12] showed that the direct-metal rapid-tooling method Electron beam melting (EBM) is also a viable method for the manufacture of free-form fabricated inserts, and a significantly higher cooling efficiency was reported, resulting in reduced cooling times and a more homogenous temperature distribution in the mold. These methods and other methods suitable for RT have been compared and discussed by Klocke [13], Karapatis [14], Radstock [15], Segal [16], Dormal [17], Kruth [18], and Wimpenny [19].

An efficient way of gaining in-depth knowledge of a process or product is to use Design of experiments (DOE). The basic idea is to perform well planned experiments in the early stage of the product development process in order to achieve the best possible product or process at the lowest cost level. By creating an orthogonal array which describes the settings of each factor, the effect of each factor can be estimated independent of the other factors. In this way, the experimental effort is optimized in reference to the information obtained, and valid and objective conclusions can be drawn. The theory behind DOE is further explained in [20]. Much work has been done in the area of optimal injection molding control using DOE, e.g. minimizing surface defects [21] and optimizing weld line strength. A more general method to determine optimal process settings has been developed where several quality measures can be chosen and weighted as objective function [22]. Another important quality criterion to take into account, especially when strict dimensional accuracy must be applied, is the warpage of the final product. Previous research dealing with warpage optimization has been focused on process parameter settings when a conventional design of the cooling system is applied, and important factors contributing to minimal warpage have been identified, like packing pressure, mold and melt temperature, packing time, and, to some extent, cooling time [23-26]. In the latter case, ideal cooling was assumed, i.e, the core and the cavity mold halves were assumed to have the same temperatures, and the cooling channels were assumed to keep a constant temperature throughout the mold. Studies considering not only simplified thin-walled parts but a cellular phone cover showed that the packing pressure was the most important factor and that interaction effects were also important contributors to the shrinkage

and warpage [27]. The process parameters are not the only contributors to the warpage, the runner and gate design also contribute and by using the length and diameter of the gate and runner as factors, the warpage of a typical plastic part can be successfully reduced [28] as well as using different rib designs as factors [29]. Using response surface methodology (RSM) is also viable in order to improve the quality of an injection molded part, and a 54% reduction of the warpage for a cellular phone cover was reported when RSM was used, and the mold temperature, packing time, packing pressure, and cooling time constituted factors in the experiment [30].

2. Experimental study

The aim with this study was to determine the effective factors controlling the dimensional accuracy of an injection-molded test part, manufactured either using a core insert with conventional cooling with straight holes and a baffle or by an conformal cooling layout. The dimensional accuracy of both layouts will be obtained by computer simulations. By using DOE, the most effective factors will be sorted out.

2.1. Test part and mold design

In cooperation with an injection molding company, which also designs and manufactures molds, a design of a test part was proposed which addressed the common and important issue with inadequate cooling in deep cores, see Fig. 1. The producer has to minimize the cycle time in order to be competitive on the market without affecting the crucial dimensional accuracy. The prime dimension of interest in this study is the distance between the two braces, which is 67 mm in the original design. For a molded part, the distance would differ from that obtained from the CAD model, due to volumetric shrinkage and flow effects. The warpage is calculated as:

$$Warpage = L_0 - L_w \tag{1}$$

where L_0 is the undeformed distance and L_w is the deformed distance after manufacturing, see Fig. 2.

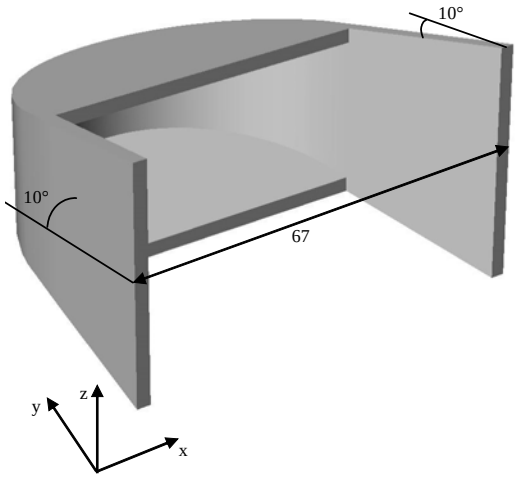

Fig. 1 Approximate part design. Draft angles are 10° and wall thickness is 3 mm.

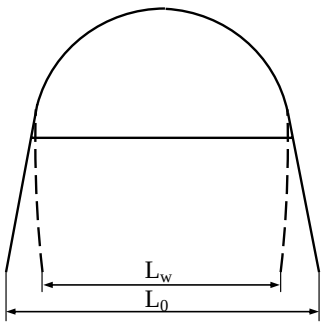

Fig. 2 Undeformed part (solid line) designed in the CAD system and deformed part (dashed line) after injection molding. The warpage is calculated as the difference between the undeformed distance, L_0, and the deformed distance, L_w.

A suitable grade of engineering plastics, POM, which also exhibits fairly extensive shrinkage, was used for the part, and the material data used for the simulations are shown in Table I.

Table I - Material data for the test part, provided by Coretech System.

Part material	POM (BASF Ultraform N2320 003)
Melt temperature	200 [°C]
Cavity temperature	90 [°C]
Ejection temperature	118 [°C]
Freeze temperature	160 [°C]
Thermal conductivity	2 [kJ/kg°C]
Specific heat	0.2 [W/m°C]
Volume	20.4 [cm^3]

Two different cooling channel layouts of the core plate were chosen for this study: a conventional cooling channel layout using a baffle (MD1) and a conformal layout (MD2), see Figs. 3 and 4. The same cooling with straight bores in the cavity plate was used for both MD1 and MD2. The gate is placed at the top center of the part (marked with an arrow in Figs. 3 and 4) with a diameter of 2.5/4 mm. The cooling channel offset from the cavity is approximately the same as the cooling channel diameter, 10 mm. The main tool body and the inserts are made of H13 tool steel, and the mold data used in the simulations are presented in Table II.

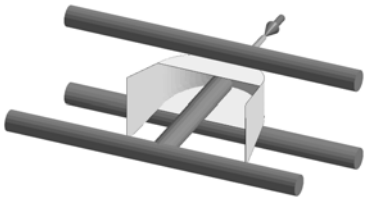

Fig. 3 Conventional cooling with straight bores in the cavity plate and a baffle in the core plate (MD1).

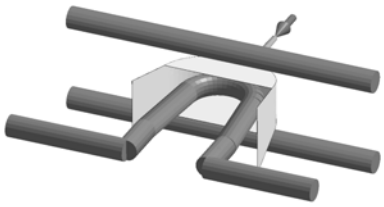

Fig. 4 Conformal cooling in the core plate and straight bores in the cavity plate (MD2).

Table II - Mold data used in the simulations.

Mold material	H13
Cooling channel diameter	10 [mm]
Cooling channel offset	10 [mm]
Runner dimension	2.5/4 [mm]
Specific heat	460 [J/kg°C][a]
Thermal conductivity	25 [W/m°C][a]
Density	7905 [kg/m^3][a]
Source:	[a]Arcam AB

2.2. Numerical model

A total number of 6,500 elements, both beam and shell elements, were used for the discretization of the model with a nominal value of 1.5 mm for the edge length of the shells but with further refinement in the gate area, see example of mesh for the free-form fabricated cooling layout in Fig. 4. The warpage in the x-direction (see Fig. 1 and Eq. 1) for the center of the braces was calculated using the results from the simulations, the packing time was set to 3 seconds in order to let the gate solidify, and the ambient temperature was set to 25 °C. The flow speed of the cooling water was set to 120 cm^3/sec in order to get well past the laminar limit of the Reynold's number of 10,000.

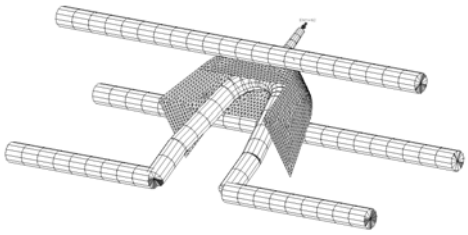

Fig. 5 Mesh of free-form fabricated cooling layout.

2.3. DOE

The process parameters chosen for the experimental design are shown in Table III. The parameters and their settings were selected in discussion with an experienced injection molder, with the aid of the values suggested by the injection molding software and after considering previous work done by other researchers. It is has been shown that the desired information often can be obtained by performing only a fraction of a full design when more than a few factors are considered, and this is known as fractional design. In this study, a fractional two-level design will be used, 2_V^{7-2}, where the filling pressure (F) and the packing pressure (G) were put on four- and five-factor interaction levels, see Table IV. This is a resolution V design where the main effects are aliased with four-factor interactions.

Table III - Process parameters chosen for the experimental design and their settings.

Parameter		**Low(-1)**	**High(+1)**	**Mid**
Temperature cavity [°C]	A	40	90	65
Temperature core [°C]	B	40	90	65
Temperature melt [°C]	C	190	210	200
Cooling time [sec]	D	6	12	9
Filling time [sec]	E	0.2	0.6	0.4
Filling pressure [MPa]	F	90	130	110
Packing pressure [MPa]	G	30	50	40

Table IV - Matrix for the experimental design and the resulting warpage values for the baffle cooling design (MD1) and the free-form fabricated layout (MD2). The warpage values when the parameters are set in the middle of the design space are given in the last row.

Experiment number	A	B	C	D	E	F	G	y_i MD1	y_i MD2
1	-1	-1	-1	-1	-1	1	-1	1.28	1.10
2	-1	-1	-1	-1	1	-1	1	1.07	0.91
3	-1	-1	-1	1	-1	-1	1	1.07	0.92
4	-1	-1	-1	1	1	1	-1	0.98	0.83
5	-1	-1	1	-1	-1	-1	1	1.59	1.37
6	-1	-1	1	-1	1	1	-1	1.50	1.29
7	-1	-1	1	1	-1	1	-1	1.47	1.26
8	-1	-1	1	1	1	-1	1	1.28	1.10
9	-1	1	-1	-1	-1	-1	1	1.63	1.66
10	-1	1	-1	-1	1	1	-1	1.60	1.63
11	-1	1	-1	1	-1	1	-1	1.57	1.62
12	-1	1	-1	1	1	-1	1	1.42	1.48
13	-1	1	1	-1	-1	1	-1	1.97	1.98
14	-1	1	1	-1	1	-1	1	1.95	1.96
15	-1	1	1	1	-1	-1	1	1.77	1.80
16	-1	1	1	1	1	1	-1	1.90	1.93
17	1	-1	-1	-1	-1	1	1	0.98	0.68
18	1	-1	-1	-1	1	-1	-1	0.96	0.64
19	1	-1	-1	1	-1	-1	-1	0.92	0.62
20	1	-1	-1	1	1	1	1	0.78	0.49
21	1	-1	1	-1	-1	-1	-1	1.38	1.10
22	1	-1	1	-1	1	1	1	1.35	1.06
23	1	-1	1	1	-1	1	1	1.17	0.90
24	1	-1	1	1	1	-1	-1	1.29	0.97
25	1	1	-1	-1	-1	-1	-1	1.56	1.44
26	1	1	-1	-1	1	1	1	1.38	1.26
27	1	1	-1	1	-1	1	1	1.38	1.28
28	1	1	-1	1	1	-1	-1	1.32	1.22
29	1	1	1	-1	-1	1	1	1.55	1.43
30	1	1	1	-1	1	-1	-1	1.66	1.55
31	1	1	1	1	-1	-1	-1	1.49	1.40
32	1	1	1	1	1	1	1	1.45	1.36
Mean								1.40	1.26
Mid								1.43	1.28

3. Results and discussion

Table IV also presents the result, or response, for design MD1 and MD2, and these data have been obtained by using the injection molding simulation software Moldex3D. The first section of this chapter will discuss the shrinkage and warpage of the part based on physical actions in- and outside the mold and what the result is in geometric measures. As seen in Table IV, regardless of the process parameter settings in the experiments, all warpage values are positive, i.e. the points **a** in Fig. 6 moves towards each other for all experiments. When the melt is cooled in the mold, it will shrink and this shrinkage can be characterized by two broad classifications; volumetric and linearized shrinkage [1]. When the part in Fig. 6 is cooled in the mold, the volumetric shrinkage will partly be compensated by the packing pressure until the gate freeze. The remaining volumetric shrinkage is dependent on the specific volume's dependence on the temperature and pressure and this shrinkage is an isotropic shrinkage, i.e. it will affect the entire part uniformly. Due to this shrinkage, the points **a** on the braces will move along the direction of the braces in the xy-plane. This will increase the warpage as described in Eq. 1 by the decrease of the distance between the points **a**.

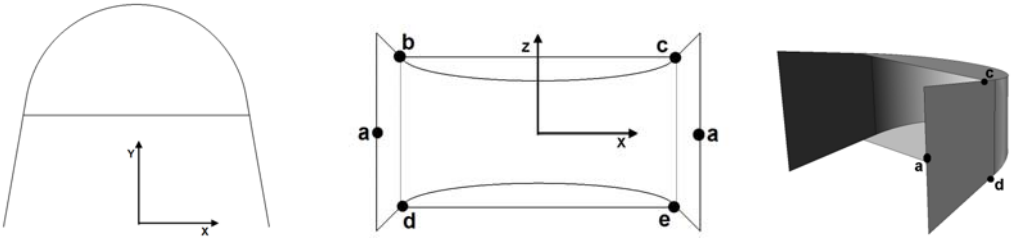

Fig. 6 Simplified shell model in different views.

The linearized shrinkage is developed as the melt flow in the cavity and these flow-induced effects can be attributed to shear forces and extensional forces induced to the polymer during filling and packing. Variations of cooling rate, direction and velocity of flow, part thickness etc. results in different layers in the polymer where the molecules have different orientations in the layers; from highly oriented to a more random orientation. Assuming that the core is subjected to a greater specific heat flux than the cavity, the temperature in the core will end up higher than in the cavity. After ejection, when the restrictions from the mold is gone, the distance between the two surfaces where points **a** are located will then decrease due to temperature induced shrinkage. During the molding process, this temperature difference leads to a thicker frozen layer on the colder side of the mold (cavity) at a higher pressure which results in a net bending moment towards the side with slower cooling rate, i.e. the hotter side (core). The warpage can also be affected in the opposite way, i.e. if the core temperature is colder than the cavity temperature, the deformed distance L_0 will in fact move towards the target distance. The last example is the case for all experiments where the core temperature is held at a low level (45°C) and when the cavity is held at a high level (65°C).

The points at the borders **b**-**c**, **d**-**e**, **c**-**e** and **b**-**d** are not as free to move while the part is in the mold. But when the part is ejected after cooling, the restrictions from the mold is gone and temperature induced shrinkage can occur as described above. When the core is hotter than the cavity, the borders **b**-**c** and **d**-**e** will move towards z=0 and the borders **b**-**d** and **c**-**e** will move outwards with respect to the z-axis (Fig. 7, left). All borders will not curve inwards due to the rather rigid corner geometry. The opposite will take place when the core is cooler than the cavity, borders **b**-**c** and **d**-**e** will move outwards and borders **b**-**d** and **c**-**e** will move inwards (Fig. 7, right). The curvature of the borders **b**-**d** and **c**-**e** will generate a curvature of the braces and hence also affect the points **a**. When the core is hotter than the cavity, the distance

between the points a will increase and the distance will decrease when the cavity is hotter than the core.

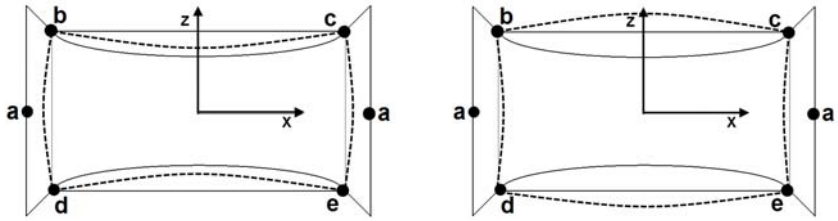

Fig. 7 Exaggerated warpage directions for hot core (left) and hot cavity (right).

Since the warpage values for all experiments are positive, i.e. the distance L_w between the points **a** is always smaller than the undeformed distance L_0, the conclusion is that the volumetric shrinkage is the main contributor of the measured warpage between the braces. The flow-induced, linearized shrinkage is not as significant.

The steps in the experimental design were analyzed by using the MATLAB R12 software with the Statistics Toolbox (www.mathworks.com) and calculating the contrasts leads to the results presented in Table V.

Table V - Contrasts for the baffle cooling design (MD1) and the conformal layout (MD2). The factors for the filling pressure (F) and for the packing pressure (G) are put on four- and five-factor interaction levels.

Contrast		MD1	MD2
L_1	**A**	-0.21	-0.34
L_2	**B**	0.41	0.61
L_3	**C**	0.30	0.29
L_4	**D**	-0.14	-0.12
L_5	**E**	-0.06	-0.05
L_6	**AB**	-0.04	-0.05
L_7	**AC**	-0.05	-0.02
L_8	**AD**	0.01	0.00
L_9	**AE**	0.03	0.02
L_{10}	**BC**	-0.07	-0.07
L_{11}	**BD**	0.01	0.01
L_{12}	**BE**	0.03	0.03
L_{13}	**CD**	-0.01	-0.01
L_{14}	**CE**	0.06	0.05
L_{15}	**DE**	0.00	0.00
L_{16}	**ABC**	-0.06	-0.07
L_{17}	**ABD**	-0.01	-0.01
L_{18}	**ABE**	-0.04	-0.03
L_{19}	**ACD**	0.00	0.00
L_{20}	**ACE**	0.02	0.01
L_{21}	**ADE**	0.00	-0.01
L_{22}	**BCD**	0.00	0.00
L_{23}	**BCE**	0.02	0.02
L_{24}	**BDE**	0.00	0.00
L_{25}	**CDE**	0.00	0.00
L_{26}	**ABCD**	0.00	0.00
L_{27}	**ABCE**	-0.01	-0.01
L_{28}	**ABDE**	-0.01	0.00
L_{29}	**ACDE**	0.00	-0.01
L_{30}	**BCDE=F**	0.00	0.00
L_{31}	**ABCDE=G**	-0.06	-0.06

By plotting the contrasts in Table V against the probability in a normal probability plot, the four most effective factors on the warpage can be detected, see Figs. 8 and 9. They are the temperatures of the melt (C), the cavity (A), the core (B), and the cooling time (D) for both of the experimental designs MD1 and MD2. These contrasts do not coincide with the straight line representing factors only affected in a random way, and hence they can also be considered as more important than the other factors. The contrasts of the factors L_1, L_2, L_3, and L_4 are depicted in Figs. 10-13. The filling time (E), the filling pressure (F), the packing pressure (G), and the interaction between all the factors are not considered to be as important which is confirmed in Table V. In order to minimize the warpage, the cavity temperature and the cooling time should be set on high levels, whilst the core temperature and melt temperature should be set on low levels. MD2 is more sensitive than MD1 to the settings of both the cavity and the core temperatures (the deviations in the interaction plots are higher for MD2 than for MD1), and, also for MD1, the core and melt temperatures are the two most important factors, but for MD2 the core and cavity temperatures are most important.

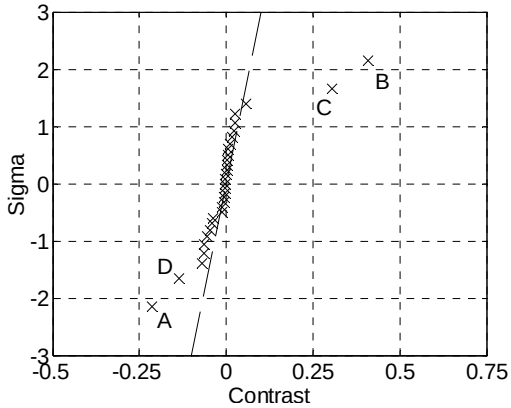

Fig. 8 Normal probability plot for the baffle cooling design (MD1).

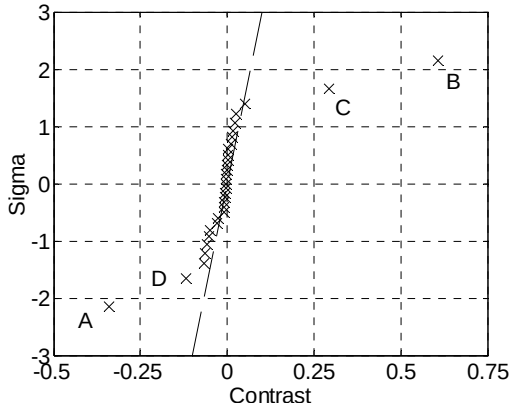

Fig. 9 Normal probability plot for the conformal cooling design (MD2).

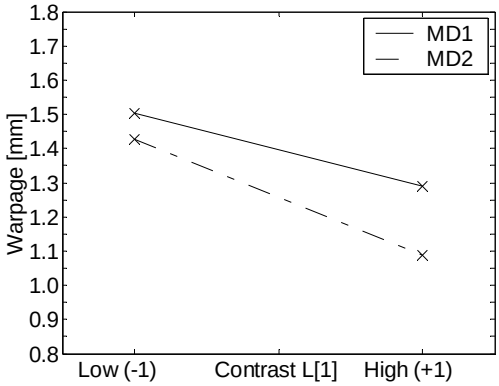

Fig. 10 The interaction of the factor cavity temperature (L_1) on the warpage.

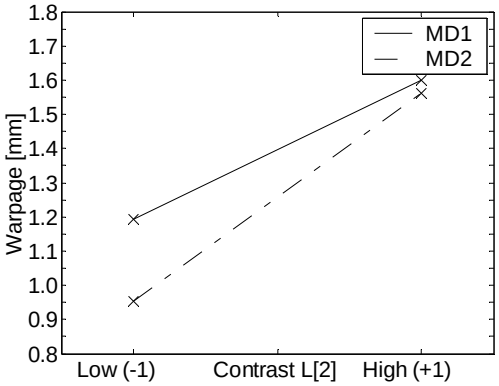

Fig. 11 The interaction of the factor core temperature (L_2) on the warpage.

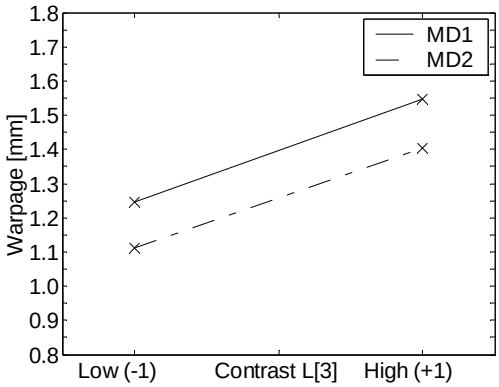

Fig. 12 The interaction of the factor melt temperature (L_3) on the warpage.

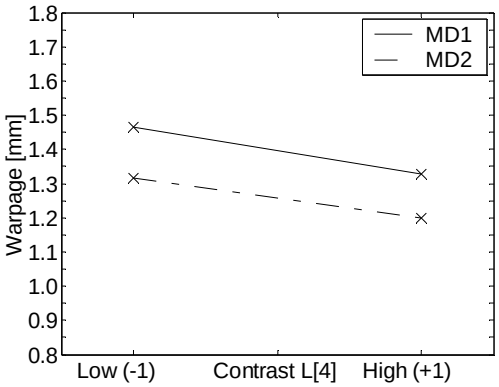

Fig. 13 The interaction of the factor cooling time (L_4) on the warpage.

In order to verify that the four chosen factors are the most important ones, a linear model, which is valid only in the tested factorial space of the response, is created according to:

$$\hat{y} = \bar{y} + \sum_{i=1}^{4} \beta_i x_i \qquad (2)$$

where $\hat{y}$ is the predictive value of the response, where $\bar{y}$ is the arithmetic mean value of the response, where $ß_i$ is half of the i:th contrast, and where the coded variables x_i represents the settings of the four factors A, B, C, and D (+1 or -1). This model is verified by examining the residual between the predictive model and the observed values in the experiments according to:

$$r_i = y_i - \hat{y}_i \qquad (3)$$

where r_i is the residual in experiment number i, where y_i is the measured response, and where $\hat{y}_i$ is the predicted value when setting the variables x_1 to x_4 in Eq. 2 according to the design matrix in Table IV. The residuals plotted against the predicted response $\hat{y}$ are depicted in Figs. 14-15, and the normal probability plots of the residuals are depicted in Figs. 16-17 for MD1 and MD2 respectively. These plots show that Eq. 2 is an adequate model for predicting the warpage, since the residuals have an expected value of zero and show scatter-like behavior for the whole range of the predicted value of the warpage, i.e. there is no relation between the residuals and the fitted values.

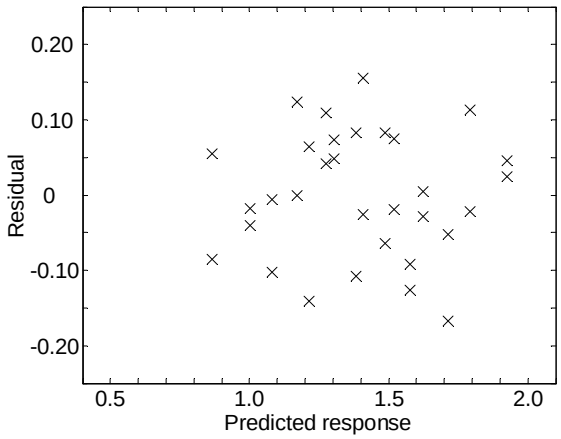

Fig. 14 Residual analysis of the baffle cooling design experiment (MD1).

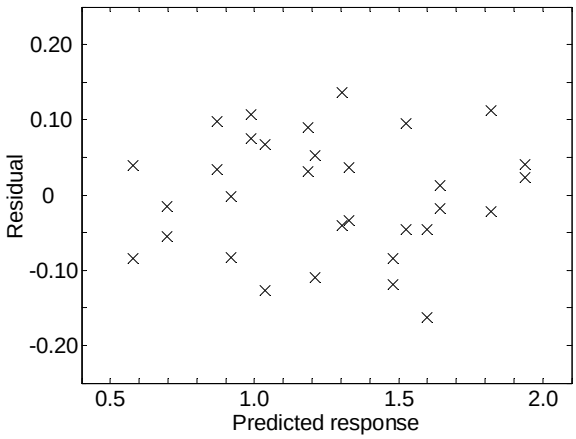

Fig. 15 Residual analysis of the conformal cooling design experiment (MD2).

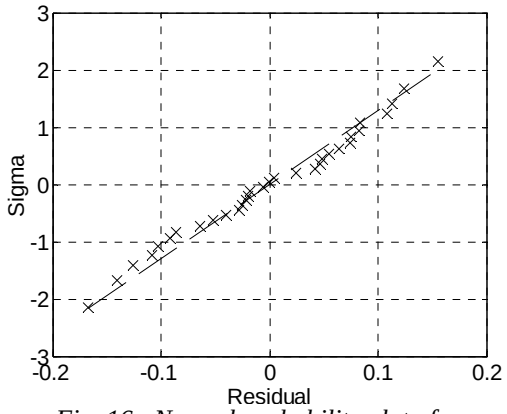

Fig. 16 Normal probability plot of residuals of the baffle cooling design (MD1).

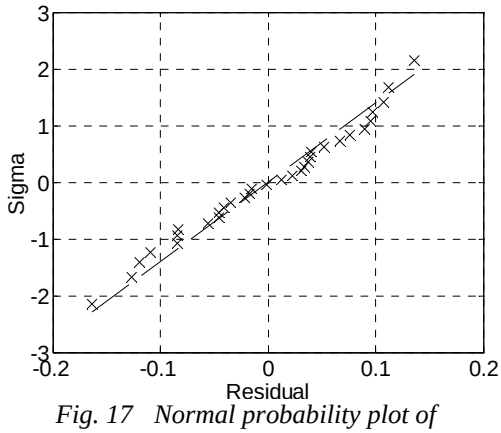

Fig. 17 Normal probability plot of residuals of the conformal cooling design (MD1).

The difference in efficiency between the layouts can be measured by comparing the warpage values of different settings for the factors. Experiments number 13 and 20 (see Table IV) give the maximum and minimum values of the warpage respectively, and in percentage the MD2 gives a reduction of the warpage of 37% compared with MD1.

4. Conclusion

DOE is a very useful tool to get a deeper knowledge about the response of different factors on a process. In this study, this method has been used to investigate the variation of the dimensional accuracy of a test part produced by injection molding with respect to seven process parameters and two different cooling channel layouts.

Numerical simulation is an essential tool in the attempt for an effective product design process but still there are limitations in the ability of describing the true physics in the injection molding process. Nevertheless, although the actual result values presented by the software is not the same results obtained in experiments, the possibility to get suggestions of how different result of interests are affected by changing several parameters are invaluable and easily accessible in comparison with carrying out shop-floor experiments.

The study shows the importance of choosing the right settings of different process parameters in order to use the effectiveness provided by free-form fabricated cooling channels. As an example, with optimal settings the warpage is reduced by 37% when using conformal cooling in comparison with a baffle cooling channel design using the same cooling time. The four most important factors influencing the warpage of this test part, for both cooling channel designs, were the temperatures of the melt, the core, the cavity, and the cooling time. The packing pressure, the filling pressure, and the filling time were not that important, and this was also the case for the interaction effects. Also, the a conformal layout is more sensitive to the settings of the temperatures of the core and the cavity in comparison with the baffle cooling channel design. So, plastic manufacturers using inserts with conformal cooling channels should be aware that there are differences in how the process parameters should be set, and, especially, that it also differs which parameters are the most important ones, in comparison with traditional cooling channel designs. If this is not taken into consideration, the benefit using conformal cooling is not fully utilized.

This work and other studies [23-27, 30] all show that it differs which process parameters are to be considered to be the most important ones influencing the warpage of an injection molded part. All of these parameters are indeed important, but for every specific case study, regardless of whether conventional cooling or conformal cooling is used, a DOE must be performed in order to sort out the most effective parameters.

In the future, this study could be extended by using optimization techniques, like stochastic methods or gradient based methods, in order to achieve the best possible process parameter setting with the objective to minimize the warpage. Another interesting study would be to minimize the cycle time with a constraint on the maximum warpage, since this is often the situation on the work shop floor, where one must minimize the cost of production whilst keeping the quality, or the warpage, within certain limits in order to be able to manufacture parts suitable for assembly.

References

[1] J. P. Beumont, R. Nagel, R. Sherman, Successful Injection Molding: Process, Design and Simulation, Carl Hanser Verlag, Munich, 2002
[2] A. Ammar, V. Leo, G. Régnier, "Corner Deformation of Injected Thermoplastic Parts", International Journal of Forming Processes, 6(1), (2003), 53-70
[3] K. M. B. Jansen, D. J. Dijk, K. P. Keizer, "Warpage of Injection Moulded Plates and Cormer Products", International Journal of Polymer Processing, 8(4), (1998), 417-424
[4] O. Denizart, M. Vincent, J. F. Agassant, "Thermal stresses and strains in injection molding: experiments and computations", Journal of Materials Science, 30((1995), 552-560
[5] D. Delaunay, P. L. Bot, R. Fulchiron, J. F. Luye, G. Regnier, "Nature of Contact Between polymer and Mold in Injection Molding. Part II; Influence of Mold Deflection on Pressure History and Shrinkage", Polymer Engineering & Science, 40(7), (2000), 1692-1700
[6] C.-H. Wu, Y.-J. Huang, "The influence of cavity deformation on the shrinkage and warpage of an injection-molded part", International Journal of Advanced Manufacturing Technology, 32 (2007), 1144-1154
[7] E. Sachs, E. Wylonis, S. Allen, M. Cima, H. Guo, Production of injection molding tooling with conformal cooling channels using the three dimensional printing process, Polymer Engineering and Science 40(5) (2000) 1232-1247
[8] K. Dalgarno, T. Stewart, Production tooling for polymer moulding using the RapidSteel process, Rapid Prototyping Journal 7(3) (2001) 173-179
[9] B. Ó. Donnchadha, A. Tansey, Conformally cooled metal composit rapid tooling, in: 1:st International Conference on Advanced Research in Virtual and Rapid Prototyping, Leiria, Portugal, 1-4 October, 2003, pp. 447-453
[10] C. Over, W. Meiners, K. Wissenbach, M. Lindemann, G. Hammann, Selective laser melting: a new approach for the direct manufacturing of metals parts and tools, in: 3:rd Conference on Laser Assisted Net Shape Engineering, Erlangen, Germany, 21-24 September, 2003, pp. 391-398
[11] K. R. Davis, T. J. Gornet, J. W. Vicars, High thermal conductivity tooling from laser direct metal deposition, in: 1:st International Conference on Advanced Research in Virtual and Rapid Prototyping, Leiria, Portugal, 1-4 October, 2003, pp. 503-507
[12] G. J. Gibbons, R. G. Hansell, Direct tool steel injection mould inserts through the Arcam EBM free-form fabrication process, Assembly Automation 25(4) (2005) 300-305
[13] F. Klocke, T. Celiker, Y.-A. Song, Rapid metal tooling, Rapid Prototyping Journal 1(3) (1995) 32-42
[14] N. P. Karapatis, J. P. S. v. Griethuysen, R. Glardon, Direct rapid tooling: a review of current research, Rapid Prototyping Journal 4(2) (1998) 77-89
[15] E. Radstock, Rapid Tooling, Rapid Prototyping Journal 5(4) (1999) 164-168
[16] J. I. Segal, R. I. Campbell, A review of research into the effects of rapid tooling on part properties, Rapid Prototyping Journal 7(2) (2001) 90-98
[17] T. Dormal, Rapid tools for injection molding, in: 4:th National Conference on Rapid and Virtual Prototyping and Applications, Lancaster, United kingdom, 20 June, 2003, pp. 139-151
[18] J. P. Kruth, X. Wang, T. Laoui, L. Froyen, Lasers and materials in selective laser sintering, Assembly Automation 23(4) (2003) 357-371
[19] D. Wimpenny, Rapid tooling options compared, in: 4:th National Conference on Rapid and Virtual Prototyping and Applications, Lancaster, U.K., 20 June, 2003, pp. 189-202
[20] G. E. P. Box, W. G. Hunter, J. S. Hunter, Statistics for Experimenters, -An introduction to design, data analysis and model building, john Wiley & Sons, New York, 1978

[21] K. H. Tan, M. M. F. Yuen, A fuzzy multiobjective approach for minimization of injection molding defects, Polymer Engineering and Science 40(4) (2000) 956-971
[22] Y. C. Lam, G. A. Britton, Y.-M. Deng, A computer-aided system for an optimal moulding conditions design using a simulation-based approach, International Journal of Advanced Manufacturing Technology 22(7-8) (2003) 574-586
[23] T. C. Chang, E. F. III, Shrinkage behavior and optimization of injection molded parts studied by the taguchi method, Polymer Engineering and Science 41(5) (2001) 703-710
[24] H. Kurtaran, B. Ozcelik, T. Erzurumlu, Warpage optimization of a bus ceiling lamp base using neural network model and genetic algorithm, Journal of Materials Processing Technology 169(2) (2005) 314-319
[25] B. Ozcelik, T. Erzurumlu, Comparison of the warpage optimization in the plastic injection molding using ANOVA, neural network model and genetic algorithm, Journal of Materials Processing Technology 171(3) (2006) 437-445
[26] M.-C. Huang, C.-C. Tai, The effective factors in the warpage problem of an injection-molded part with a thin shell feature, Journal of Materials Processing Technology 110 (2001) 1-9
[27] S. J. Liao, D. Y. Chang, H. J. Chen, L. S. Tsou, J. R. Ho, H. T. Yau, W. H. Hsieh, Optimal Process Conditions of Shrinkage and Warpage of Thin-Wall Parts, Polymer Engineering and Science 44(5) (2004) 917-928
[28] C. Yen, J. C. Lin, W. Li, M. F. Huang, An abductive neural network approach to the design of runner dimensions for the minimization of warpage in injection mouldings, Journal of Materials Processing Technology 174(1-3) (2006) 22-28
[29] T. Erzurumlu, B. Ozcelik, Minimization of warpage and sink index in injection-molded thermoplastic parts using Taguchi optimization method, Materials & Design 27(10) (2006) 853-861
[30] K.-T. Chiang, F.-P. Chang, Analysis of shrinkage and warpage in an injection-molded part with a thin shell feature using the response surface methodology, The International Journal of Advanced Manufacturing Technology (2006)

Paper F

Effective Injection Molding with Rapid Tooling and Optimization

L-E Rännar and C-G Gustafson

submitted to the International Journal of Advanced Manufacturing Technology

Effective injection molding with rapid tooling and optimization

LARS-ERIK RÄNNAR[1,2]

CLAES-GÖRAN GUSTAFSON[2]

[1)] *Mid Sweden University, Dept. of Engineering, Physics and Mathematics, Akademigatan 1, SE-831 25 Östersund, Sweden*

[2)] *Norwegian University of Science and Technology, Dept. of Engineering Design and Materials, Richard Birkelandsvei 2B, N-7491, Trondheim, Norway)*

Abstract

In this paper, a study is presented where rapid tooling (RT) and optimization have been used in order to minimize the warpage of an injection molded part. Few papers have been found in which it is described that RT in combination with optimization has been used to improve the injection molding process. In the present work, a free-form fabricated (FFF) cooling channel layout manufactured by RT is compared with a conventional cooling channel layout using straight holes and a baffle. The investigation is conducted on a test part in order to investigate a common and important issue for the injection molding industry: inadequate cooling in deep cores. Furthermore, three different optimization routines were used to solve the same optimization problem, and, in a comparison, the most effective one, with respect to the number of function calls, was the Method of Moving Asymptotes (MMA). The warpage of an FFF cooling channel layout was reduced by 56% in comparison with the original parameter setting, and, in comparison with the conventional layout, the warpage was reduced by 36% in favor of the FFF layout.

Keywords

Injection molding, rapid tooling (RT), optimization, simulation, cooling, warpage

1. Introduction

Injection molding is one of the most important methods to manufacture plastic products. With the process, it is possible to make products suitable for many different applications. Some of the properties characterizing the injection molding process are the ability to produce parts in large volumes, with excellent finish and dimensional accuracy, good repeatability and a fairly short processing time. One of the main drawbacks is the mold cost. The mold is custom-designed and in order to produce parts according to the market specification, the mold undergoes a costly iterative process where variations of the part, the mold, the material and the process have to be made to produce a part ready for the market.

Rapid prototyping, or free-form fabrication (FFF), refers to a group of technologies in which an additive approach in utilized when building physical models, tooling components or even production parts. In contrast to CNC machines, which subtract material, FFF joins liquid, powder, or sheets to form parts by using plastic, metal, ceramic, cellulose or composites. The first method commercialized in the late eighties is called Selective laser sintering (SLS) and today FFF has evolved into three market segments: rapid prototyping (RP), rapid tooling (RT) and rapid manufacturing (RM) [1]. In recent years, several FFF methods, where metal is used as building material, have appeared on the market. Many of them have been used for RT, and they can be divided into two groups: indirect and direct methods. Indirect methods use RP master patterns to produce molds, while the direct approach builds the tool insert without any intermediate casting step. The different methods for direct and in-direct RT have been compared and discussed by Klocke [2], Karapatis et. al. [3], Radstock [4], Segal et. al. [5], Dormal [6], Kruth et. al. [7], and Wimpenny [8].

The technology of FFF will enable a completely new approach when designing cooling systems for injection molding. The engineers have a completely new freedom when designing molds, since they are not restricted to conventional machining technologies like drilling but can focus on how to make the cooling as effective as possible, e.g. by making cooling channels that follow the geometry. This is also a strong argument for using simulation software, since these new methods turn all previous know-how about process setting upside down, and the best way to get an accurate estimate of the finished product is to utilize simulation in the product development process.

Optimization answers the question of how a product should be designed in order to behave the way the designer wants while satisfying all constraints. This is in contrast to the conventional design process in which the parameters of interest are altered from one simulation to another until an acceptable design has been conceived. This is a tedious, time- and cost-consuming activity by which it is hard and, in most of the practical cases, impossible to achieve the best possible design, i.e. the optimal design. The engineering optimization process benefits greatly from the revolution in the computer technology and the numerical calculations in the recent past, but still the optimization process is time-consuming and to choose a suitable optimization algorithm for a certain design problem is not an easy task. Fairly new methods like Particle swarm optimization (PSO) and Ant colony optimization (ACO), which are referred to as non-conventional or stochastic methods, compete with the more classical methods like Newton's method, Sequential linear programming (SQP), etc., and the designer must weigh the pros and cons of the different methods in order to make use of them as efficiently as possible. Previous research in the area of the optimization of the injection molding process, specifically about cooling time and warpage issues, has been focused on molds manufactured by traditional methods. Park et.al. [9] optimized the weighted

sum of the temperature non-uniformity over the part surface and the cooling time using the gradient-based CONMIN algorithm. Process parameters, coordinates and radii were used as design variables. Tang et.al. [10] used both the part average temperature and the temperature gradients throughout the mold as objective function using cooling channel size, locations and coolant flow rates as design variables. Qiao [11] presented a hybrid optimizer using a combined gradient-based and stochastic optimization routine. In this work, the temperature distribution over the part surface of a rectangular plate was minimized using the location of the cooling channels as design variables. Li [12] proposed a design synthesis approach in order to decompose a complex plastic part shape into simpler shapes and then develop an initial cooling system for the whole part based on the cooling systems obtained for the individual features.

2. Aim and objective

No studies have been found where RT in combination with optimization has been used in order to improve the injection molding process. The aim with the present study is to minimize the warpage of a test part, which was designed in order to replicate an important problem for the injection molding industry, namely inadequate cooling in a deep core. Also, the study aims to investigate the efficiency of different optimization algorithms applied to this problem.

3. Theory

3.1. Simulation

The use of computer-aided engineering (CAE) alone is not a redeemer in the product development process but it is an important tool in order to gain a deeper understanding of the product being developed. By using an injection molding simulation software and provide it with data about the material, part design, mold design and process parameters, the iterative process between the design engineer and the mold designer can be reduced significantly, and studies have shown that mold alteration costs can be reduced up to 50% when using injection molding simulation [13].

The software used in this study to simulate the injection molding process is Moldex3D (www.moldex3d.com), and the theory behind the process can be described as a three-dimensional, transient problem with a moving melt front where non-Newtonian flow and coupled heat transfer are also involved. Here, two-dimensional shell elements are used to represent the part geometry. Hence the generalized Hele-Shaw (GHS) was used to model the flow of an inelastic, viscous polymer melt under non-isothermal conditions. In order to solve the equations for the pressure, flow and temperature fields, a coupled finite-element/finite-difference method is used to solve the equations describing the GHS polymer melt front. The method uses finite elements to describe the planar coordinates, whereas the gap wise and time derivatives are expressed in terms of finite differences. The cooling phase of the process is described by solving a steady-state Laplace equation for the cycle-averaged temperature distribution throughout the mold and where the heat transfer phenomena in the boundary between the part and the mold is governed by a one-dimensional Poisson equation. The formulations and computations are described in [14].

Studies have shown that commercial softwares have limitations in describing the true physics related to warpage. In Moldex3D (R7, shell formulation), the molded part is assumed to be an orthotropic, linear, thermal, elastic material that obeys the Duhamel-Neumann constitutive

law [15] during the warpage calulations. So. the part deformation is assumed to be linear, elastic and static. During the flow calculations, no visco-elastic effects are considered like elongational flow etc., but asymmetric thermal conditions and volumetric effects during package are considered. The corner deformation of injection-molded parts was studied by Ammar et.al. [16] and they showed that the spring forward effect, which is not considered in commercial softwares, is the main contributor to deformation of a corner. Jansen et.al. [17] showed that the warpage increased linearly with applied temperature difference between the mold halves. More interesting, they also showed that a plate geometry curved towards the colder side of the mold when a high holding pressure was applied. At lower pressures, the plate curved towards the colder side which is the phenomena commercial softwares are describing independent of the applied pressure. Mold deformation is also o source of discrepancy between simulated and experimental results. Delauney et.al. [18] and Wu & Huang [19] showed that packing pressure history applied to mold deformation analysis could improve the warpage predictions for the molded part.

3.2. Optimization

For a design engineer there are often several possible solutions to a given problem. By using optimization, the engineer can rely on the optimization method to find the set of design variables that minimize, or maximize, a given function without violating any constraints. This can be written in a standard form as:

$$\begin{aligned} &\text{Find a vector} && \mathbf{x} = (x_1\ x_2\ \ldots\ x_n) && \\ &\text{which minimizes} && f(\mathbf{x}) && \\ &\text{such that} && \mathbf{h}_i(\mathbf{x}) = 0, && i = 1, 2, \ldots I \\ & && \mathbf{g}_j(\mathbf{x}) \le 0, && j = 1, 2, \ldots J \\ & && x_k^l \le x_k \le x_k^u, && k = 1, 2, \ldots n \end{aligned} \qquad (1)$$

where **x** is a vector of design variables which is bounded by side constraints x^l and x^u, where $f(\mathbf{x})$ is the cost, or objective, function, and where $h(\mathbf{x})$ and $g(\mathbf{x})$ are the vectors describing the equality and inequality constraints respectively. This is called a constrained problem, but if no equality or inequality constraints exist, it is called an unconstrained problem, and the latter formulation will be used in the present study.

3.2.1. Sequential Quadratic Programming (SQP)

SQP is a generalization of Newton's method for unconstrained optimization where the objective function is replaced by a quadratic approximation. This is done by formulating a QP subproblem based on a quadratic approximation of the Lagrangian function. SQP is used by the built-in function *fmincon()* in the MATLAB Optimization Toolbox. An overview of SQP is found in [20].

3.2.2. Method of Moving Asymptotes (MMA)

MMA is a first-order gradient-based method, i.e. it makes use of the first-order derivatives of the objective and constraint functions, and the basic idea is that the creation and solution of a sequence of sub-problems converge for the solution of the original problem. The sub-problem is of rather simple form: it is a linearization of the original functions and requires only one function evaluation of the original objective and of the constraint functions and their derivatives. One of the main advantages with MMA is its ability to converge to a solution fast and stable in comparison with other linear approximation methods [21].

3.2.3. Simulated Annealing (SA)

SA was developed in the mid-eighties, and the method describes the annealing process in which a substance is heated above its melting temperature and then gradually cooled down to form a crystalline lattice. This lattice, which is composed of millions of atoms organized in a structured way, is one example of nature's ability to form optimal structures. The atoms in the material have a high energy level when the temperature is high, but, when the material is cooled down, the ability of the atoms to move is reduced, and if the temperature is decreased too fast, defects in the crystalline lattice are formed because amorphous parts are introduced into the crystalline lattice. The system will then end up with a higher energy state than the optimal crystalline lattice. The optimum energy state can be seen as the optimum solution to the problem, while the temperature decrease is analogous to a locally performed optimization. The optimization is expressed by a sequence of iterations, and in each iteration the cost function is calculated by randomly modifying the variables. If the value of the cost function is decreasing, the old variable set is replaced by the new one, but if the cost function is increasing, the new variable set can be accepted or rejected. The acceptance of the new set is based on the value of the probability density function of the Bolzman distribution, and this feature of the SA makes it possible to climb out of local minima [22].

4. Case Study

4.1. Geometry and optimization formulation

The quality of an injection molded part can be defined in different ways depending on the usage of the product. The warpage is in many cases one of the most important quality factors, e.g. when the plastic product is a part of an assembled system. If the dimensional accuracy is poor, the mounting process will be slowed down and, in the worst case, even impossible to perform. The geometry of the test part in this study (Fig. 1) was conceived in cooperation with an experienced injection molder and designer in order to replicate an important issue for the injection molding industry; inadequate cooling in a deep core. The geometry of the part prevents a short cooling time due to the heat from the molten polymer which is concentrated in the core, and, generally, the greater temperature difference is through the part thickness and over part areas, the greater the warpage in the final product will be. In this study, the warpage between the two braces, as indicated in Fig. 2, is the objective function, and due to orientation effects and different temperature distributions during the molding. This distance after manufacturing will differ from that obtained from the CAD system.

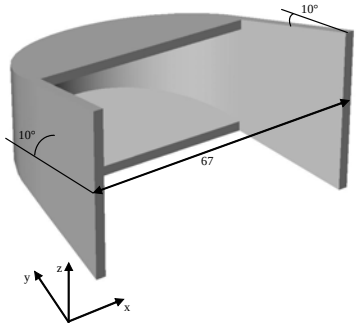

Fig. 1 Part design with a thickness of 3 mm and a draft angle of 10°.

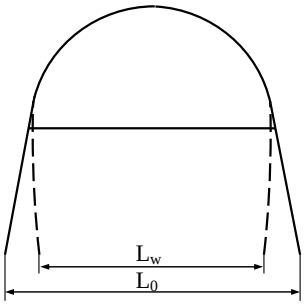

Fig. 2 The warpage depicted as the difference between the undeformed part (solid line) designed in the CAD system and the deformed distance after manufacturing (dashed line).

The warpage is calculated as:

$$Warpage = L_0 - L_w \quad (2)$$

where L_0 is the undeformed distance measured 67.00 mm in the CAD system, and where L_w is the deformed distance obtained after conducted simulations.

Previous research dealing with minimizing the warpage of injection molded parts has shown that crucial factors contributing to minimal warpage are packing pressure, mold and melt temperature, packing time, and, to some extent, cooling time [23-26]. Taking into consideration previous research where a design of experiments (DOE) was conducted on the same test part, four variables were chosen for the optimization in this study: the temperatures in the cavity and in the core, the melt temperature, and the cooling time. The settings of the side constraints were selected with the aid of the values suggested from the injection molding software and after discussion with an experienced injection molder. The variables, their initial values and their side constraints are presented in Table I, and other data used in the simulations are presented in Table II. The two different mold designs are depicted in Figs. 3-4.

Table I - The design variables, their initial values, and their side constraints.

Variable		$\mathbf{x^0}$	$\mathbf{x^l}$	$\mathbf{x^u}$
Temperature cavity [°C]	x_1	65	40	90
Temperature core [°C]	x_2	65	40	90
Temperature melt [°C]	x_3	200	190	210
Cooling time [sec]	x_4	9	6	12

Table II –Material data.

Part	**Material**	POM (BASF Ultraform N2320 003)
	Volume	20.4 [cm^3]
	Melt flow index	7.5 [g/10min][a]
	Ejection temperature	118 [°C][a]
	Freeze temperature	160 [°C][a]
	Thermal conductivity	2 [kJ/kg°C][a]
	Specific heat	0.2 [W/m°C][a]
Mold	**Material**	H13
	Specific heat	460 [J/kg°C][b]
	Thermal conductivity	25 [W/m°C][b]
	Density	7905 [kg/m^3][b]
	Cooling channel diameter	10 [mm]
	Cooling channel offset	10 [mm]
	Runner dimension	2.5/4 [mm]
Process	**Filling time**	0.4 [s]
	Filling pressure	110 [MPa]
	Packing pressure	25 [MPa]
	Source:	[a]CoreTech System, Taiwan [b]Arcam AB, Sweden

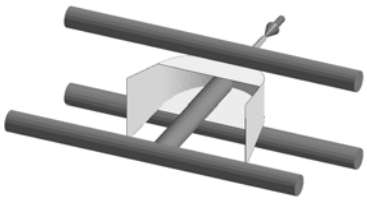

Fig. 3 The conventional cooling channel design (MD1) using straight holes in the cavity and a baffle in the core.

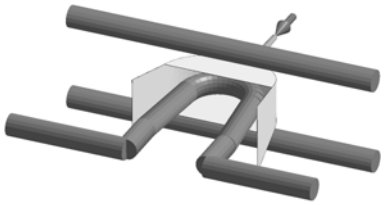

Fig. 4 The FFF cooling channel design (MD2) using straight holes in the cavity and a conformal cooling channel in the core.

The nominal value for the edge length of the shell elements for the part was set to 1.5 mm with further refinement in the gate area. A total number of 6,400 shell elements was used. In this problem, no equality or inequality constraints were used, so, to conclude, the optimization problem can be formulated as:

$$\begin{aligned} &\text{Find a vector} && \mathbf{x} = (x_1\ x_2\ x_3\ x_4) \\ &\text{which minimizes} && f(\mathbf{x}) \\ &\text{such that} && x_k^l \le x_k \le x_k^u, \qquad k = 1-4 \end{aligned} \tag{3}$$

where x_1 is the cavity temperature, x_2 is the core temperature, x_3 is the melt temperature, x_4 is the cooling time, $f(\mathbf{x})$ is the warpage according to Eq. 2, and where x^l and x^u are the lower and upper bounds of the four design variables respectively.

4.2. Software environment

In order to use different optimization algorithms and different solvers, a versatile MATLAB-driven environment for optimization studies called *VerOpt* has been developed [27]. The optimization problem is defined in the *VerOpt* software, as well as paths and names of the input and output files of the external solver, which is the injection molding software in this study. After executing *VerOpt*, the optimization is conducted automatically: the external solver is started with the appropriate input file. After the analysis, when the results from the output files are read in the form of the warpage, the objective function is analyzed, a new design variable set is calculated, and the external solver starts again, see Fig 5.

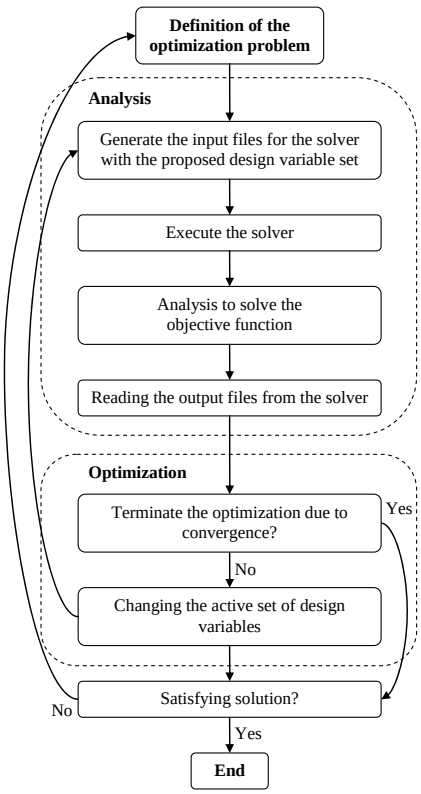

Fig. 5 The VerOpt process.

5. Results and discussions

The efficiency of the different optimization algorithms is evaluated by comparing the number of function calls which are executed to converge for an optimum solution, see Table III. The convergence was set to 0.001, that is, when the change in the objective function between two iterations is less than 0.001, the optimization was terminated automatically. Due to the stochastic behavior of SA, a slightly different approach to measure the convergence was used. The objective function when using SA is not always decreasing during the optimization, so for SA the number of function calls for convergence was decided by analyzing the iteration history graphs.

Table III - Optimization results for the three algorithms SQP, MMA and SA.

	SQP		**MMA**		**SA**	
	MD1	***MD2***	***MD1***	***MD2***	***MD1***	***MD2***
x_1	90	90	90	90	89	89
x_2	40	40	40	40	41	41
x_3	190	190	190	190	192	192
x_4	12	12	12	12	12	12
$f(x)$	0.87	0.56	0.87	0.56	0.88	0.60
$f(x_0)$	1.43	1.28	1.43	1.28	1.43	1.28
Function calls	124	102	18	18	121	125

As seen in Table III, the warpage is minimized when setting the cavity temperature and the cooling time at their high level and the core and melt temperature at their low level. With the two gradient-based methods SQP and MMA it is possible to find this setting, and consequently to find the same result for the objective function, whereas with SA it is not. MMA uses14-18% of the number of function calls compared with SQP and SA, although SA does not reach the optimum solution. By using the gradient-based algorithms, the warpage was reduced by 39% for cooling channel design MD1 and by 56% for cooling channel design MD2. This specific study seems to yield a convex problem, where a global optimum exists and where the side constraints are active. For these characteristic, gradient-based methods, especially MMA, are more efficient than stochastic methods.

For economic reasons, the gradients for SQP and MMA were calculated using forward finite differences, see Eq. 4 for the differentiation of a function on one variable. The function is denoted $f(\mathbf{x})$, the value for which the derivative is calculated, is denoted x_0 and the step-size is denoted h. In this study, the differentiation of the objective function by data rather than by an analytical expression makes it a classical ill-posed problem, and choosing the right step-size h is of vital importance in order to give a good approximation of the derivate. A large step-size gives a poor approximation of the derivate at point x_0, i.e. truncation errors, whilst a small step-size implies a loss of significant digits, i.e. a round-off error.

$$f'(x_0) = \frac{f(x_0 + h) - f(x_0)}{h} \tag{4}$$

The step-size h was calculated according to Eq. 5, where eps is the precision with which the objective function can be calculated. In the output files from Moldex3D, *eps* is 0.0001 which gives a value of h of 0.01.

$$h = \sqrt{eps} \tag{5}$$

6. Conclusions

This study shows that by using FFF cooling channels, it is possible to decrease the warpage of a part with a deep core by 36%, in comparison with a conventional cooling channel layout using a baffle. It also shows the viability of the use of optimization for engineering problems, and in this study the warpage for the test part was reduced by 56% for the FFF cooling channel design and by 39% for the conventional cooling channel design in comparison with the initial set of design variables. The most efficient method for this problem was the first-order, gradient-based method MMA but for more complex problems with a non-convex solution space, i.e. where possible local minima exists, SA or other stochastic methods would benefit more, due to their ability not to get trapped in local minima. By using gradient-based algorithms for such a problem, the global minimum is hard or sometimes even impossible to find, even if several different staring points are used for the optimization.

References

[1] T. T. Wohlers, Wohlers Report 2005, Wohlers Associates, Fort Collins, 2005.
[2] F. Klocke, T. Celiker, Y.-A. Song, Rapid metal tooling, Rapid Prototyping J 1 (1995) 32-42.
[3] N. P. Karapatis, J. P. S. v. Griethuysen, R. Glardon, Direct rapid tooling: a review of current research, Rapid Prototyping J 4 (1998) 77-89.
[4] E. Radstock, Rapid Tooling, Rapid Prototyping J 5 (1999) 164-168.
[5] J. I. Segal, R. I. Campbell, A review of research into the effects of rapid tooling on part properties, Rapid Prototyping J 7 (2001) 90-98.
[6] T. Dormal, Rapid tools for injection molding, in: 4:th National Conference on Rapid and Virtual Prototyping and Applications, Lancaster, U.K., 2003 139-151.
[7] J. P. Kruth, X. Wang, T. Laoui, L. Froyen, Lasers and materials in selective laser sintering, Assembly Autom 23 (2003) 357-371.
[8] D. Wimpenny, Rapid tooling options compared, in: 4:th National Conference on Rapid and Virtual Prototyping and Applications, Lancaster, U.K., 2003 189-202.
[9] S. J. Park, T. H. Kwon, Optimal cooling system design for the injection molding process, Polym Eng Sci 38 (1998) 1450-1462.
[10] L. Q. Tang, C. Chassapis, S. Manoochehri, Optimal cooling system design for multi-cavity injection molding, Finite Elem Anal Des 26 (1997) 229-251.
[11] H. Qiao, A systematic computer-aided approach to cooling system optimal design in plastic injection molding, Int J Mech Sci 48 (2006) 430-439.
[12] C. L. Li, A feature-based approach to injection mould cooling system design, Comput-Aided Des 33 (2001) 1073-1090.
[13] G. Menges, W. Michaeli, P. Mohren, How to make injection molds, Hanser Publishers, Munich, 2000.
[14] C. L. Tucker, (Ed.), Fundamentals of Computer Modeling for Polymer Processing; Hanser Publishers: Munich, 1989.
[15] Y. C. Fung, P. Tong, Classical and Computational Solid Mechanics, World Scientific Publishing, 2001.
[16] A. Ammar, V. Leo, G. Régnier, Corner Deformation of Injected Thermoplastic Parts, International Journal of Forming Processes 6 (2003) 53-70.
[17] K. M. B. Jansen, D. J. Dijk, K. P. Keizer, Warpage of Injection Moulded Plates and Cormer Products, International Journal of Polymer Processing 8 (1998) 417-424.
[18] D. Delaunay, P. L. Bot, R. Fulchiron, J. F. Luye, G. Regnier, Nature of Contact Between polymer and Mold in Injection Molding. Part II; Influence of Mold Deflection on Pressure History and Shrinkage, Polymer Engineering & Science 40 (2000) 1692-1700.
[19] C.-H. Wu, Y.-J. Huang, The influence of cavity deformation on the shrinkage and warpage of an injection-molded part, Int J Adv Manuf Tech 32 (2007) 1144-1154.
[20] J. S. Arora, Introduction to Optimum Design, Elevier Academic Press, San Diego, 2004.
[21] K. Svanberg, The method of moving asymptotes - a new method for structural optimization, Int J Numer Eng 24 (1987) 359-373.
[22] S. Kirkpatrick, C. D. Gelatti Jr, M. P. Vecchi, Optimization by simulated annealing, Sci 220 (1983) 671-680.
[23] M.-C. Huang, C.-C. Tai, The effective factors in the warpage problem of an injection-molded part with a thin shell feature, J Mater Process Technol 110 (2001) 1-9.
[24] H. Kurtaran, B. Ozcelik, T. Erzurumlu, Warpage optimization of a bus ceiling lamp base using neural network model and genetic algorithm, J Mater Process Technol 169 (2005) 314-319.

[25] S. J. Liao, D. Y. Chang, H. J. Chen, L. S. Tsou, J. R. Ho, H. T. Yau, W. H. Hsieh, Optimal Process Conditions of Shrinkage and Warpage of Thin-Wall Parts, Polym Eng Sci 44 (2004) 917-928.
[26] B. Ozcelik, T. Erzurumlu, Comparison of the warpage optimization in the plastic injection molding using ANOVA, neural network model and genetic algorithm, J Mater Process Technol 171 (2006) 437-445.
[27] J. Holmberg, L.-E. Rännar, Versatile Optimization, in: Nordic MATLAB Conference, Oslo, Norway, 2001 207-212.